THE PHYSICAL REVIEW

A JOURNAL OF EXPERIMENTAL AND THEORETICAL PHYSICS

CONDUCTED BY

THE

AMERICAN PHYSICAL SOCIETY

BOARD OF EDITORS

Managing Editor John T. Tate, University of Minnesota, Minneapolis

G. Breit, P. W. Bridgman, L. W. McKeehan; I. S. Bowen, R. S. Mulliken, H. D. Smyth; E. U. Condon, C. J. Davisson, F. K. Richtmyer

---

NOVEMBER 15, 1929

Theory of Complex Spectra - - - - - - - - - - - - J. C. Slater [illegible]

Phenomena in Oxide Coated Filaments - - - - - - - - Joseph A. Becker [illegible]

A New Method for the Study of Voltage-Intensity Relations and its Application to the Mercury 2537A Line - - - - - - - - - - - Floyd C. [illegible] [illegible]

Magnetic Moment of the Oxygen Atom - - - - - - O. R. Kurt and T. E. Phipps [illegible]

On the Theory of the Smekal-Raman Effect in Hydrogen-Like Atoms - - - - - - - - - - - - - - - - - - Boris Podolsky and Vladimir Rojansky [illegible]

On Life and Concentration of Metastable Atoms and the Quenching of Mercury Resonance Radiation - - - - - - - - - - - - - - - E. Gaviola [illegible]

Energy Changes by a Variation from the Crystallographic Group - - - H. M. [illegible] [illegible]

Letters to the Editor - - - - - - - - - - - - - - - - [illegible]

Book Reviews - - - - - - - - - - - - - - - - - [illegible]

PUBL[illegible]

EDITORS OF THIS REVIEW

[illegible] E. Ives	University of Chicago, Chicago, Ill.
[illegible] F. G. Swann	Bartol Research Foundation, Philadelphia, Pa.
[illegible] A. L. Hammerschlag	Columbia University, New York City
[illegible] G. H. Pegram	Columbia University, New York City
John T. Tate	University of Minnesota, Minneapolis, Minn.
[illegible] S. Lee	University of California, Berkeley, Calif.

THE PHYSICAL REVIEW

[illegible] American Physical Society at [illegible] Ahlers St., Menasha, Wis. [illegible] University of Minnesota, Minneapolis, Minn. Two volumes annually, [illegible] each volume.

[illegible] From July 1, 1896, to January 1, 1913, the Review was conducted by Edwin [illegible] Hall and Frederick Bedell, with the financial support of Cornell [illegible]. Four volumes were issued annually; subsequent volumes, semi-[illegible] volumes in all.

On January 1, 1913, the Review was transferred to the American [illegible] commenced on the first page of the new series which was then begun. [illegible] has been conducted by a Board of Editors elected by the Society. Semi-[illegible] regularly January and July. Since July 1, 1916, the Review has been issued [illegible].

[illegible] reference is referred to page 2 of the advertisements for further information.

[illegible] Subscription, throughout the Postal Union, $5.00 in advance.

[illegible] single number of current volumes, $1.60.

[illegible] Foreign postage, $0.20, in advance.

[illegible] Back volumes: Back Numbers, $2.00 per copy for issues prior to [illegible] 1916, $1.60 per copy for issues subsequent thereto. Postage is free [illegible] subscription order; otherwise postage is extra. No bound volumes can be [illegible] subscribers desiring to purchase a limited number of Page Series, Vol. 1, No. 1 [illegible] Second Series, Vol. 7, No. 4, January 1916; Vol. 7, No. 2, February [illegible], April 1916; and Vol. 7, No. 5, May 1916 (at $1.00 each).

[illegible] Back issues will be supplied by the Editor on request. Copy for such numbers [illegible] Minneapolis two months prior to the date of issue; old copy is [illegible] destroyed. Send communications about back numbers, George Ellett, [illegible], Wis.

[illegible] Change in allowed subscription upon resignation of members of the American [illegible].

[illegible] Notice and Complaints of failure to receive the Review, in the case of [illegible] delivery, should be addressed to the Secretary; in the case of [illegible] Menasha, Wis., or to the Editor. New copies can [illegible] to complaint of non-delivery only if notice of non-delivery is [illegible] months of date of issue.

[illegible] Communications should be addressed to the Physical Review, University of [illegible].

[illegible] Entered as second-class matter [illegible], at the Post Office at Menasha, Wis., under the Act of October 3,

Second Series *November 15, 1929* *Vol. 34, No. 10*

THE

PHYSICAL REVIEW

THE THEORY OF COMPLEX SPECTRA

By J. C. Slater
Jefferson Physical Laboratory, Harvard University

(Received June 7, 1929)

Abstract

Atomic multiplets are treated by wave mechanics, without using group theory. In part 1 Hund's scheme for multiplet classification is derived directly from theory. Part 2 is devoted to the computation of the energy distances between multiplets, and comparison of these distances with experiment in some typical examples. There is no treatment of the separations between the various terms of a multiplet, since that has been done elsewhere, but only between one multiplet and another. It is found that Hund's rule, that terms of large L and S values lie lowest, has no general significance; the present theory leads to the same results as the rule when it is obeyed experimentally, but many cases which were exceptions to that rule are in agreement with the theory. The method of calculation of multiplet distances is described in sufficient detail, with the necessary tables of coefficients, etc., so that further checks with experiment could easily be made.

THE theory of complex spectra is treated in this paper by the method of wave mechanics. The results of the calculation may be divided into two parts: first, the classification of the terms into multiplets; second, the energy values of these multiplets. The first part contains no new results of physical interest, for it leads precisely to Hund's[1] scheme of classification, and uses almost the identical steps that Hund uses. Its value lies in the fact that this well-known scheme is shown in an elementary way to follow directly from wave mechanics. The second part, however, is almost entirely new, and it leads to definite formulas for the intervals between the different multiplets in spectra, intervals which could previously be considered only very roughly from an empirical rule of Hund, which proves to have no general significance. These calculations, of course, give the intervals in terms of certain integrals, which we do not calculate, but merely estimate well enough to permit some comparison with experiment. The agreement is in general fairly good. A third part would be also included, dealing with the intervals within the multiplets, produced by the magnetic interaction, were

[1] F. Hund, Linienspektren und periodisches System der Elemente, Springer.

it not that Goudsmit[2] has already answered the question by a method closely analogous to that used here.

It will be noted that the objects of the present paper resemble closely those aimed at by Heisenberg, Wigner, Hund, Heitler, Weyl, and others,[3] who employ the methods of the group theory. That method is not used at all in the present calculation,and, in contrast, no mathematics but the simplest is required, until one actually comes to the computation of the integrals. This, it is believed, is in itself sufficient justification for paralleling to some extent work already done. The simplification is achieved largely by introducing the spin at the very beginning of the calculation, rather than later. Thus we need only consider antisymmetric wave functions, which can be treated very simply as determinants, and can avoid the other symmetry characters, with which the other papers have been mostly concerned. The process of building up wave functions of the proper symmetry by using determinants is not new; it is found in Dirac's earlier papers, and has been used, for example, by Waller and Hartree.[4] The spin function, however, is introduced into the determinant in the present paper in a new and more satisfactory way. The results which we obtain, concerning the diagonal term of the energy with respect to the antisymmetric wave functions, are of the sort found by the group theory, and also by the recent method of Dirac,[5] but it seems worth while to derive them in a simple fashion.

The essentially new results of the present paper, those relating to energy, in the second part, come from the fact that we consider the whole degeneracy, that coming from orbital as well as spin angular momentum, which most of the other papers have failed to do. The present method is essentially equivalent to the others in that it gives sums of energies, rather than individual energies. When it is applied to the case in which the degeneracy with respect to orbital angular momentum is not considered, it leads, as do the others, merely to the sum of all terms of a given multiplicity; the writer is indebted to Dr. Bloch for pointing out that in that case all the results of Heitler can be easily demonstrated by the present method. But we make the observation that, by considering the whole problem with all its degeneracy, the method of energy sums can be used much more effectively, so much so that in most important cases we can get the actual energies of the individual terms. In connection with this, it should be noted that in several cases the actual perturbation problems have been solved directly, rather than by the method of energy sums, obtaining results[6] that hold even when the magnetic energy is appreciable.

[2] S. Goudsmit, Phys. Rev. **31**, 946 (1928).

[3] W. Heisenberg, Zeits. f. Physik **41**, 239 (1927). E. Wigner, Zeits. f. Physik **40**, 492, 883, etc. (1927). F. Hund, Zeits. f. Physik **43**, 788 (1927). W. Heitler, Zeits. f. Physik **46**, 47 (1928). H. Weyl, Gruppentheorie und Quantenmechanik, Hirzel, 1928.

[4] I. Waller and D. R. Hartree, Proc. Roy. Soc. **A124**, 119 (1929). The writer is indebted to Dr. Hartree for calling his attention to this paper.

[5] P. A. M. Dirac, Proc. Roy. Soc. **A123**, 714 (1929).

[6] W. V. Houston, Phys. Rev. **33**, 297 (1929). J. A. Gaunt, Trans. Camb. Phil. Soc. (1929).

PART 1. THE CLASSIFICATION OF MULTIPLETS

1. As a preface, we remind the reader of the theory of multiplets, as developed before wave mechanics. This theory considered the interactions of the various angular momenta of the parts of an atom, and treated the various energy levels resulting from different relative orientations of these parts. In a logical development of atomic structure it would follow directly after Bohr's theory of electron orbits; for Bohr went as far as was possible on the assumption that each electron moved in a field with spherical symmetry, so that its orientation with respect to the rest of the atom was a matter of no concern. We start then, as Bohr finished, with an atom composed of a number of electrons, each characterised by a total quantum number n, and an azimuthal quantum number l, the latter determining the angular momentum, and being often regarded as a vector (normal to the plane of the orbit, in Bohr's theory, but this is of no importance). The orientation of this vector in space was arbitrary, on account of the spherical symmetry. As an additional part of the formulation, we need to consider the electronic spin of Goudsmit and Uhlenbeck: each electron has an angular momentum (with consequent magnetic moment) entirely apart from the momentum l which it acquires by its motion. This additional angular momentum, denoted by s, (which like l, is often regarded as a vector), can likewise be oriented arbitrarily in space, without reference to the direction of l. Since the values which n, l, and s can take on, and the notation, are rather significant, we observe that l can equal 0, 1, 2, $\cdots$; n can be any integer greater than or equal to $(l+1)$; and s is always equal to $1/2$. The values of n and l are denoted by symbols, as $1s$, $2s$, $\cdots$; $2p$, $3p$ $\cdots$; $3d$, $4d$, $\cdots$; $4f$, $5f$ $\cdots$; referring respectively to the cases where n and l are 10, 20, $\cdots$; 21, 31, $\cdots$; 32, 42, $\cdots$; etc. Then the structure of an entire atom in a given state can be given, as far as Bohr's theory is concerned, by giving the n and l of each electron, denoted as in the example: $(1s)^2$ $(2s)^2$ $(2p)^6$ $(3s)^2$, meaning that there are two $(1s)$ electrons, two $(2s)$, six $(2p)$, two $(3s)$. Another state of the same atom (in this case magnesium) would be $(1s)^2$ $(2s)^2$ $(2p)^6$ $(3s)$ $(3p)$; and so on. These two states would be often abbreviated $3s$ and $3p$ respectively. The spin, having always the same value, need not be mentioned at this stage.

Having described the atom to the degree of accuracy considered by Bohr, we next must consider that the angular momentum vectors really are coupled together; there are differences of energy depending on orientation, and a consequent splitting up of each energy level into a number of different ones. In the commonest case, which alone we shall consider, the coupling can be considered in several stages. First, the l's of the various electrons group themselves into a vector sum L, which takes on only integral values, 0, 1, 2, $\cdots$, as the separate l's do. Each such arrangement gives a different energy, and a different term in the spectrum. The terms with L equal respectively to 0, 1, 2, 3, $\cdots$, are called S, P, D, F, $\cdots$ terms. Second, the spins of the electrons group themselves into a vector sum S, taking on the integral or half integral values (for any case, the orientation where all s's are

parallel is allowed; if it is integral, only integral S's are allowed, and if it is half integral, only half integers are allowed for S). The different values of S lead to terms of different multiplicities, as we shall see in a moment, and different energies; thus $S=0$ gives singlets, $S=1/2$ doublets, $S=1$ triplets, etc. Finally L and S are coupled together, their sum being called J, and being integral or half integral to correspond with S. Since J can vary from $|L+S|$ to $|L-S|$, there are (if $L>S$) $2S+1$ different terms so obtained. These terms are the various terms of a single multiplet, which is named singlet ($2S+1=1$), doublet ($2S+1=2$), etc., to agree with the number of terms. The energies involved in going from one value of L to another, or of S to another, are generally large; they are (as one sees from wave mechanics) electrostatic energies. On the other hand, the energy of orientation of L with respect to S is small, coming from magnetic interaction of the parts of the atom, so that the different levels of a multiplet (same L and S, different J) lie near enough together to be grouped together. If one neglects the magnetic interaction as a first approximation, the levels of a multiplet all have just the same energy. As to notation, we speak, for example, of $^3P_2$, meaning a triplet P term with $J=2$. And if we wish to indicate the state of the electrons which produce the multiplet terms, we write it as $(1s)^2\,(2s)^2\,(2p)^6\,(3s)\,(3p)\,^3P_2$, which would often be abbreviated $(3p)\,^3P_2$.

The process of coupling can also be described in the language of space quantization. If one has an angular momentum vector, as l, acted on by no torques, so that its direction is arbitrary, it is legitimate to choose any axis in space, and consider that the component of the vector along this direction can take up any one of a set of values, integrally spaced between the parallel and antiparallel orientations. Thus, if m_l is the component of l along this axis, m_l can equal $l, l-1, l-2, \cdots -l$. These $(2l+1)$ values are considered to denote $(2l+1)$ separate stationary states, all with the same energy. Now we follow by this method the process of coupling, beginning with the uncoupled vectors, and carrying it through to the case where the l's are coupled to give L, and the s's to give S, but the magnetic interactions are not considered. In the uncoupled case, each electron has its own m_l and m_s. As the coupling forces are introduced, torques appear which make the components of the individual l's and s's vary with time, so that the same space quantization is no longer possible. But the torques are internal; they cannot change the total angular momentum. The total sum of all the l's and the sum of all the s's, and their components along the axes, remain constant, and hence quantized: $\sum m_l$ and $\sum m_s$ are quantized even when the coupling has taken its full value. On the other hand, when the electrons are coupled, the atom consists of vectors L and S, each separately free, so that these can be space quantized, giving components M_L and M_S along the axis. We need now only identify the M_L and M_S for the coupled system with the $\sum m_l$ and $\sum m_s$ for the uncoupled one, to get the correspondence necessary to show what multiplets appear from any combination of electrons. The exact method is easily shown from an example.

For illustration, we take the coupling of two p electrons. Each has $l=1$; the first has principal quantum number n, the second n'. For each, we can have $m_l=1,\ 0,\ -1$; $m_s=1/2,\ -1/2$; that is, $2(2l+1)=6$ different sets (m_l, m_s), each representing a stationary state. With the combined atom, there are 36 combinations of one state of the first electron with one of the second. These are partly given in Table I. Two different notations are

TABLE I. *Two p electrons.*

First notation	Second notation	Σm_l	Σm_s	Notes
$(n\ 1\ 1\ \frac{1}{2})\ (n'\ 1\ 1\ \frac{1}{2})$	$\{(n\ 1\ 1)\ (n'\ 1\ 1)\}\ \{\ \}$	2	1	Exc
$(n\ 1\ 0\ \frac{1}{2})\ (n'\ 1\ 1\ \frac{1}{2})$	$\{(n\ 1\ 0)\ (n'\ 1\ 1)\}\ \{\ \}$	1	1	A
$(n\ 1\ -1\ \frac{1}{2})\ (n'\ 1\ 1\ \frac{1}{2})$	$\{(n\ 1\ -1)\ (n'\ 1\ 1)\}\ \{\ \}$	0	1	
$(n\ 1\ 1\ -\frac{1}{2})\ (n'\ 1\ 1\ \frac{1}{2})$	$\{(n'\ 1\ 1)\}\ \{(n\ 1\ 1)\}$	2	0	
$(n\ 1\ 0\ -\frac{1}{2})\ (n'\ 1\ 1\ \frac{1}{2})$	$\{(n'\ 1\ 1)\}\ \{(n\ 1\ 0)\}$	1	0	
$(n\ 1\ -1\ -\frac{1}{2})\ (n'\ 1\ 1\ \frac{1}{2})$	$\{(n'\ 1\ 1)\}\ \{(n\ 1\ -1)\}$	0	0	
$(n\ 1\ 1\ \frac{1}{2})\ (n'\ 1\ 0\ \frac{1}{2})$	$\{(n\ 1\ 1)\ (n'\ 1\ 0)\}\ \{\ \}$	1	1	A
$(n\ 1\ 0\ \frac{1}{2})\ (n'\ 1\ 0\ \frac{1}{2})$	$\{(n\ 1\ 0)\ (n'\ 1\ 0)\}\ \{\ \}$	0	1	Exc
$(n\ 1\ -1\ \frac{1}{2})\ (n'\ 1\ 0\ \frac{1}{2})$ etc.	$\{(n\ 1\ -1)\ (n'\ 1\ 0)\}\ \{\ \}$	-1	1	

used in this table for comparison. First we simply give the four quantum numbers $(n\ l\ m_l\ m_s)$ for each of the electrons. For the other scheme of notation, which is often convenient in practice, we take advantage of the fact that each m_s is capable of only the two values $1/2$, $-1/2$: we set up two brackets, one containing the symbols $(n\ l\ m_l)$ of each electron with $m_s=1/2$, the second containing the symbols for those with $m_s=-1/2$. Such a bracket symbol, in which the arrangement of terms within a bracket is of no significance, is equivalent to a state of the first sort. After each symbol is given the value of $\sum m_l$ and of $\sum m_s$ for that state. Finally, after some of the terms, are notes which will be explained later.

The values of $\sum m_l$ and $\sum m_s$ are conveniently plotted by giving $\sum m_s$ as abscissa, $\sum m_l$ as ordinate, and putting a dot for each state. Thus in Fig. 1, a, we give a single p state; and in b, the points for the sum of the two (the numbers indicate the number of states with the same $\sum m_s$, $\sum m_l$). But now in Fig. 1, b, each point should also represent the M_L, M_S of one of the multiplets existing in the coupled atom. This can be brought about in but one way: by assuming the multiplets $^1S\ ^1P\ ^1D\ ^3S\ ^3P\ ^3D$, whose separate representations are shown below (in Fig. 1, d—i), and whose patterns, if superposed, would just give Fig. 2b. Thus it must be that two p electrons produce these multiplets. But that is just what our other method gives; for two l's, each equal to unity, can add to give $L=0,\ 1,\ 2$, (S, P, D terms); while two s's, each $1/2$, can give $S=0,\ 1$ (singlet, triplet). In every case, the two methods lead to the same result, just as here.

The scheme as described above will result, in an atom with many electrons, in an enormous variety of terms, comparatively few of which are realized in actual atoms. The principle limiting the number is the exclusion principle of Pauli. It cannot be stated in the language of vectors, but only in

terms of the space quantization just described. It is: no two electrons can have identical sets of numbers $(n\ l\ m_l\ m_s)$; further, two combinations of electrons which differ only in the interchange of the quantum numbers of two electrons are to be treated as identical. Stated in terms of the bracket method of writing the electronic combinations, this means that no two sets of quantum numbers $(n\ l\ m_l)$ within a bracket can be identical; and that the order of arrangement within a bracket is immaterial. By these restrictions, the number of terms is often enormously decreased. Many points on our diagrams are removed, and just the remaining ones must be fitted into multiplets, resulting in a much smaller number. For example, in our Table I, the two electrons have the same l; hence, if they have also the same total quantum number (that is, if $n=n'$), they cannot both have the same set of m_l and m_s. Thus the two terms marked *Exc* (and many other terms not

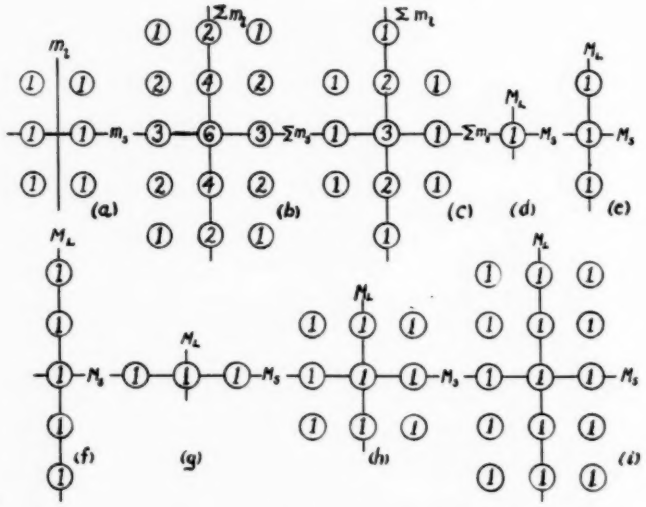

Fig. 1. (a) Single p electron; (b) Two p electrons; (c) Two equivalent p electrons; (d) ^1S (e) ^1F; (f) ^1D; (g) ^3S; (h) ^3P; (i) ^3D.

included in the table) must be excluded; and the two terms marked A (and many more pairs) are to be considered identical. When the terms not allowed are removed, the new pattern in place of Fig. 1b proves to be Fig. 1c; and this is the superposition of ^3P ^1S ^1D, which then are the multiplets allowed with two equivalent p electrons (that is, two electrons, each with $l=1$, and with the same n). As a general thing, the exclusion principle is active only when there are equivalent electrons; its many properties, as in limiting the number of electrons in a closed shell, are well known and need not be elaborated.

2. In quantum mechanics, we meet the problem of complex spectra as one step in the approximate solution of the wave equation for the atom. There are two fundamental principles which govern the structure of matter: quantum dynamics, and the principle of antisymmetry which shows itself

in the exclusion principle and the Fermi-Dirac statistics. The first states that only those energy levels are possible which are characteristic numbers of Schrödinger's equation for the system; the second further restricts the possible energies to those connected with characteristic functions antisymmetric in the electrons. Our whole object is to find such characteristic functions and numbers. And as before, the first step is to approximate by supposing that the separate electrons move in fields of force with spherical symmetry, so that there is no tendency for orientation of the various angular momenta. There are various ways of doing this; one scheme which gives good results is that of Hartree.[7] For simplicity in description we shall imagine that scheme modified slightly in one detail; according to it, each electron moves in a field of force slightly different from the others. We shall neglect the difference, assuming that all the electrons move in precisely the same field. And this field is to be so chosen as to give the best agreement with the correct values even without further corrections.

An electron moving in a central field of force, according to wave mechanics, is characterized by the same two quantum numbers n and l that we have previously described. The arbitrary direction of the angular momentum is, as before, most conveniently described by quantizing the component m_l in a fixed direction. Similarly the orientation of the spin is most conveniently given by specifying its component m_s in the same fixed direction. Thus each electron in an atom, in the approximation in which we can neglect the interactions of their rotations, is specified by the four quantum numbers $n\ l\ m_l\ m_s$, just as it was before. All relations of these numbers remain unchanged. But now, each electron has a wave function—a function of its coordinates (and, as we shall describe presently, of a coordinate representing its spin) depending on the numbers $n\ l\ m_l\ m_s$, which is a solution of Schrödinger's equation for a particle in a central field. We can denote the function for the ith electron by $u(n_i/x_i)$, where n_i stands for the four numbers $n_i l_i m_{li} m_{si}$, and x_i symbolizes the four coordinates (three of position, one of spin) of the ith electron. Now it is well known that the product of these functions, for all the electrons $(1 \cdots N)$ of the atom, gives a function which approximately satisfies Schrödinger's equation. That is, $u(n_1/x_1)u(n_2/x_2) \cdots u(n_N/x_N)$ is an approximate solution. But it is not antisymmetric in the electrons, so that it does not satisfy the exclusion principle. To build up an antisymmetric solution, we first note that we still have an approximate solution, connected with the same energy value, if we interchange any two x's, obtaining for example $u(n_1/x_2)\ u(n_2/x_1) \cdots u(n_N/x_N)$. We still have an approximation with the same energy if we make a linear combination of any such solutions. Then we can make the one possible combination which is antisymmetric, and it will both satisfy the exclusion principle, and will be an approximate solution of Schrödinger's equation. This combination is conveniently written as a determinant:

[7] D. R. Hartree, Proc. Camb. Phil. Soc. **24**, 89 (1928). See also J. C. Slater, Phys. Rev. **32**, 339 (1928) for discussion of Hartree's method and application of some of present results to it.

$$\begin{vmatrix} u(n_1/x_1) & u(n_1/x_2) & \cdots & u(n_1/x_N) \\ \cdots & \cdots & \cdots & \cdots \\ u(n_N/x_1) & u(n_N/x_2) & \cdots & u(n_N/x_N) \end{vmatrix}$$

It is obviously antisymmetric, for interchanging, say, x_1 and x_2 interchanges two columns of the determinant, which by a familiar property merely changes the sign. It can be shown that it is the only antisymmetric combination of these functions. And it leads at once to the familiar interpretation of the exclusion principle. For if two of the functions had the same quantum numbers (say $n_1 = n_2$, symbolizing equality of four quantum numbers), then the corresponding rows of the determinant would be identical (since they contain the functions $u(n_1/x_1) = u(n_2/x_1)$, $u(n_1/x_2) = u(n_2/x_2)$, etc.) and by another familiar rule, the determinant will vanish. Thus there is no solution corresponding to the case where two electrons have the same set of quantum numbers. Further, the determinant treats all electrons alike; hence we cannot count as separate two states which differ only by the interchange of the quantum numbers of two electrons. Our exclusion principle then coincides with the one previously described.

We now have, corresponding to each set of quantum numbers, or to each independent bracket expression of quantum numbers (as given in Table I), which is allowed by Pauli's principle, a single, antisymmetric function of the electrons, which is an approximate solution of Schrödinger's equation. Our next task is, beginning with this, to introduce the interaction between the various angular momenta, and to try to improve the agreement with Schrödinger's equation, without destroying the property of antisymmetry. We use essentially the method of perturbations. The fundamental result of this method is that, if we take the approximate but incorrect wave function, and compute the matrix of the real energy with respect to this, the diagonal terms of this matrix are good approximations to the actual energy values of the problem. The errors remaining are of the order of the square of the ratio of non-diagonal to diagonal terms. Since we can easily show in our case that the non-diagonal terms here are really small, this method will give a good approximation to the energy values. We are then to take the real energy operator (involving the interactions between electrons, rather than with fictitious central fields), find its matrix with respect to the wave functions already determined and take these diagonal terms as energy levels.

There is, however, one case in which our criterion for the accuracy of this approximation is not valid. This is the case where a number of terms lie close together. Then in the first place one can no longer say that the errors are as small as we have assumed; in the second place, since we are generally interested in the energy differences between the neighboring terms, we really demand a much greater accuracy than usual, to give this difference correctly. Thus this case—that of degeneracy—demands special treatment. We see that, in our case, we actually meet this difficulty, for the various wave functions with the same values of n's and l's, but different m_l's and m_s's,

have very nearly the same energy, and yet the energy differences, giving the separations between multiplet levels, are just what we wish to find. Thus the problem of degeneracy is the essential part of the calculation for complex spectra. We may describe the situation this way: the non-diagonal energy terms connected with transitions between states with different n's and l's for the electrons are negligible; but those between states with the same n's and l's but different m_l's although they may be no greater

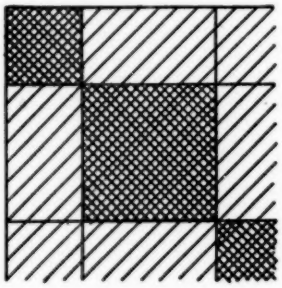

FIG. 2

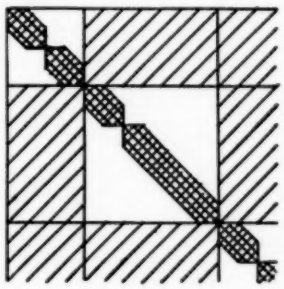

FIG. 3

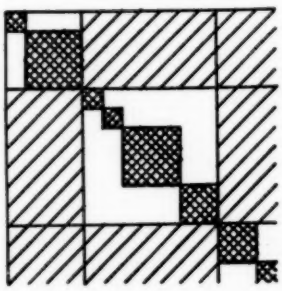

FIG. 4

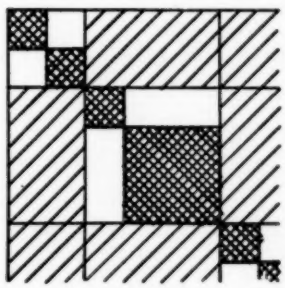

FIG. 5

Figs. 2–5. Figures 2, 3, 4 represent the energy matrix schematically. In Fig. 2, it is with respect to the unperturbed wave functions. The terms in the double shaded squares represent transitions between two states with the same electron quantum numbers. These terms are all significant; those outside the squares are negligible. In Fig. 3 we have made the linear combinations to the perturbed wave functions, reducing each square to a diagonal matrix. Fig. 4 is with respect to unperturbed wave functions, as is Fig. 2; but we take account of the fact that there are no components between states of different $\sum m_l$, $\sum m_s$. In Fig. 4, energy levels are arranged according to the values of $\sum m_l$, $\sum m_s$. Fig. 5 (see Note 3) represents the matrix of angular momentum, in the final perturbed wave functions. Each square represents a separate multiplet. In Figs. 3 and 5 the terms are arranged according to multiplets.

numerically, are not negligible for our purpose. This situation can be described graphically. Suppose we make a scheme for the energy matrix, giving stationary states (the incorrect ones that we determine from the central field, denoted by the numbers $n_1 \cdots m_{sN}$) along the two sides of a square array, and putting in the matrix components. Then if we arrange together all terms with one set of n's and l's, then those with another set, and so on, we see that the matrix components in the double shaded regions

of Fig. 2 are all important (even the non-diagonal ones); but those in the singly shaded regions are negligible. The method of treatment is now this: we take a particular square of the matrix, as A, coming from transitions between different states with the same n's and l's. And, by linear combinations of the wave functions connected with these states, we reduce the matrix to a diagonal one. This can always be done for a finite matrix. Then we do the same thing with each such double-shaded square. The result after that is then a matrix of the form shown in Fig. 3. Here the only important non-diagonal terms have disappeared; so that we can take the diagonal terms as the approximate energy values of the real problem, with assurance that the errors are not large. We observe that, after this is done, there will still be just as many wave functions connected with each set of values of the n's and l's as before.

In our problem of complex spectra, there is a feature which greatly simplifies the calculation. For we shall prove[8] that the energy has no matrix components connected with transitions in which $\sum m_l$ or $\sum m_s$ change (if we neglect the magnetic energy, as we are doing for the present). To show the effect of this graphically, we can arrange the terms, first according to the n's and l's, as we have done; but under each such classification, we can arrange according to $\sum m_l$ and $\sum m_s$. Then the original energy matrix really has the simplified form shown in Fig. 4. And the process of removing the important non-diagonal terms reduces to separate linear combinations between the functions of each set having a given set of n's, l's, $\sum m_l$, and $\sum m_s$. Generally the number of functions actually present in one of these groups is very small; thus the problem by this method becomes very simple, and can be readily carried out. As a result of it, we see that the number of states with a given set of n's and l's, and a given $\sum m_l$ and $\sum m_s$, remains unchanged as we apply the interaction between angular momenta. And this is the essential point required in the classification of the terms.

3. The essential features of the perturbation theory as applied to complex atoms have been described; and we can now make connections with Hund's scheme for classifying the terms. Each unperturbed wave function can be described by its set of $(n\ l\ m_l\ m_s)$ for each electron (Pauli's principle being actually satisfied by our condition of antisymmetry). Then, just as before, we can make a table of all the possible terms with any set of n's and l's; we can find $\sum m_l$ and $\sum m_s$ for each of the terms; and we can make a diagram, as before, plotting $\sum m_l$ against $\sum m_s$, obtaining just the sort of point diagram that was shown in Fig. 1, b or c. The small square arrays of matrix components, in Fig. 4, are just the components between different terms represented by coincident points in Fig. 1, b and c. The components between terms lying at different points on the $\sum m_l$—$\sum m_s$ diagram are zero. Now we have just proved that, even when the interactions are considered, we still have the same diagram representing the number of states with each set of $\sum m_l$ and $\sum m_s$. To verify Hund's method completely, we need only show that we can correctly break up this diagram into a number of separate

[8] See Note 1 for the proof.

ones, as Fig. 1, d—i, each representing a separate multiplet. Obviously we can separate the diagram into rectangular arrays of points (that is, sets of wave functions with particular values of $\sum m_l$ and $\sum m_s$), but there are other conditions that must be satisfied to make these wave functions really represent a multiplet.

In looking for the conditions that a set of wave functions must satisfy to represent a multiplet, we first observe that, so long as we neglect magnetic energies, they must all have the same energy value. Now after we have made our linear combinations, we shall have perfectly definite wave functions, each with a perfectly definite energy value (the diagonal terms in Fig. 3). Without proof, it is not obvious that we can pick out sets of functions, with different $\sum m_l$ and $\sum m_s$, but all with the same energy. Even if we can (and we shall prove that it is possible),[9] the set of functions must satisfy further conditions. Somehow we must work in the fact that they all represent the same vector L, and the same S, but with different orientations in space. Now the wave functions corresponding to an angular momentum vector with different orientations have perfectly definite relations, which are expressed by computing the matrix components of the angular momentum. If, then, our group of terms of the same energy really is to represent a multiplet, the matrix of angular momentum must also have the required form. But we shall prove that this also is the case.[9] Thus, with these proofs given, we see that we have a perfect right to separate the wave functions into a group of multiplets, as Hund does. Since the method of doing this is unique, the result must give precisely the same classification of multiplets that Hund finds. And since at present we wish only classification, we need not actually make the linear combinations, and get the diagonal matrix of H, at all.

It remains to be proved that the terms, after making the proper linear combinations, really can be divided up into groups of terms, having the following properties: every wave function of the group has the same energy value; and the angular momentum matrix has just the same values that it would if the wave functions referred to the vectors L and S with their various orientations in space. The details of the proof are given in the notes[9]; but we can state the essential features. First we show, by fundamental methods, that the total angular momentum matrix can have components only between states of the same energy. Since we can show that the angular momentum matrix is not diagonal, this proves that there must be at least several states of each energy, in order that the angular momentum can have components between them. This breaks up the terms associated with a given set of n's and l's into sets each of the same energy. Next we show that each of these sets is just the sort we need for a multiplet. We do this by detailed consideration of the angular momentum matrix; the essential point being that the entire matrix can be determined uniquely from certain commutation relations between the x, y, z components of the angular momentum vector, and that these relations are just the same for the whole atom as for a single angular momentum vector, so that we must have just the same matrix. We then

[9] See Note 2.

have the complete proof that the wave functions of the atom really break up into sets each having all the properties of a multiplet; the M_L—M_S diagram of such a multiplet is just as we assumed in the first section; and the result is that the method of finding what multiplets arise from any configuration of electrons, is precisely the method of Hund.

Part 2. Determination of the Energies

1. To find the energy values of the multiplets, the natural procedure is to solve the various problems of linear combination encountered above, find the correct wave functions, and compute the diagonal terms of the energy with respect to them. But we can find a simpler way, a way that even here will allow us to omit the actual calculation of the wave functions altogether. This is done by the use of the principle that the sum of a number of energy values is in some cases not changed by applying a perturbation, even if the individual values are. The principle is this: given a set of wave functions $u_1 \cdots u_i$; make a set of orthogonal linear combinations of them, $u_1' \cdots u_i'$. Consider the diagonal terms of a matrix, as the energy matrix, referred to the original wave functions: say $E_1 \cdots E_i$. Consider also the diagonal terms of the matrix of the same function, referred to the new wave functions, as $E_1' \cdots E_i'$. Then $E_1 + \cdots + E_i = E_1' + \cdots + E_i'$. In our case, we can use this as follows. We consider a set of terms, all with the same n's, l's, $\sum m_l$, $\sum m_s$ (that is, the terms connected with a small square in Fig. 4, or with coincident points in Fig. 2b and c). Before making our linear combinations, we can easily calculate the diagonal terms of the energy. We can add these terms for all the wave functions. Then the sum is equal to the sum of the corresponding energy values after making the linear combinations; that is, it is the sum of certain energy values that we wish to calculate. By proper use of this method, we can generally get the energies of all the multiplets.

To make the process clear, we shall illustrate by the case of two equivalent p electrons, shown in Fig. 2c. We compute the energy of the function $\sum m_s = 0, \sum m_l = 2$; that is, the energy of the configuration $\{(n11)\}\ \{(n11)\}$. But there is only one function connected with this point in the diagram. Hence the sum degenerates to one term. The process of making linear combinations is not necessary here; the corresponding square matrix array in Fig. 4 has but one row and column. Thus the energy we have found is also the energy of the term after interaction is considered; and comparison with (f) shows that it is the energy of the ^1D multiplet. Similarly the point $\sum m_s = 1, \sum m_l = 1$, gives the energy of ^3P. Again, $\sum m_s = 1, \sum m_l = 0$ or -1, and $\sum m_s = -1$ $\sum m_l = 1, 0, -1$, should all give the energy of P; and in consequence of certain identities between the energy matrix components, these actually do give the same result as before. Also, the point $\sum m_s = 0$, $\sum m_l = 1$, has two wave functions, for the states $\{(n\ 1\ 0)\}\ \{(n1\ 1)\}$ and $\{(n1\ 1)\}\ \{(n1\ 0)\}$. We calculate the energies of these terms, and add. And the result should, and does, come out to be the sum of the ^1D and ^3P energies. Finally, the point $\sum m_l = 0, \sum m_s = 0$ has three wave functions. We add their energies, and the result should be the sum of the energies of

^1D, ^3P, and ^1S. Since the first two of these energies are known, we need only subtract them from the sum to get the energy of ^1S. Thus the energies of all the multiplets are computed, without finding any perturbed wave functions at all. It is readily seen that extension of the same scheme will give complete information in all cases except where there is more than one multiplet of the same kind; for example, if a given configuration of electrons contains two ^2D multiplets, the method will give only the sum of the two terms. To get the individual terms, we must carry through the more elaborate scheme of taking linear combinations. But such cases are not found among the more important terms, so that in practical use the limitation is not important.

For actual use, the essential step is to find the energy values referred to the original wave functions; then it is simply a matter of adding and subtracting to get the energies of the multiplets. This is merely a problem of integration; for we know the original wave functions (they are the determinants mentioned above), and we can easily find the matrix components of energy with respect to them. The process is somewhat complicated, however, in many cases, and a careful arrangement of the arithmetic simplifies it greatly. To work out the actual method properly, we shall have to go more into detail than we have about the whole problem. This calculation will be made in sections 2 and 3; finally we give a number of examples of calculation of energy in section 4.

2. Our problem in the present section is this: to compute the diagonal term of the energy with respect to one of the approximate wave functions, written as a determinant, which we discussed earlier. If H represents the energy operator, and

$$u = \begin{vmatrix} u(n_1/x_1) & \cdots & u(n_1/x_N) \\ \cdots & \cdots & \cdots \\ u(n_N/x_1) & \cdots & u(n_N/x_N) \end{vmatrix}$$

is the wave function, we then have as the desired diagonal term

$$\frac{\int u^* H u dv}{\int u^* u dv}.$$

The functions u are determinants; that is, sums of the $N!$ terms formed from the product $u(n_1/x_1) \cdots u(n_N/x_N)$ by carrying out all permutations of the coordinates $x_1 \cdots x_N$, even permutations having the coefficient $+1$, odd ones the coefficient -1. The product u^*u is then a double sum, and each of the integrals would be likewise; except that, in consequence of orthogonality relations, they really reduce to single sums, of which all the terms are identical.

We consider first the energy integral. The energy operator H consists, as we shall see, of three parts: first, a constant, which we need consider

no further; second, a sum of terms each depending on the coordinates of a single electron, and all the same in form, which we can write $H(x_1)+\cdots+H(x_N)$; third, a sum of terms (the Coulomb repulsions) each depending on the coordinates of two electrons, which we can write explicitly as Σ(all pairs) e^2/r, where r is the distance between the two. The whole integral then consists of a constant, and two triple sums, two of the summations being over the permutations found in u and u^*, the third over the terms in the energy operator. Consider a single term out of this triple sum, of the sort connected with the coordinates of just one electron. Then, if the permutations involved in u and u^* are different, at least two x's must have different quantum numbers in the product; for example, we may have

$$u^*(n'/x_k)u^*(n''/x_l)u(n'''/x_k)u(n''''/x_l),$$

where n' is different from n''', and n'' different from n''''. When we multiply this by a function of one electron, and integrate, there will always be at least one product (as $u^*(n'/x_k)u(n'''/x_k)$), which by orthogonality will integrate to zero. Thus the only terms which are not zero are those where we have the same permutation in u and in u^*; the double sum over permutations reduces to a single one. We are left, then, with

$$\Sigma(\text{permutations of } x_1\cdots x_N)\int u^*(n_1/x_1)\cdots u^*(n_N/x_N)$$
$$(H(x_1)+\cdots+H(x_N))u(n_1/x_1)\cdots u(n_N/x_N)dx_1\cdots dx_N.$$

A single integral from this sum, by normalization, immediately reduces to

$$\left[\int u^*(n_1/x_1)H(x_1)u(n_1/x_1)dx_1+\cdots+\int u^*(n_N/x_N)H(x_N)u(n_N/x_N)dx_N\right].$$

If we let these terms be $I(n_1),\cdots I(n_N)$, we see that the whole is simply the sum of the I's, counted $N!$ times; so that this part of the energy integral is $N!(I(n_1)+\cdots+I(n_N))$, where it will be observed that the sum of terms $H(x_i)$, each depending on the coordinates of one electron, has been changed into a sum of terms each depending on a single set of quantum numbers.

Next we take the terms e^2/r_{kl} in the energy. As before, we take a typical term of the triple summation. If it happens that the same permutation occurs both in u and u^*, then the integral will reduce to

$$J(n;n')\int u^*(n/x_k)u^*(n'/x_l)e^2/r_{kl}u(n/x_k)u(n'/x_l)dx_kdx_l,$$

which we will call $J(n;n')$. Each permutation will yield, from terms of this kind, the summation over all pairs x_kx_l; this reduces to the summation of J's over all pairs $n\,n'$; and the $N!$ permutations finally give, from terms of this sort, $N!\sum$(pairs of n's) $J(n;n')$. Next, it may be that the permutation in u^* differs from that in u by the interchange of two electron coordinates.

If in addition the term e^2/r_{kl} happens to refer to the particular coordinates $x_k x_l$ which have been interchanged, we have an integral which reduces to

$$K(n;n')=\int u^*(n/x_l)u^*(n'/x_k)e^2/r_{kl}u(n/x_k)u(n'/x_l)dx_k dx_l,$$

which we call $K(n;n')$. Such terms all occur with negative sign; for, since the permutation in u^* differs by one interchange from that in u, one of the terms is always an even, the other an odd, permutation, resulting in a coefficient -1 in the double sum. Then by a similar argument to that above, these terms yield a contribution $-N!\sum$(pairs of n's) $K\ (n\ ;\ n')$ to the energy integral. Finally, if the term of u^* differs from that of u by more than a single interchange, there will always be at least one coordinate whose wave functions will integrate to zero on account of orthogonality, so that no other terms exist.

Finally we need the normalization integral $\int u^*u\ dv$. Formally, we can find this as we did the first part of the energy integral, replacing $H(x_1)+\ldots+H(x_N)$ by unity. This results in replacing $\sum I(n)$ by unity; so that the integral is just $N!$. Thus division by the normalization factor simply removes the factor $N!$ which occurs in each term of the energy integral. We have then, for the diagonal term of the energy which we desire, constant $+\sum(n$'s$)I(n)$ $+\sum$(pairs of n's) $J\ (n;\ n')-\sum$(pairs of n's$)K(n;\ n')$.

3. Now we must consider the exact form of the wave function, to compute I, J and K. In connection with this, we must answer the question which no doubt will be felt at this point, as to the part which the spin plays in the calculations. We begin by considering the individual functions $u(n_i/x_i)$. Each such function is a solution of Schrödinger's equation for an electron in a central field. Let the potential of such a field be $U(xyz)$. Then Schrödinger's equation is

$$H_1u=\left(-\frac{h^2}{8\pi^2m}\left(\frac{\partial^2}{\partial x^2}+\frac{\partial^2}{\partial y^2}+\frac{\partial^2}{\partial z^2}\right)+U\right)u=\epsilon u.$$

Here u is a function of x, y, z, and certain coordinates representing the spin, depending parametrically on n, l, m_l, and m_s; ϵ is a function of the quantum numbers alone. To describe the spin, we proceed as Pauli[10] does: we use as a coordinate the component of the spin along our fixed axis, m_s (which thus appears both as quantum number and as coordinate). Thus we could write our equation

$$H_1u(n\ l\ m_l\ m_s/x\ y\ z\ m_s)=\epsilon(n\ l\ m_l\ m_s)u(n\ l\ m_l\ m_s/x\ y\ z\ m_s).$$

Since H_1 is independent of the spin coordinate m_s, (neglecting magnetic interactions), we can separate variables, writing u as a product of a function of xyz, and a function of m_s:

$$u(n\ l\ m_l\ m_s/x\ y\ z\ m_s)=u(n\ l\ m_l/x\ y\ z)u(m_s/m_s).$$

[10] W. Pauli Jr., Zeits. f. Physik **43**, 601 (1927).

The function $u(m_l/m_s)$ is to be interpreted as follows: m_s (the quantum number) can have two possible values, $\pm\frac{1}{2}$, and we have a different wave function for each quantum number. For example, we may have $u(\frac{1}{2}/m_s)$. But now assuming that the quantum number is $\frac{1}{2}$, we know that the wave function is different from zero only if the spin points along the positive axis, so that m_s (the coordinate) is $\frac{1}{2}$; for $m_s = -\frac{1}{2}$, there is no wave function. Thus $u(\frac{1}{2}/\frac{1}{2})=1$, $u(\frac{1}{2}/-\frac{1}{2})=0$. We can then write $u(\frac{1}{2}/m_s)=\delta(\frac{1}{2}/m_s)$. Similarly $u(-\frac{1}{2}/m_s)=\delta(-\frac{1}{2}/m_s)$; and we can write the whole symbolically as $u(m_s/m_s)=\delta(m_s/m_s)$. We now have

$$u(n\,l\,m_l\,m_s/x\;y\;z\;m_s) = u(n\,l\,m_l/x\;y\;z)\delta(m_s/m_s).$$

And for the first factor, the equation is

$$H_1 u(n\,l\,m_l/x\;y\;z)=\epsilon(n\,l)u(n\,l\,m_l/x\;y\;z),$$

where, since the energy does not depend on m_l or m_s, we have left out those quantum numbers in describing ϵ.

The solution of the central field problem is well known. We separate variables in spherical coordinates $r\,\theta\,\phi$. Then we have

$$u(n\,l\,m_l/x\;y\;z)=R(n\,l/r)\Theta(l\,m_l/\theta)\Phi(m_l/\phi)$$

where

$$\Theta(l\,m_l/\theta)=\left[\frac{(2l+1)(l-|m_l|)!}{(l+|m_l|)!}\right]^{1/2} P_l^{|m_l|}(\cos\theta)$$

where

$$P_l^{|m_l|}(\cos\theta)=\frac{1}{2^l l!}\sin^{|m_l|}\theta\frac{d^{|m_l|+l}(-\sin^2\theta)^l}{d(\cos\theta)^{|m_l|+l}}$$

and

$$\Phi(m_l/\phi)=e^{im_l\phi}/(2\pi)^{1/2}.$$

Thus we have

$$u(n\,l\,m_l\,m_s/x\;y\;z\;m_s)=R(n\,l/r)\Theta(l\,m_l/\theta)\Phi(m_l/\phi)\delta(m_s/m_s).$$

To proceed further, we must investigate the value of H operating on the product of u's. By definition,

$$H=-\frac{h^2}{8\pi^2 m}\sum_{i=1}^{N}\left(\frac{\partial^2}{\partial x_i^2}+\frac{\partial^2}{\partial y_i^2}+\frac{\partial^2}{\partial z_i^2}\right)+V,$$

where V is the potential energy, given by

$$V=\sum_{i=1}^{N}\left(-\frac{Ze^2}{r_i}\right)+\sum_{1}^{N}(i>j)\frac{e^2}{r_{ij}},$$

where r_i is the distance of the ith electron from the nucleus, r_{ij} the distance between the ith and jth electrons. Thus we have

$$Hu(n_1/x_1)\cdots u(n_N/x_N)=-\frac{h^2}{8\pi^2 m}\left(\frac{\partial^2 u(n_1/x_1)}{\partial x_1^2}+\frac{\partial^2 u(n_1/x_1)}{\partial y_1^2}\right.$$
$$\left.+\frac{\partial^2 u(n_1/x_1)}{\partial z_1^2}\right)u(n_2/x_2)\cdots u(n_N/x_N)\cdots+Vu(n_1/x_1)\cdots u(n_N/x_N).$$

But by our assumptions,

$$\frac{-h^2}{8\pi^2 m}\left(\frac{\partial^2 u(n_1/x_1)}{\partial x_1^2}+\frac{\partial^2 u(n_1/x_1)}{\partial y_1^2}+\frac{\partial^2 u(n_1/x_1)}{\partial z_1^2}\right)=(\epsilon(n_1)-U(x_1))u(n_1/x_1),$$

etc. Thus we are left with

$$Hu(n_1/x_1)\cdots u(n_N/x_N)=\left[\sum_{i=1}^{N}(\epsilon(n_i)-U(x_i))+V\right]u(n_1/x_1)\cdots u(n_N/x_N).$$

This is of the form used above: Constant$+\sum H(x)+\sum e^2/r$, where constant $=\sum(n)\epsilon(n)$, and $H(x)=-U(x)-Ze^2/r$.

We are now ready to compute the integrals I, J, and K. We must first note that by integrating over the coordinates of one electron, we really mean integrating over the $dx\,dy\,dz$, and summing over the spins:

$$\int dv\equiv\sum_{-1/2}^{1/2}(m_s)\int dxdydz.$$

Thus, for example, we have the normalization and orthogonality of the individual wave functions:

$$\int u^*(n'/x)u(n''/x)$$
$$\equiv\sum_{-1/2}^{1/2}(m_s)\delta(m_s'/m_s)\delta(m_s''/m_s)$$
$$\int u^*(n'l'm_l'/xyz)u(n''l''m_l''/xyz)dxdydz$$
$$=\delta(m_s'/m_s'')\delta(n'l'm_l'/n''l''m_l'').$$

This orthogonality is all that is needed in the proofs of the preceding paragraphs.

For the integral I, we have

$$I(nlm_lm_s)=\sum_{-1/2}^{1/2}(m_s)\delta(m_s/m_s)\delta(m_s/m_s)$$
$$\int u^*(nlm_l/xyz)H(xyz)u(nlm_l/xyz)dxdydz.$$

The summation over m_s merely reduces to the factor unity, independent of m_s. When we insert the value of $H(xyz)$, we note that the result is also

independent of m_l; for H is a function of r only, the functions of angles integrate to unity, and we are left with

$$I(nlm_lm_s)=I(nl)=-\int R^2(nl/r)(U(r)+Ze^2/r)4\pi r^2dr.$$

Next we are to find J and K. For J, we have

$$J(nlm_lm_s;n'l'm_l'm_s')$$
$$=\sum_{-1/2}^{1/2}(m_s)_k\sum_{-1/2}^{1/2}(m_s)_l\ \delta(m_s/(m_s)_k)\delta(m_s'/(m_s)_l)\delta(m_s/(m_s)_k)\delta(m_s'/(m_s)_l)$$
$$\int u^*(nlm_l/x_ky_kz_k)u^*(n'l'm_l'/x_ly_lz_l)e^2/r_{kl}u(nlm_l/x_ky_kz_k)u(n'l'm_l'/x_ly_lz_l)$$
$$dx_kdy_kdz_kdx_ldy_ldz_l.$$

The summation again reduces to unity, independent of m_s and m_s'. Then our quantity reduces to the integral, which we can write

$$J(nlm_lm_s;n'l'm_l'm_s')=J(nlm_l;n'l'm_l').$$

Similarly we have

$$K(nlm_lm_s;n'l'm_l'm_s')$$
$$=\sum_{-1/2}^{1/2}(m_s)_k\sum_{-1/2}^{1/2}(m_s)_l\ \delta(m_s/(m_s)_l)\delta(m_s'/(m_s)_k)\delta(m_s/(m_s)_k)\delta(m_s'/(m_s)_l)$$
$$\int u^*(nlm_l/x_ly_lz_l)u^*(n'l'm_l'/x_ky_kz_k)e^2/r_{kl}u(nlm_l/x_ky_kz_k)u(n'l'm_l'/x_ly_lz_l)$$
$$dx_kdy_kdz_kdx_ldy_ldz_l.$$

The summation reduces to $\delta(m_s/m_s')$; so that we are left with

$$K(nlm_lm_s;n'l'm_l'm_s')=\delta(m_s/m_s')K(nlm_l;n'l'm_l'),$$

where the integral is symbolized by the last K. We thus observe that these exchange integrals only exist for electrons with spins parallel to each other.

We are now to compute

$$J(nlm_l;n'l'm_l')$$

and

$$K(nlm_l;n'l'm_l')$$

We recall the expression for u previously given. Also we use the familiar expansion

$$\frac{1}{r(xx')}=\sum(k,m)\frac{(k-|m|)!}{(k+|m|)!}\frac{r(a)^k}{r(b)^{k+1}}P_k^{|m|}(\cos\theta)P_k^{|m|}(\cos\theta')\exp(im(\phi-\phi'))$$

where $r(xx')$ is the distance between (xyz) and $(x'y'z')$, and where $r(a)$ is the smaller, $r(b)$ the greater, of r and r'. Forming the expression for J, we have integrals of the form $\int_0^{2\pi}\exp(im\phi)d\phi$ which vanish unless $m=0$.

The double sum over k and m thus reduces to a single one over k, m being always zero. Then we easily have

$$J(nlm_l;n'l'm_l') = \sum(k)a^k(lm_l;l'm_l')F^k(nl;n'l')$$

where

$$a^k(lm_l;l'm_l') = \frac{(2l+1)(l-|m_l|)!}{(l+|m_l|)!}\frac{(2l'+1)(l'-|m_l'|)!}{(l'+|m_l'|)!}$$
$$\int_0^\pi [P_l^{|m_l|}(\cos\theta)]^2 P_k^0(\cos\theta)\frac{\sin\theta}{2}d\theta$$
$$\int_0^\pi [P_{l'}^{|m'_l|}(\cos\theta')]^2 P_k^0(\cos\theta')\frac{\sin\theta'}{2}d\theta'$$

and

$$F^k(nl;n'l') = e^2(4\pi)^2\int_0^\infty\int_0^\infty R^2(nl/r)R^2(n'l'/r')\frac{r(a)^k}{r(b)^{k+1}}r^2r'^2drdr'.$$

One notes that the a's can be computed once for all, in terms of the spherical harmonics; the special properties of the atom in question appear only in the integrals F.

In a similar way we form K. Here the integrals over ϕ are of the form $\int_0^{2\pi}\exp i(m_l-m_l'+m)\phi\, d\phi$, vanishing unless $|m| = |m_l-m_l'|$. Thus we have

$$K(nlm_l;n'l'm_l') = \sum(k)b^k(lm_l;l'm_l')G^k(nl;n'l'),$$

where

$$b^k(lm_l;l'm_l') = \frac{(k-|m_l-m_l'|)!}{(k+|m_l-m_l'|)!}\frac{(2l+1)(l-|m_l|)!}{(l+|m_l|)!}\frac{(2l'+1)(l'-|m_l'|)!}{(l'+|m_l'|)!}$$
$$\left[\int_0^\pi P_l^{|m_l|}(\cos\theta)P_{l'}^{|m_l'|}(\cos\theta)P_k^{|m_l-m_l'|}(\cos\theta)\frac{\sin\theta}{2}d\theta\right]^2$$

and

$$G^k(nl;n'l') = e^2(4\pi)^2\int_0^\infty\int_0^\infty R(nl/r)R(n'l'/r)R(nl/r')R(n'l'/r')\frac{r(a)^k}{r(b)^{k+1}}r^2r'^2drdr'.$$

Using the values of the associated spherical harmonics one can compute the various a's and b's; although the writer has not succeeded in setting up closed formulas for them, since this would involve the integrals of products of three spherical harmonics, an unfamiliar form.[11] We give a table, including all the coefficients involved with s, p, d electrons (that is, $l, l' \leq 2$).

We have now obtained the diagonal term of energy which we desired: in section 2 we have found it in terms of certain integrals I, J, K, and in section 3 we have evaluated those integrals. Before passing to the examples, we should note one fact: that in finding the energy differences between multiplets, one needs only the integrals J and K, which do not depend

[11] See, however, J. A. Gaunt, l. c. Whether one has formulas or not, the table of values is certainly most convenient for computation.

TABLE OF $a^k(lm_l; l'm_l')$.
(Note: in cases with two ± signs, the two can be combined in any of the four possible ways).

Electrons	l	m_l	l'	m_l'	$k=0$	2	4
ss	0	0	0	0	1	0	0
sp	0	0	1	±1	1	0	0
	0	0	1	0	1	0	0
pp	1	±1	1	±1	1	1/25	0
	1	±1	1	0	1	−2/25	0
	1	0	1	0	1	4/25	0
sd	0	0	2	±2	1	0	0
	0	0	2	±1	1	0	0
	0	0	2	0	1	0	0
pd	1	±1	2	±2	1	2/35	0
	1	±1	2	±1	1	−1/35	0
	1	±1	2	0	1	−2/35	0
	1	0	2	±2	1	−4/35	0
	1	0	2	±1	1	2/35	0
	1	0	2	0	1	4/35	0
dd	2	±2	2	±2	1	4/49	1/441
	2	±2	2	±1	1	−2/49	− 4/441
	2	±2	2	0	1	−4/49	6/441
	2	±1	2	±1	1	1/49	16/441
	2	±1	2	0	1	2/49	−24/441
	2	0	2	0	1	4/49	36/441

TABLE OF $b^k(lm_l; l'm_l')$
(Note: in cases where there are two ± signs, the two upper, or the two lower, signs must be taken together).

Electrons	l	m_l	l'	m_l'	$k=0$	1	2	3	4
ss	0	0	0	0	1	0	0	0	0
sp	0	0	1	±1	0	1/3	0	0	0
	0	0	1	0	0	1/3	0	0	0
pp	1	±1	1	±1	1	0	1/25	0	0
	1	±1	1	0	0	0	3/25	0	0
	1	±1	1	∓1	0	0	6/25	0	0
	1	0	1	0	1	0	4/25	0	0
sd	0	0	2	±2	0	0	1/5	0	0
	0	0	2	±1	0	0	1/5	0	0
	0	0	2	0	0	0	1/5	0	0
pd	1	±1	2	±2	0	2/5	0	3/245	0
	1	±1	2	±1	0	1/5	0	9/245	0
	1	±1	2	0	0	1/15	0	18/245	0
	1	±1	2	∓1	0	0	0	30/245	0
	1	±1	2	∓2	0	0	0	9/245	0
	1	0	2	±2	0	0	0	15/245	0
	1	0	2	±1	0	1/5	0	24/245	0
	1	0	2	0	0	4/15	0	27/245	0
dd	2	±2	2	±2	1	0	4/49	0	1/441
	2	±2	2	±1	0	0	6/49	0	5/441
	2	±2	2	0	0	0	4/49	0	15/441
	2	±2	2	∓1	0	0	0	0	35/441
	2	±2	2	∓2	0	0	0	0	70/441
	2	±1	2	±1	1	0	1/49	0	16/441
	2	±1	2	0	0	0	1/49	0	30/441
	2	±1	2	∓1	0	0	6/49	0	40/441
	2	0	2	0	1	0	4/49	0	36/441

explicitly on the central field U at all. The integral I is needed only in finding the center of gravity of a multiplet system. The reason is that I depends only on n and l, and so is the same for all the various degenerate states with which we start our perturbation problem.

4. *Examples. One electron outside closed shells.* We need take but one case: a $3p$ electron outside completed K and L shells. Thus the scheme of electrons is $(1s)^2(2s)^2(2p)^6 3p$. We must now consider the various antisymmetric wave functions which are possible. By the method of symbolization mentioned above, in which we group in separate brackets the quantum numbers of electrons with parallel and antiparallel spins, we see that there are six wave functions, which we give below, together with the values of $\sum m_l$ and $\sum m_s$:

	Σm_l	Σm_s
$\{(100)(200)(211)(210)(21-1)(311)\}$ $\{(100)(200)(211)(210)(21-1)\}$	1	$\frac{1}{2}$
$\{(100)(200)(211)(210)(21-1)(310)\}$ $\{(100)(200)(211)(210)(21-1)\}$	0	$\frac{1}{2}$
$\{(100)(200)(211)(210)(21-1)(31-1)\}\{(100)(200)(211)(210)(21-1)\}$	-1	$\frac{1}{2}$
$\{(100)(200)(211)(210)(21-1)\}$ $\{(100)(200)(211)(210)(21-1)(311)\}$	1	$-\frac{1}{2}$
$\{(100)(200)(211)(210)(21-1)\}$ $\{(100)(200)(211)(210)(21-1)(310)\}$	0	$-\frac{1}{2}$
$\{(100)(200)(211)(210)(21-1)\}$ $\{(100)(200)(211)(210)(21-1)(31-1)\}$	-1	$-\frac{1}{2}$

We note that the arrangement of $\sum m_l, \sum m_s$, is just that for a single multiplet ^2P. There are no cases in which more than one term has a given value of $\sum m_l, \sum m_s$; thus there is no need of applying the sum rule at all. The diagonal terms of the energy, computed with respect to these six wave functions, should give directly the energies of the six terms of the multiplet. But now we come back to our general principle; these six terms must have the same energy. We must actually compute the energies by our rules, and see that they are the same in each of the six functions. As has been mentioned before, we need only use the J and K terms. These terms, we recall, were $\sum(\text{pairs})J - \sum(\text{pairs with par. spins})K$. Now in these sums, many terms are the same for each of the six wave functions; all the terms, in fact, relating to pairs of electrons both in the closed shells. These terms can exert no influence on the multiplet separations, or anything of that sort. Thus we can leave them out, for our present purpose, as we left out the terms depending on the integrals I. The only terms we need retain are those in which our $3p$ electron is a member of the pairs. Thus for the first wave function we must compute the following:

$$2J(311;100)+2J(311;200)+2J(311;211)+2J(311;210)+2J(311;21-1)$$
$$-K(311;100)-K(311;200)-K(311;211)-K(311;210)-K(311;21-1).$$

For the second and third, we substitute respectively 310, 31-1 in place of 311; the fourth, fifth, and sixth evidently give the same three results already given. Let us now group these terms according to the shells that the $3p$'s interact with:

$$1s: 2J(311;100)-K(311;100)$$
$$2s: 2J(311;200)-K(311;200)$$
$$2p: 2J(311;211)+2J(311;210)+2J(311;21-1)-K(311;211)$$
$$-K(311;210)-K(311;21-1).$$

For the interaction with $1s$, we have

$$2J(311;100)=2\sum(k)a^k(11;00)F^k(31;10)=2F^0(31;10)$$
$$-K(311;100)=-\sum(k)b^k(11;00)G^k(31;10)=-\tfrac{1}{3}G^1(31;10).$$

Before going further, let us find the corresponding terms in the interaction of a 310 electron with the $1s$ shell:

$$2J(310;100)=2\sum(k)a^k(10;00)F^k(31;10)=2F^0(31;10)$$
$$-K(310;100)=-\sum(k)b^k(10;00)G^k(31;10)=-\tfrac{1}{3}G^1(31;10).$$

That is, the interaction integrals of an outer p electron with an s shell are the same whether the p electron has $m_l=1$ or 0 (or -1, as one immediately verifies). We shall show the same result to hold for the interaction with the $2p$ shell: for the (311) electron, the terms are

$$\begin{aligned}
&2J(311;211)+2J(311;210)+2J(311;21-1)-K(311;211)\\
&\quad -K(311;210)-K(311;21-1)\\
&=2\sum(k)a^k(11;11)F^k(31;21)+2\sum(k)a^k(11;10)F^k(31;21)\\
&\quad +2\sum(k)a^k(11;1-1)F^k(31;21)-\sum(k)b^k(11;11)G^k(31;21)\\
&\quad -\sum(k)b^k(11;10)G^k(31;21)-\sum(k)b^k(11;1-1)G^k(31;21)\\
&=2\sum(k)(a^k(11;11)+a^k(11;10)+a^k(11;1-1)F^k(31;21)\\
&\quad -\sum(k)(b^k(11;11)+b^k(11;10)+b^k(11;1-1))G^k(31;21)\\
&=6F^0(31;21)-G^0(31;21)-\tfrac{2}{5}G^2(31;21).
\end{aligned}$$

Similarly for the (310) electron interacting with the $2p$ shell, we have

$$\begin{aligned}
&2\sum(k)(a^k(10;11)+a^k(10;10)+a^k(10;1-1)F^k(31;21)\\
&\quad -\sum(k)(b^k(10;11)+b^k(10;10)+b^k(10;1-1))G^k(31;21)\\
&\quad =6F^0(31;21)-G^0(31;21)-\tfrac{2}{5}G^2(31;21).
\end{aligned}$$

This agrees with the former value, showing that the interaction of either a 311 or a 310 (or, by a simple extension, a 31–1) electron with a completed p shell, give the same result, independent of m_l. Putting all these results together, all six levels of the ^2P multiplet give the same energy, by direct computation. Of course, this is merely a check of our general theorem that all the levels of any multiplet must have the same energy. The special properties of the a's and b's which lead to this result could be proved by use of that theorem.

Any configuration outside closed shells. We have just seen that the interaction energy of a single electron with a closed shell is independent of the m_l of the outer electron. We have proved this by direct computation for a p electron interacting with s or p shells, but we could extend the result to the general case, from our general theorem that all the terms of any multiplet have the same energy. But this has an important bearing on our general problem. For in any case an atom consists of a certain number of electrons

outside closed shells, and the central closed shells. In the various unperturbed wave functions which we are to use, the outer electrons have different m_l's. In the energies of the terms, we are to compute all J's and K's connected with pairs of electrons in the atom. We have already seen that all pairs, both of which are in closed shells, will give identical contributions to each of the unperturbed terms. But now we can go further: all sets of pairs, in which one is an outer electron, the other one of the electrons of a closed shell, will, when summed over the electrons of the closed shell, give the same result for each unperturbed state. That is, as far as multiplet separations are concerned, closed shells exert no influence at all; they affect only the position of the whole set of multiplet terms. It is well known that the classification of the terms is independent of the existence of closed shells; this proves that the energy relations also depend only on the outer electrons.[12] For the rest of our examples, then, we shall consider only those electrons which are outside closed shells.

Two electrons outside closed shells, one in s state (helium, alkaline earths). Suppose we have the scheme (ns), $(n'p)$, for example. There are, in this case, the unperturbed wave functions symbolized by

	Σm_l	Σm_s
$\{(n\,0\,0)(n'\,1\,1)\}$	1	1
$\{(n\,0\,0)(n'\,1\,0)\}$	0	1
$\{(n\,0\,0)(n'\,1\,-1)\}$	−1	1
$\{(n\,0\,0)\}\{(n'\,1\,1)\}$	1	0
$\{(n\,0\,0)\}\{(n'\,1\,0)\}$	0	0
$\{(n\,0\,0)\}\{(n'\,1\,-1)\}$	−1	0
$\{(n'\,1\,1)\}\{(n\,0\,0)\}$	1	0
$\{(n'\,1\,0)\}\{(n\,0\,0)\}$	0	0
$\{(n'\,1\,-1)\}\{(n\,0\,0)\}$	−1	0
$\}\{(n\,0\,0)(n'\,1\,1)\}$	1	−1
$\}\{(n\,0\,0)(n'\,1\,0)\}$	0	−1
$\}\{(n\,0\,0)(n'\,1\,-1)\}$	−1	−1

By our general scheme of classification, we have a ^1P and ^3P term. The terms with $\sum m_l, \sum m_s$ equal respectively to (1 1), (0 1), (−1 1), (1 −1), (0 −1), (−1 −1), belong to the ^3P state. On the other hand, the remaining terms, as (1 0), are each degenerate. The sum of the energies of two such terms equals the sum of the ^1P and ^3P energy. Thus for example we have

$$^3P: \{(n\,0\,0)(n'\,1\,1)\}$$

$$^3P + {}^1P: \{(n\,0\,0)\}\{(n'\,1\,1)\} + \{(n'\,1\,1)\}\{(n\,0\,0)\} = 2\{(n\,0\,0)\}\{(n'\,1\,1)\}.$$

That is, for the energies, we have

$$^3P: J(n\,0\,0; n'\,1\,1) - K(n\,0\,0; n'1\,1)$$

$$^3P + {}^1P = 2J(n\,0\,0; n'\,1\,1).$$

Therefore $^1P = J(n\,0\,0; n'\,1\,1) + K(n\,0\,0; n'\,1\,1)$

The singlet and triplet are thus given by a definite value $\pm K(n\,0\,0; n'\,1\,1)$. This checks with Heisenberg's[13] calculation of this case; our integral K is readily seen to be the same exchange integral which he computes.

[12] See W. Heitler, Zeits. f. Physik **46**, 70 (1928).

[13] W. Heisenberg, Zeits. f. Physik **39**, 499 (1926).

Shell of equivalent p electrons. (Elements C, N, O, F, etc.) p^2. This is the case shown in Fig. 1c. There are 15 wave functions, of which we give those with $\sum m_l \geq 0, \sum m_s \geq 0$; for simplicity we omit the total quantum number from our descriptions, so that (1 0), for example, stands for (n 1 0). Then, correlating the $\sum m_l$, $\sum m_s$ with the multiplets represented (from the figure), we have

Multiplet	M_l	M_s	Wave function
^1D	2	0	$\{(1\ 1)\}$ $\{(1\ 1)\}$
$^1D+{}^3P$	1	0	$\{(1\ 0)\}$ $\{(1\ 1)\}$
	1	0	$\{(1\ 1)\}$ $\{(1\ 0)\}$
$^1D+{}^3P+{}^1S$	0	0	$\{(1\ 1)\}$ $\{(1\ -1)\}$
	0	0	$\{(1\ 0)\}$ $\{(1\ 0)\}$
	0	0	$\{(1\ -1)\}$ $\{(1\ 1)\}$
^3P	1	1	$\{(1\ 1)\ (1\ 0)\}$ $\{\ \}$
^3P	0	1	$\{(1\ 1)\ (1\ -1)\}$ $\{\ \}$

Now we have for the energies

$$^1D: J(n\,1\,1; n\,1\,1) = F^0(n\,1;\,n\,1) + \frac{1}{25}F^2(n\,1; n\,1)$$

$$^3P: J(n\,1\,1; n\,1\,0) - K(n\,1\,1; n\,1\,0) = F^0(n\,1; n\,1) - \frac{2}{25}F^2(n\,1; n\,1) - \frac{3}{25}G^2(n\,1; n\,1)$$

We note that, for equivalent electrons, the F's and G's of the same indices are equal. Hence

$$^3P = F^0(n\,1; n\,1) - \frac{5}{25}F^2(n\,1; n\,1).$$

We can check the same value from the other ^3P term ($\Sigma m_l = 0$, $\Sigma m_s = 1$) and from the two terms giving $^1D + {}^3P$. Finally we have

$$^1D+{}^3P+{}^1S: J(n\,1\,1; n\,1\,-1) + J(n\,1\,0; n\,1\,0) + J(n\,1\,-1; n\,1\,1)$$
$$= 3F^0(n\,1; n\,1) + \frac{6}{25}F^2(n\,1; n\,1).$$

Therefore $^1S = F^0(n\,1; n\,1) + \frac{10}{25}F^2(n\,1; n\,1)$.

We note that the term $F^0(n\ 1;\ n\ 1)$ is common to all the levels; thus we can leave it out, as we have all the terms which do not affect the separation. We note from its definition that $F^2(n\ 1;\ n\ 1)$ is positive. Thus we see that of the three multiplets, the ^3P lies lowest, ^1D next, ^1S highest, in accordance with Hund's rule that the terms of largest L and S lie lowest. The separations are in a simple ratio: $^3P - {}^1D = 6/25\ F^2(n\ 1;\ n\ 1)$, and $^1D - {}^1S = 9/25\ F^2(n\ 1;\ n\ 1)$ so that the ratio is 2 to 3.

We should find an example in the lowest levels of C, $(1s)^2\ (2s)^2\ (2p)^2$; these levels, however, have not been observed, as far as the writer knows. For Si $(1s)^2\ (2s)^2\ (2p)^6\ (3s)^2\ (3p)^2$, however, the term values are[14] $^3P = 65{,}615$,

[14] McLennan and Shaver, Roy. Soc. Canada **18**, 1, (1924). A. Fowler, Proc. Roy. Soc. **A123**, 422 (1929).

$^1D = 59{,}466$, $^1S = 50{,}370$, giving $^3P - {}^1D = 6149$, $^1D - {}^1S = 9096$, the first giving $F^2(3\,1;\,3\,1) = 25{,}602$, the second $F^2(3\,1;\,3\,1) = 25{,}267$, in good agreement.

p^3. The method is so similar to that used for p^2 that the calculations need not be given in detail. The multiplets are $^4S\ ^2D\ ^2P$, the ^4S lying lowest and ^2P highest, again in agreement with Hund's rule. The separations are given by $^4S - {}^2D = 9/25\ F^2(n\,1;\,n\,1)$ $^2D - {}^2P = 6/25\ F^2(n\,1;\,n\,1)$. An example is found in the normal N spectrum, $(1s)^2\ (2s)^2\ (2p)^3$, observed by Compton and Boyce.[15] They find $^4S = 117{,}345$, $^2D = 98{,}143$, $^2P = 88{,}537$, giving $^4S - {}^2D = 19{,}200$, $^2D - {}^2P = 9{,}600$. From the first, $F^2(2\,1;\,2\,1) = 53{,}400$, and from the second, it is 40,000; a somewhat poorer agreement than before, probably on account of the tighter binding of the electrons.

p^4. Here the relations prove to be as in p^2 as regards energy, as well as in the arrangement of terms: $^3P - {}^1D = 6/25\ F^2(n\,1;\,n\,1)$ $^1D - {}^1S = 9/25\ F^2(n\,1;\,n\,1)$. An example is normal O, $(1s)^2\ (2s)^2\ (2p)^4$. Here it is estimated[16] that, counting terms up from ^3P as zero, $^1D = 25{,}500$, and $^1S = 65{,}000$, giving $^3P - {}^1D = 25{,}500$, $^1D - {}^1S = 39{,}500$. From the first, $F^2(2\,1;\,2\,1) = 106{,}000$, and from the second 109,700, a very good agreement. It is interesting to note the increase in the integral from N to O on account of the tighter binding.

p^5 and p^6 yield each only one multiplet, so that they need not be considered.

Shell of equivalent d electrons (Iron group) d^2. The multiplets are $^3F\ ^3P\ ^1G\ ^1D\ ^1S$. When we work out the separations, however, it appears that they are not arranged in this order; the singlet terms are anomalous, disobeying Hund's rule, in that the ^1D lies lower than ^1G. Except for this, however, the arrangement is as we should expect, ^3F lying below ^3P, and being the lowest term of the combination. The separations are given by

$$^3F - {}^3P = (135/441)\ F^2(n\,2;\,n\,2) - (75/441)\ F^4(n\,2;\,n\,2)$$
$$^3F - {}^1G = (108/441)\ F^2(n\,2;\,n\,2) + (10/441)\ F^4(n\,2;\,n\,2)$$
$$^3F - {}^1D = (45/441)\ F^2(n\,2;\,n\,2) + (45/441)\ F^4(n\,2;\,n\,2)$$
$$^3F - {}^1S = (198/441)\ F^2(n\,2;\,n\,2) + (135/441)\ F^4(n\,2;\,n\,2)$$

The separations now depend on the two parameters $F^2(n\,2;\,n\,2)$ and $F^4(n\,2;\,n\,2)$, which bear no fixed relation to each other. Nevertheless we can estimate their relative magnitude. For by definition F^k is the integral of a certain function of r_1 and r_2, multiplied by r_a^k/r_b^{k+1} where r_b is the greater, r_a the less, of r_1 and r_2. Thus increasing k necessarily decreases the integrand, and hence the function F: $F^4(n\,2;\,n\,2) < F^2(n2\ ;\,n\,2)$. Rough calculation indicates that the decrease is about to a half. If then we provisionally take F^4 to be half of F^2, we have the separations in the ratio

$$^3F - {}^3P: 135 - 37 = 98 \qquad ^3F - {}^1D: 45 + 22 = 67$$
$$^3F - {}^1G: 108 + 5 = 113 \qquad ^3F - {}^1S: 198 + 67 = 265.$$

The order of terms is thus expected to be $^3F\ ^1D\ ^3P\ ^1G\ ^1S$.

[15] K. T. Compton and J. C. Boyce, Phys. Rev. **33**, 145 (1929).

[16] McLennan, McLeod, and Ruedy, Phil. Mag. Sept., 1928, p. 558. These values are estimated from the energy level diagram in that paper.

Experimentally we find an example in the normal spectrum of Ti,[17] $(1s)^2\ (2s)^2\ (2p)^6\ (3s)^2\ (3p)^6\ (4s)^2\ (3d)^2$. Here the order of terms is in fact just what our calculation predicts, the exception to Hund's rule being found experimentally. The observed separations are approximately

$$^3F-{}^3P=\ 8500 \qquad {}^3F-{}^1D=\ 7200$$

$$^3F-{}^1G=12100 \qquad {}^3F-{}^1S=15100.$$

If we assume that F^4 is really half of F^2, these give $F^2(n\ 2;\ n\ 2)$ equal respectively to 38,000, 47,000, 41,000, 72,000, in fair agreement except for the last one. This last results from the ^1S, which is not nearly so far above the rest of the terms as the theory would indicate—probably because the second order corrections for this term would be large, and would have the effect of depressing it. The agreement with observations can be somewhat, but not much, improved by taking a slightly different ratio of F^4 to F^2.

$d^3..d^8$. We shall give only the lowest terms for the rest of the d shell. The terms of highest multiplicity prove to lie in general lower than the others, as the rule would predict. Of these, we have for d^3: $^4F\ ^4P$; d^4, ^5D; d^5, ^6S; d^6, ^5D; d^7, $^4F\ ^4P$; d^8, $^3F\ ^3P$. Evidently the only cases where there are significant separations in the multiplets of highest multiplicity are the $d^2\ d^3\ d^7\ d^8$ F–P separations. When one calculates, one discovers the fact that all these are given by the same formula, $(135/441)F^2(n\ 2;\ n\ 2)-(75/441)F^4(n\ 2;\ n\ 2)$. This permits an interesting comparison with experiment: we can compare the observed separations for Ti (d^2), V(d^3), Co(d^7) and Ni (d^8). We should expect these to increase regularly with the number of d electrons. Experimentally this separation is about 8000 for Ti, 9500 for V, 14000 for Co, 15000 for Ni, indicating a fairly uniform increase of about 1000 to 1500 for the addition of one d electron.

Non-equivalent p's: Two *p's*: pp'. The multiplets are $^3D\ ^3P\ ^3S\ ^1D\ ^1P\ ^1S$. The triplets are particularly interesting, and we give their separations. If the principal quantum numbers of the electrons are n and n', they are

$$^3D-{}^3P=-6/25F^2(n\ 1;n'\ 1)+2G^0(n\ 1;n'\ 1)-4/25G^2(n\ 1;n'\ 1)$$

$$^3D-{}^3S=9/25F^2(n\ 1;n'\ 1)-9/25G^2(n\ 1;n'\ 1).$$

The significant feature of these results is that they depend in such a complicated way on several integrals. That is, in a case like this— and it is the simplest set of multiplets that can be built up from non-equivalent electrons—we must not look for simple numerical relations between the separations, or even for a definite, fixed order for the terms. We may rather expect that, as we go from one element to another, the relative order of terms can change.

We find an example in N^+ $(1s)^2\ (2s)^2\ 2p\ 3p$.[18] Here the experimental separations are approximately $^3D-{}^3P=4000$ $^3D-{}^3S=2300$, disobeying Hund's rule, in that ^3S lies below ^3P. We can make from these figures a rough estimate of the integrals F and G. We note that G differs from F in having

[17] H. N. Russell, Astroph. Jour. **66**, 283 (1927).

[18] A. Fowler, Proc. Roy. Soc. **A107**, 31 (1925).

the product $R(n/x_1)\ R(n'/x_1)$ in its integrand instead of $R^2(n/x_1)$. The first is less than the second—very much less if the orbits n and n' are of decidedly different size, for then either $R(n/x_1)$ or $R(n'/x_1)$ will be small through most of the range of x_1. Thus each G integral is small compared to the corresponding F. It is reasonable to suppose that G^0 is of the same order of magnitude as F^2. Further, G^2 will be smaller than G^0, by analogy with what we have already seen, and as a rough assumption we may take $G^2=\frac{1}{2}\ G^0$. Thus we have the two equations

$$4000=-(6/25)F^2+(48/25)G^0$$
$$2300=(9/25)F^2-(9/50)G^0,$$

giving $F^2(2\,1;3\,1)=7900$, $G^0(2\,1;3\,1)=3070$, $G^2(2\,1;3\,1)=1535$.
These values are reasonable, but provide no definite check for the equations.

Five equivalent p's, one other p: p^5p'. Again we have $^3D\,^3P\,^3S\ ^1D\ ^1P\ ^1S$, by combination of the p' with the ^2P of p^5. But now it proves that the triplet separations are quite different, and have a much simpler formula. We have

$$^3D-{}^3P=(6/25)F^2(n\,1;n'\,1)$$
$$^3D-{}^3S=-(9/25)F^2(n\,1;n'\,1)$$

depending on only one parameter (the others all cancel out, seemingly, although perhaps not really, by chance). Thus we can predict definitely the order of terms: ^3S lies lowest, then ^3D, finally ^3P, in direct contradiction to Hund's rule. We find an example, however, in Ne $(1s)^2\ (2s)^2\ (2p)^5\ 3p$, Paschen's p terms,[19] and it definitely verifies the contradiction. Experimentally, Paschen's $2p_{10}$, which is the ^3S, lies well below any others. On account of the wide multiplet separations it is impossible to show any good check of the ratio 2:3 for the $^3D-{}^3P$ and $^3D-{}^3S$ separations. If one takes centers of gravity of Paschen's terms, one finds

$$^3D-{}^3P=570 \qquad ^3D-{}^3S=-2023$$

the first giving $F^2(2\,1;\,3\,1)=2370$, the second 5620. The correct figure is probably between these. It is interesting to note the agreement as to order of magnitude of this with the same one, 7900, for N^+.

Notes

1. We wish to prove that the energy has no matrix components (taken with reference to the incorrect, approximate wave functions) connected with transitions in which $\sum m_l$ or $\sum m_s$ changes. The essential part of the proof is the demonstration that the energy operator H commutes with the operators connected with $\sum m_l$ or $\sum m_s$. For $\sum m_s$ the proof is obvious: $\sum m_s$ is a quantity depending only on the spins, H only on the coordinates, and operators depending on entirely independent quantities always commute. For $\sum m_l$, the essential point is that $\sum m_l$ is the operator connected with an infinitesimal rotation of space about the z axis, and on account of the fact that H is in-

[19] F. Paschen, Ann. d. Physik **60**, 405 (1920).

dependent of orientation, such a rotation does not affect it, and so commutes with it. To be more specific, one can write the three components of angular momentum of an electron in operator form, using the operators for linear momentum. Put in spherical coordinates, the z component of angular momentum is represented by the operator $(h/2\pi i)\partial/\partial\phi$. Operating on a single electron wave function with the factor $e^{im_l\phi}$, this operator reduces to the multiplication by $m_l h/2\pi$, so that it has a diagonal matrix, and m_l measures the z component of angular momentum, in units $h/2\pi$. Then the operator connected with $\sum m_l$ is $-i\sum\partial/\partial\phi$, where the sum is over the ϕ's of the various electrons in the many-electron wave function; this operator is in the many electron problem again a diagonal matrix. This holds, we note, even with the incorrect, unperturbed wave functions. Except for the factor $-i$, this operator simply represents the change in the function it operates on, if all φ's are increased by the same amount; that is, if the whole electronic system is rotated rigidly. Then we have

$$\left(-i\sum\frac{\partial}{\partial\phi}\right)Hu=-i\sum\frac{\partial H}{\partial\phi}u-iH\sum\frac{\partial}{\partial\phi}u.$$

But on account of its spherical symmetry, $\Sigma\partial H/\partial\phi=0$. Hence

$$\left(-i\sum\frac{\partial}{\partial\phi}\right)Hu=H\left(-i\sum\frac{\partial}{\partial\phi}\right)u, \quad \text{or}$$

$$(\sum m_l)H-H(\sum m_l)=0,$$

showing that the operator $\sum m_l$ commutes with H.

Knowing that both $\sum m_l$ and $\sum m_s$ commute with H, and that both have diagonal matrices, the rest of the proof is simple. We merely write down the commutation laws in matrix form:

$$\sum(n'')\sum m_l(n'/n'')H(n''/n''')-H(n'/n'')\sum m_l(n''/n''')=0.$$

On account of the diagonal relation, this amounts to

$$(\sum m_l(n'/n')-\sum m_l(n'''/n'''))H(n'/n''')=0.$$

This cannot be satisfied unless either $\sum m_l(n'/n')=\sum m_l(n'''/n''')$ or unless $H(n'/n''')=0$; that is, H has matrix components different from zero only if $\sum m_l$ has the same values in initial and final states. The same proof holds for $\sum m_s$.

2. *Theorems regarding angular momentum.* It is assumed that we have wave functions which, although not exact, are the good approximations used in this paper; that is, linear combinations have been made so that the energy matrix has components different from zero only between states of decidedly different energy; it is diagonal as far as the states are concerned which come from one set of electron quantum numbers. We wish to show first that matrix components of angular momentum have non-negligible components only between states of the same energy (or diagonal term of the energy matrix). Suppose we let the operators connected with the three com-

ponents of orbital angular momentum be M_L^x, M_L^y, M_L^z, where M_L^z is the quantity usually denoted by M_L, and is equal to $\sum m_l$. Similarly for spin we have M_S^x, M_S^y, M_S^z. Now we have seen that M_L^z and M_S^z commute with H; and, since there is nothing peculiar about the z axis, we can equally well show that M_L^x, M_L^y, M_S^x, M_S^y commute with H. Thus for example $M_S^x H - H M_S^x = 0$, or in matrix form

$$\sum(n'')M_S^x(n'/n'')H(n''/n''') - H(n'/n'')M_S^x(n''/n''') = 0.$$

We can write this, for non-diagonal terms,

$$M_S^x(n'/n''')[H(n'''/n''') - H(n'/n')]$$
$$= -\sum(n'' \neq n', n''')[M_S^x(n'/n'')H(n''/n''') - H(n'/n'')M_S^x(n''/n''')].$$

The non-diagonal terms of the energy, $H(n''/n''')$, etc., are by hypothesis different from zero only if n'' and n''' refer to states with different electron quantum numbers, and even so they are small of the first order. If the right side were precisely zero, we should have obviously the result that $M_S^x(n'/n''')$ was different from zero only if $H(n'''/n''')$ was equal to $H(n'/n')$ which is what we wished to show. As it is, this result is true only to the first order of small quantities: M_S^x can have other, small components, and $H(n'''/n''')$ can differ from $H(n'/n')$ by small quantities. Thus we should expect that our approximate wave functions for a multiplet would give only approximately equal energies. This is not true, however, when we actually calculate by our method; the energies are precisely equal. The reason can be easily seen. Let the states n' and n''' be both connected with the same electron quantum number. Then the matrix components on the left side of the equation above are all found in terms of integrals over wave functions of those particular electron quantum numbers. The matrices on the right, however, involve other states, n'', which must refer to different electron quantum numbers, so that the right side would involve different, independent integrals. The two sides could not be in general equal unless each was zero. Hence the result is: if the approximate wave functions are computed by our method, the angular momentum has components, between two states of the same electron quantum numbers, only if both states have the same energy. Its components between states of different electron quantum number are small of the first order. From now on, we can neglect the latter terms, as we did with the energy. Thus the matrix of the angular momentum is of the form shown in Fig. 5. This can be compared with Fig. 3, showing the matrix of the energy in the final wave functions; but Fig. 3 should now be numbered to show that the diagonal terms of energy within one of the small squares of Fig. 5 (that is, in a multiplet) are all equal.

We have shown that the wave functions connected with a set of n's and l's are divided into groups, each wave function of a group having the same energy value, and the angular momentum having components only between different wave functions of a group, not from one group to another. We wish now to show that the matrix components of angular momentum within such a group are really such as to indicate a vector of magnitude L, and

another S. To do this, we first note that M_{L^x}, M_{L^y}, M_{L^z}, M_{S^x}, M_{S^y}, M_{S^z} satisfy the commutation relations

$$M_{L^y}M_{L^z}-M_{L^z}M_{L^y}=-\frac{h}{2\pi i}M_{L^x},\ \text{etc.},$$

$$M_{S^y}M_{S^z}-M_{S^z}M_{S^y}=-\frac{h}{2\pi i}M_{S^x},\ \text{etc.},$$

$$M_{L^x}M_{S^x}-M_{S^x}M_{L^x}=0,\ \text{etc.}$$

We show these by proving them for the separate m_l's and m_s's of the separate electrons, and then combining by the relations $M_{L^x}=\sum m_{l^x}$, etc. For the separate electrons, the results for the m_l's are well known; for the m_s's, the results come directly from Pauli's theory of the electron spin. We also note; that M_{L^z} and M_{S^z} have diagonal matrices, with diagonal values M_L and M_S (in units of $h/2\pi$). Now it can be proved[20] that if we have a set of matrices related by the commutation rules $M_{L^y}M_{L^z}-M_{L^z}M_{L^y}=-(h/2\pi i)M_{L^x}$, etc.; if these have components only between a limited set of statesand if M_{L^z} forms a diagonal matrix; then the whole matrix is uniquely determined, except for a phase constant; further, M_{L^z} must have integral, or half integral, characteristic values M_L, ranging from a value $-L$ to L; the states can be described by the values of M_L, so that can be taken as a quantum number. Then the matrix components prove to be given by

$$M_{L^x}(M_L/(M_L+1))M_{L^x}((M_L+1)/M_L)=\frac{1}{4}\left(\frac{h}{2\pi}\right)^2[L(L+1)-M_L(M_L+1)]\cdots$$

$$M_{L^z}(M_L/M_L)=M_L$$

$$[(M_{L^x})^2+(M_{L^y})^2+(M_{L^z})^2](M_L/M_{L'})=\left(\frac{h}{2\pi}\right)^2L(L+1)\delta(M_L/M_{L'}).$$

Such a set of matrix components is the unique description of a vector L, in its $(2L+1)$ possible orientations. Similar results apply to M_S.

In our case, these relations lead immediately to the following results. In the first place, the M_{L^x}'s depend only on orbital coordinates, the M_{S^x}'s only on spins. Thus the M_{L^x}'s can have components only between two wave functions in which the spin appears in the same way (and which thus have the same M_S). Similarly M_{S^x}'s can have components only between states of the same M_L. Therefore for each M_S there are a number of states of the multiplet, with different M_L's and having matrix components of the M_{L^x}'s between them as given above. These different sets of states, on the other hand, can differ only in the spin function, so that the components of M_{L^x}'s are the same for each set with each M_S. Similarly, for each M_L, there are a number of states, with different spin functions but with the same orbital functions, different M_S's, and components of M_{S^x}'s just as above. The result is an array of terms which can be plotted in precisely the rectangular form used in the paper, and corresponding to the $(2L+1)$ orientations of the vector L, combined with the $(2S+1)$ orientations of S.

[20] Born, Heisenberg, and Jordan, Zeits. f. Physik **35**, 557 (1926).

PHENOMENA IN OXIDE COATED FILAMENTS

By Joseph A. Becker
Bell Telephone Laboratories, 463 West Street, New York, N. Y.

(Received October 4, 1929)

Abstract

A theory of the changes in activity in oxide coated filaments is proposed. From a comparison of the behavior of these filaments and filaments with composite surfaces such as thorium on tungsten, caesium on tungsten, and caesium on oxygen on tungsten it appears probable that oxide coated filaments owe their high activity to adsorbed metallic barium. The changes in emission from a coated filament produced by changes in plate potential and by currents sent into or drawn from it, are ascribed to electrolysis of the oxide. When electrons are sent into a coated filament barium is deposited on the surface and the activity increases until an optimum is reached beyond which the activity decreases. When current is drawn from the oxide, oxygen is deposited on the surface. If the oxygen is beneath the adsorbed barium, it increases the activity; if it is above the barium, it decreases the activity. Both barium and oxygen diffuse readily from the surface into the oxide and vice versa. This theory is tested, confirmed, and extended by numerous experiments.

An experimental technique is employed by which relative rates of evaporation of small amounts of electropositive and electronegative materials can be determined with considerable precision. The same technique might be useful in a number of similar investigations. Metallic barium or oxygen which evaporate from a coated filament are allowed to deposit on one side of a flat tungsten ribbon whose thermionic activity is followed. When the plausible assumption is made that an optimum activity is obtained when the tungsten is covered with a single layer of electropositive material, the relative rates of evaporation can be converted to absolute rates. This technique is also employed to determine the factors which control the evaporation of oxygen from a coated filament.

Experimental results.—(1) *Metallic barium evaporates* from a well broken down coated filament provided that the temperature is not too high and that no appreciable currents are drawn. (2) *Oxygen evaporates* if an emission limited current is drawn and the temperature is high enough. (3) *Metallic barium* which is deposited on the surface of the oxide either by electrolysis or by evaporation from an outside source, *produces changes in activity* of the same sort as are produced by barium on tungsten. (4) *Barium or oxygen diffuse* readily to and from the surface of the oxide (5) *Oxygen* brought to the surface of the oxide by drawing current from it, *increases* the *activity* under some circumstances *and decreases it* under others. (6) *Most of the current through the oxide is carried by electrons* but a small part is carried by ions; the ratio depends upon the temperature, the composition of the oxide, and the plate potential. It appears that *the conductivity of the oxide does not obey Ohm's law* and that some of the conductivity is due to a diffusion current which may flow against an opposing field. (7) *The complex time changes* that occur in coated filaments *are described* in a systematic manner.

Introduction

A METALLIC filament which is covered with one or more of the oxides of calcium, strontium, or barium is called an oxide coated filament. It has long been known that such filaments when properly treated are exceedingly good emittors of electrons. They have found considerable use in

thermionic vacuum tubes and in scientific investigations. The object of this paper is to present a scientific description of some of the processes occurring in some oxide coated filaments and to propose a comprehensive theory to account for these processes.

There are two types of oxide coated filaments: those in which some or all of the oxides have been made to combine chemically with the metallic core of the filament, and those in which the oxides are uncombined. The latter appear pure white. In the combined filaments, the chemical compounds are decomposed when the tube is pumped. This leaves a finely dispersed metal mixed with the oxides and gives the filaments a grayish appearance. A method of preparation of combined filaments is described by Arnold.[1] The preparation of uncombined filaments is described by Schottky, Rothe and Simon, Volume 13, Part 2 of the Wien-Harms "Handbuch der Experimental-physik" pp. 215 and 305.[2] The reader will find a good discussion of published articles on oxide coated filaments in this same volume. The author's experience with barium oxide+strontium oxide combined filaments has been more extensive than with others.

In either type of filament, but particularly in combined filaments, it is found that the thermionic activity is greatly enhanced by what has been variously termed the activation, formation, or breakdown process. We shall call it the breakdown process. This process consists in glowing the oxide coated platinum filament at about 1500°K for several minutes; a rather high positive potential gradient is then applied to the filament for something like two to thirty minutes. During this time the emission from the filament increases greatly. When it attains rather large values such as 0.1 to 1.0 amps. per cm^2, the applied field and the filament temperature are so adjusted that the current is just limited by space charge. The detailed procedure to be followed for any particular filament constitutes an art and is beyond the scope of this article. The processes that go on during this time will be discussed below. The behavior of the filament before and after breakdown is considerably different.

Throughout this article we shall frequently use the term "activity" of the filament. As a measure of the activity we shall take the emission current at one particular temperature or at a series of temperatures. These temperatures will all be low and the plate potential will have a small constant value in order that the currents may remain essentially constant during the time required to determine the activity.

One of the outstanding characteristics of a coated filament is its complex behavior. For example, coated filaments show changes in activity with time following upon or accompanying (1) changes in temperature, (2) changes in plate potential and (3) current sent into or drawn from the filament. While all coated filaments show time changes with these three variables, the magnitude and even the direction of the change in activity depends greatly on the chemical and physical composition of the oxide as well as on the previous

[1] H. D. Arnold, Phys. Rev. **16**, 70 (1920).

[2] The title to this volume is "Glühelektroden und Technische Elektronenröhren"

treatment both immediate and remote. From this it is apparent that the coated filament is an extremely complex system. In our attempt to discover the processes going on in this complex system, we have found it convenient to be guided by a tentative hypothesis or unifying picture, and the reader may find it helpful to consider this hypothesis.

Hypothesis or Theory of the Action in Coated Filaments

In constructing such a hypothesis it is desirable to consider simpler types of filaments and to compare them with oxide coated filaments. The simplest kind of filament is one having an atomically clean and homogeneous surface such as clean tungsten, tantalum, or molybdenum. For any of these filaments the emission is determined solely by the temperature and plate potential; it is independent of the time of treatment at any previous temperatures, plate potentials or emission currents.

A somewhat more complex type of filament is illustrated by thoriated tungsten,[3] caesium on tungsten,[4,5] or barium on tungsten. These filaments have composite surfaces: the tungsten surface is more or less covered by a partial layer, a complete layer, or more than one atom layer of a foreign element. The activity, or emission at a testing temperature and fixed plate potential, now depends on the kind of foreign element and on θ, the fraction of the surface covered with it. Figure 1 shows the logarithm of the emission for barium on tungsten at 1100°K as a function of θ. Note that the activity is increased by a factor of about 10^{11} by a complete layer of barium. Since the amount of barium on the surface can be changed by heating the filament, it follows that in this case the activity can be greatly modified by a temperature treatment. On the other hand, experiment shows that the activity and θ are not affected by the plate potential or by the electron current sent into or drawn from the filament.

A still more complex filament is one with a doubly composite surface such as caesium and oxygen on tungsten. In this case experiment apparently shows that the activity depends upon (1) the number of caesium atoms per cm², (2) the number of oxygen atoms per cm², and (3) the relative position of the caesium and the oxygen. The activity increases with the amount of caesium until the surface is covered with a monatomic caesium layer; then it decreases as the second layer is formed. If we start with a monatomic layer of caesium and add increasing amounts of oxygen to the hot filament, the activity is increased even more, provided the amount of oxygen is small; as more and more oxygen is added, the activity comes to a maximum and then decreases. Temperature treatments change the concentration of caesium and of oxygen and consequently they also change the activity. Temperature may also affect the activity by changing the relative position of the caesium and oxygen.

That the activity depends on whether the caesium is on top of the oxygen or the oxygen on top of the caesium, is not yet established by direct experi-

[3] Langmuir, Phys. Rev. **22,** 357 (1923).
[4] Langmuir and Kingdon, Proc. Roy. Soc. **107A,** 61 (1925).
[5] Becker, Phys. Rev. **28,** 341 (1926).

ments. This view is based on the author's interpretation of temperature changes in the analogous case of barium and oxygen on tungsten and on the theory of the cause of the increase in activity for composite surfaces.* On this view,** if oxygen is deposited on top of a monatomic layer of caesium on tungsten and stays there, the activity should decrease; but if thermal agitation causes the oxygen to settle down between the tungsten and the caesium, the activity should increase. Such surface rearrangements take place apparently at temperatures lower than those necessary to produce other surface changes such as surface migration, diffusion inward, or evaporation. Temperature treatments can thus change the activity by changing the amount of caesium, amount of oxygen, or their relative positions. But even with this complex filament, the activity is independent of plate potential and the amount of current sent into or taken out of the filament.

Since coated filaments show changes in activity with temperature treatments in much the same way as do filaments with composite surfaces, it is quite natural to assume that coated filaments also have a composite surface of presumably metallic barium† on the oxide. This view is supported by another striking similarity between oxide coated filaments and filaments which are known to have composite surfaces. In both cases the emission current increases quite appreciably as the plate potential is increased more and more, while the emission current from an atomically clean surface saturates quite well.[6+]

Because of these two similarities, the author in private laboratory reports proposed the hypothesis that the enhanced activity of oxide coated filaments is due to metallic barium on the surface of barium oxide. Numerous experiments made in this laboratory have fully confirmed this hypothesis. The same or a similar hypothesis was proposed by Koller[7] in 1925, Rothe[8] in 1926, Espe[9] in 1927, and Detels[10] in 1927.

This hypothesis takes into account the similarities in coated and composite surface filaments but it fails to take into account the dissimilarities. It has been emphasized above that the activity of a coated filament is changed by changes in plate potential and by the current sent into or drawn from it, while the activity of other forms of composite surface filaments is not. It follows that an additional hypothesis must be made for

* See 15 below.

** This view was held by Mr. Ryde of the G. E. Laboratory at Wembley, England in 1928. He was kind enough to discuss the matter with the author on his visit to America.

† Throughout this article barium will be used as representative of the group of alkaline earths. It is to be understood that calcium and strontium act qualitatively like barium.

[6] See "On Electrical Fields near Metallic Surfaces" by Becker and Mueller, Phys. Rev. **31,** 431 (1928).

[+] In oxide coated filaments poor saturation may sometimes be produced by additional causes such as heating effects in the oxide or localized space charges.

[7] Koller, Phys. Rev. **25,** 671 (1925).

[8] Rothe, Zeits. f. Physik **36,** 737 (1926).

[9] Espe, Wissenschaftliche Veröffentlichungen aus dem Siemens Konzern, **5,** 29 and 46 (1927).

[10] Detels, Jahrbuch der Drahtlosen Telegraphie und Telephonie **30,** 10 and 52 (1927.

coated filaments. Electrolysis of the oxides naturally suggests itself since it has been known for many years that heated salts and in particular some oxides are electrolized. This was shown by the work of Bose,[11] Horton,[12] and Spanner.[13] From what is known of the conductivity of oxides, it may safely be postulated that the current perpendicular to the surface of the oxide may be carried partly by electrons and partly by ions, presumably of barium and oxygen.

This hypothesis too was proposed by the author in private laboratory reports. It had previously been held by Fredenhagen[14] in 1913, who believed, however, that the emission of electrons was caused by chemical recombination of barium and oxygen. The electrolytic hypothesis was also held by Rothe,[8] Espe,[9] and Detels.[10] They and others showed that an oxide coated filament which has been heated to a high temperature for a considerable time does not give off appreciable quantities of gas if no current is drawn from it, but that considerable gas is given off when curernt is subsequently drawn. Detels[10] showed that this gas was oxygen by collecting it in a Geissler tube and showing that its spectrum was identical with that of a similar tube filled with pure oxygen. J. E. Harris in these laboratories first showed that if large currents are drawn from a barium oxide+strontium oxide coated filament, barium and strontium are present in the core, while if a similar filament is glowed even more severely but without drawing currents, no barium or strontium are found in the core. It is thus clearly established by numerous and varied experiments that some electrolysis takes place in oxide coated filaments and that the products are the ones to be expected. It is proper, therefore, to attempt to account for the observed changes in activity with drawing current or sending current into the filament on the basis of the electrolytic theory.

On the electrolytic theory, if electrons are sent into a coated filament from another source, barium is deposited on the outer surface of the oxide while oxygen is deposited on the interface between the core and the coating. Since thermionic emission depends on surface conditions and not on the conditions many layers beneath the surface, the barium should directly and immediately affect the activity while the oxygen should not do so. If barium on barium oxide produces the same effects as does barium on the tungsten, the activity should increase, pass through an optimum and then decrease as more barium is deposited on the surface. Experiments to be described below show that this is precisely what happens. These experiments will also be used to determine quantitatively the factors that determine the amount of electrolysis.

If, on the other hand, electrons are drawn from a coated filament, barium is deposited on the core-oxide interface and oxygen on the outer surface. The barium should not affect the activity directly and immediately but may

[11] Bose, Ann. d. Physik **9**, 164 (1902).
[12] Horton, Phil. Mag. **11**, 505 (1906).
[13] Spanner, Ann. d. Physik **75**, 609 (1924).
[14] Fredenhagen, Leipziger Berichte **65**, 42 (1913).

do so if it subsequently diffuses to the oxide surface. The oxygen, however, should affect the activity directly and immediately. From analogy with caesium and oxygen on tungsten discussed above, the change in activity due to additional oxygen should depend on the amount of barium, the amount of oxygen, and also on the position of the oxygen relative to any surface layers of barium or barium-oxide. The experiments described below fulfill this expectation. They show that when current is drawn from a coated filament, the activity sometimes decreases, while at other times it increases to a maximum and then decreases. Which of these behaviors is exhibited depends upon the degree of breakdown of the filament, the temperature, and the plate potential.

Another supplementary hypothesis is required to account for the complex behavior in coated filaments. It is to be expected that the barium and oxygen which are produced by electrolysis will diffuse into the oxide and from the oxide to the outer surface where they produce their effect on the activity. On account of the open or spongy structure of the oxides on these filaments, we should expect diffusion to take place very readily since it has been shown that surface migration of adsorbed atoms takes place at temperatures at which evaporation is negligible.[15] At temperatures near 1000°K there should be a continuous interchange of barium and oxygen atoms between the surface and the interior of the oxide.

The various phases of the proposed hypothesis have been thoroughly tested, confirmed, and extended by the experiments which are described below. For this reason it seems proper to speak of the theory rather than the hypothesis of oxide coated filaments.

Experimental Tubes

Most of the experiments were performed with two tubes designated by 12-J and 89-B. Figure 2 shows the plate and filament assembly of tube 12-J. The plates were made of preglowed nickel. The dimensions are given in the figure. Usually only the current to the center plate was measured; the end plates served as guard plates. F_1 and F_3 are oxide coated filaments. The core consisted of a 95 percent platinum, 5 percent nickel alloy in the form of a ribbon $10.2\times0.030\times0.0054$ cm. They were coated with about 20,000 molecular layers of barium oxide and strontium oxide and were flashed at 1000°K in air to form some barium and strontium platinates and nickelites. F_1 was broken down on the pumps, while F_3 was merely glowed but thoroughly degassed. During the course of the experiments, F_3 was subsequently broken down. F_2 is a tungsten ribbon $7.05\times0.0381\times0.003$ cm. Material from any filament can be vaporized onto any other filament. All the filaments were kept taut and straight by means of molybdenum springs not shown in the figure. This plate and filament assembly was inserted in one end of an appropriate lead glass tube. At the other end a Buckley ionization manometer[16] was attached. The tube was thoroughly pumped and had magnesium "get-

[15] Becker, "The Life History of Adsorbed Atoms and Ions" Proc. Am. Electrochem. Soc. **55**, 153 (1929).

[16] Buckley, Proc. Nat. Acad. Sci. **2**, 683 (1916).

ter." After it was sealed off and cleaned up by glowing the thoriated tungsten filaments in the manometer and the broken down coated filament, the pressure was ordinarily about 1×10^{-8} mm Hg and the activity of the filaments was not affected by gas even over long periods of time.

Tube 89-B was similar to 12-J. It differed from it in three significant respects: (1) The tungsten ribbon F_W was about 10 cm long instead of 7.05 cm.

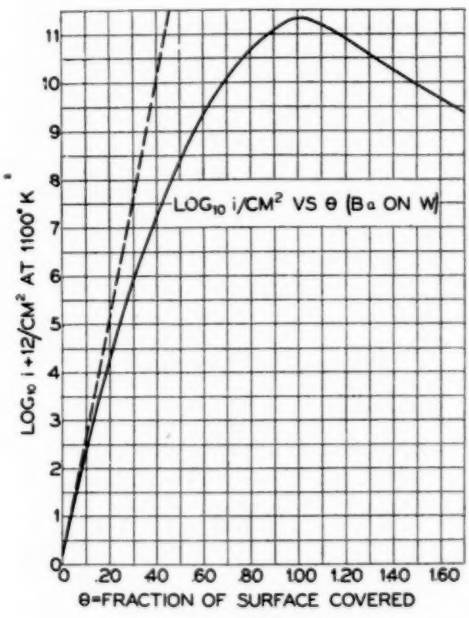

Fig. 1.

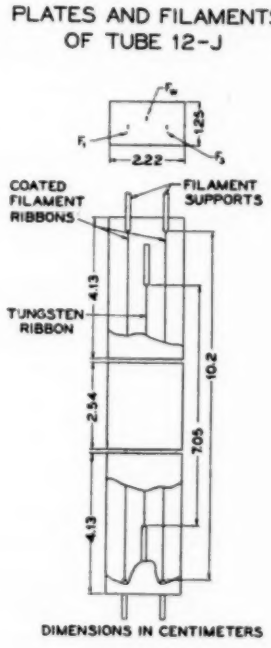

Fig. 2.

This reduced the effects of end cooling. (2) The middle collector or plate was 1.27 cm high instead of 2.53 cm. This too reduced end-cooling effects and also minimized effects due to non-uniformities along the filament. (3) A movable nickel shield could be placed between the unbroken down coated filament and the other two filaments. This permitted experiments which could not be performed in 12-J.

Experimental Results

The experimental results will be divided into eight groups which tend to show that: (1) Metallic barium evaporates from a well broken down coated filament; (2) Oxygen evaporates if an emission limited current is drawn and the temperature is high enough; (3) The high activity of oxide coated filament results from metallic barium on the oxide surface; (4) Barium diffuses readily to and from the surface of the oxide; (5) Oxygen affects the activity in various ways; (6) Oxygen diffuses readily to and from the surface of the oxide; (7) Most of the current through the oxide is carried by electrons but a small part is carried by ions; the ratio depends upon the temperature, the composition of the oxide, and the plate potential; (8) The complex time changes that occur can be interpreted in terms of these processes.

(1) Evaporation of metallic barium from oxide coated filaments. That metallic barium evaporates from a well broken down coated filament was shown by the following experiments. In tube 12-J, after filament F_3 had been broken down and thoroughly aged, it was glowed at 1260°K for about 10 minutes while the tungsten filament F_W, which had previously been cleaned off, was cold. F_3 and the whole tube were then allowed to cool and the activity of F_W was determined at a series of testing temperatures which were as low as possible so that no appreciable time changes took place during the test. It was found that the activity of F_W had increased appreciably. F_3 was then again glowed as previously while F_W was cold. When the tube was cool, the activity was again determined at a series of low testing temperatures. This process was repeated a number of times. Whenever necessary, the emission from F_W was extrapolated or interpolated to 1100°K.

When the log of these emission currents reduced to a cm² were plotted against the total time of flashing F_3 at 1260°K, a curve similar to Fig. 1 was obtained: Log i rises rapidly at first, then more and more slowly until it passes through an optimum beyond which it decreases. By appropriate experiments, it was shown that in equal intervals of time of glowing F_3, equal quantities of material were deposited on F_W so that θ, the fraction of its surface covered, is directly proportional to the time of glowing F_3 at a fixed temperature. That θ is equal to unity for the optimum activity is based on (1) analogy with caesium on tungsten for which it was proven[5] and (2) the author's theory of the emission from composite surfaces[15] from which it follows that θ should be equal to unity at the optimum activity for all electropositive materials adsorbed on strong electronegative surfaces. The exact shape of the curve in Fig. 1 was obtained by correcting the observed curve for non-uniform deposition on various portions of one side of F_W.

When F_W was subsequently glowed at 1100°K, the activity increased until it reached practically the same optimum as before; then the activity decreased and approached a steady value. When the temperature of F_W was increased again, the activity decreased, at first rapidly and then more and more slowly. This process was continued at successively higher temperatures until the activity of clean tungsten was reached at a temperature of about 1700°K.

Apparently something evaporated from F_3 and activated F_W. When F_V was subsequently heated, this something disappeared from the surface of F_W. If this whole behavior could be repeated even in some of its quantitative aspects, with a source known to contain barium, it would be fair to infer that the material that evaporated from a well broken down coated filament is barium.

This inference was established by an experiment performed by J. M. Eglin[17] of these laboratories. He built and worked with tube 5-E which was just like 12-J except that the two coated filaments were replaced by two filaments consisting of an alloy core of 95 percent platinum, 5 percent nickel and metallic barium. The barium was obtained from barium-azide and was

[17] Eglin, Phys. Rev. **31**, 1127 (1928).

alloyed with the filaments in a separate tube by a process which is now well known.[2] If such barium alloy filaments are thoroughly aged to free them of nitrogen, and are then glowed at 1200°K, chiefly barium evaporates from them. The changes in activity of the tungsten filament obtained in this tube were just like those described in the preceding paragraphs for tube 12-J. Even more significant is the fact that the optimum activity obtained in these two tubes agreed quite closely with each other.

Figure 3 is in part intended to show how close this agreement is. It is a plot of the emission vs. the power supplied to F_W per cm² on a coordinate paper devised by C. J. Davisson of these laboratories. If the emission from a filament obeys Richardson's $T^{1/2}$ equation and if the watts dissipated increase with T^4, then the "power emission" line should be straight. Line No. 1 shows the observed optimum for tube 12-J. Line No. 2 is for tube 5-E. This line has been slightly corrected for the fact that the tungsten ribbons in the two tubes were not quite identical. This correction, which amounted to about a factor of 8 at the lower currents and 2 at the higher currents, was based on the power emission lines for clean tungsten and on the heating currents necessary to make the filaments barely visible in a dark room. Line No. 3 is for a similar optimum from a coated filament in tube 89-B. Note that none of the three lines is straight. This is due to the fact that at temperatures below about 1000°K, the end cooling is appreciable and becomes more marked at lower temperatures. Line 4 is line 1 corrected for end cooling by approximate methods. Since in 89-B the end-cooling correction should be less than in the other two tubes because the filament was 10 cm long instead of 7.05 cm line 3 should be everywhere higher than lines 1 and 2. The figure shows that this is so. The agreement between line 2 for barium on tungsten and lines 1 and 3 for two cases of material vaporized from well broken down coated filaments on tungsten, is almost as good as between two successive determinations of the same line. Line 5 in the lower right corner shows the emission from clean tungsten. An approximate temperature scale is added below the power scale. The close agreement of the optimum lines and the similarity of the general behavior in the three tubes make it very probable that barium evaporates from a well broken down coated filament at temperatures near 1250°K.

If in similar experiments the coated filament were not well broken down or if its temperature were too high, or if current was being drawn from it during the vaporization process, then another element presumably oxygen either free or in the form of an oxide, was vaporized over with the barium. This oxygen showed itself in the following four ways: (1) The log i vs. θ curve of Fig. 1 instead of rising rapidly and then more slowly, rose slowly and then approached the trend shown in Fig. 1. If the oxygen ratio was rather high, the activity actually decreased during the first few minutes of flashing; then it started to rise. (2) If about 0.9 layer was deposited on F_W and if F_W was then glowed at successively higher temperatures, the activity decreased to a value below that of clean tungsten. At still higher temperatures, near 1800°K the activity increased again to that of clean tungsten. This behavior

is analogous to that for caesium and oxygen on tungsten.[5] (3) If more than one layer was deposited, the temperature required to pass backward through the optimum at a reasonable rate was considerably higher than if no oxygen was vaporized. The oxygen apparently holds the barium more tenaciously than does clean tungsten. This too is analogous to its behavior for caesium on oxygen on tungsten. (4) The optima were not definite but depended on the amount of oxygen coming over with the barium. Comparatively small amounts of oxygen increased the optimum line to a value of about five times that for barium on tungsten. Large amounts of oxygen lowered the optimum line more and more. This also is analogous to caesium on oxygen on tungsten, but in this case, the optimum caesium on tungsten line can be increased several hundredfold by the proper amount of oxygen.

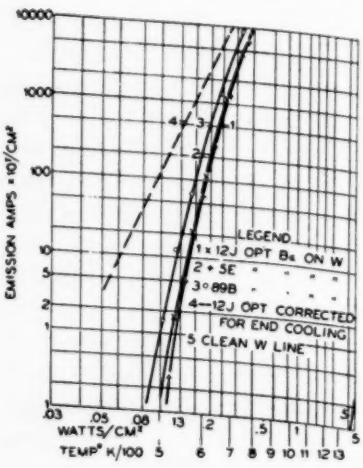
EMISSION AMPS = 10⁷/CM²
LEGEND
1 x 12J OPT Ba ON W
2 • 5E " " "
3 • 89B " " "
4 — 12J OPT CORRECTED FOR END COOLING
5 CLEAN W LINE
WATTS/CM²
TEMP° K/100

Fig. 3.

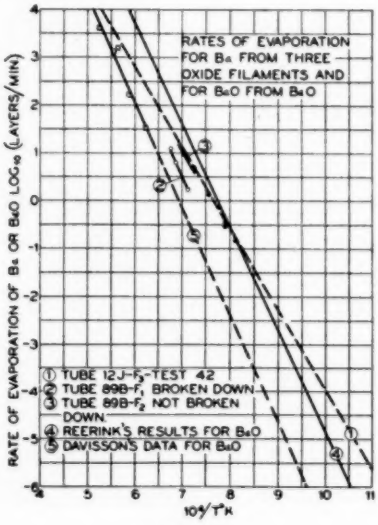
RATES OF EVAPORATION FOR Ba FROM THREE OXIDE FILAMENTS AND FOR BaO FROM BaO
RATE OF EVAPORATION OF Ba OR BaO LOG₁₀ (LAYERS/MIN)
① TUBE 12J-F₂-TEST 42
② TUBE 89B-F₁ BROKEN DOWN
③ TUBE 89B-F₂ NOT BROKEN DOWN
④ REERINK'S RESULTS FOR BaO
⑤ DAVISSON'S DATA FOR BaO
10⁴/T°K

Fig. 4.

An interesting deduction from these experiments is that barium and oxygen do not permanently combine chemically on a hot tungsten surface. Another way of stating this, is that barium oxide is decomposed on a hot tungsten surface.

The peak or optimum activity phenomenon furnishes us with a convenient and powerful method for determining rates of evaporation of electropositive materials at various temperatures. All that need be done is to determine the time required for the activity of F_W to reach its optimum and to compute from the geometrical relationships the number of layers that must evaporate from the primary to deposit one layer on the tungsten. In this way the number of layers evaporating per minute at a series of temperatures was determined for several coated filaments.

In Fig. 4 the log of the evaporation rate expressed in layers per minute has been plotted as a function of $1/T$. Curves 1, 2 and 3 are for the evaporation of barium from oxide coated filaments.* Line 4 represents the data

* θ, the fraction of the surface covered with barium may have been different from one

obtained by Reerink for barium oxide from barium oxide which was reported in an article by Zwikker.[18] The points through which line 5 has been drawn are experimental values obtained by C. J. Davisson in these laboratories several years ago. He showed also that the rate of evaporation of strontium oxide from strontium oxide was negligibly small compared to barium oxide from barium oxide. The filaments which furnished the data for line 1, 2 and 3 consisted of a mixture of barium oxide and strontium oxide. Presumably the evaporation rate of barium oxide from this mixture is somewhat less than it would have been from a pure barium oxide surface. From this and from a comparison of the slopes of lines 1 to 3, and lines 4 and 5, it follows that at low temperatures chiefly barium should evaporate while at sufficiently high temperatures chiefly oxide should evaporate.†

It should be pointed out that this method of determining evaporation rates at various temperatures might well be used for a study of the precise way in which the evaporation depends upon the temperature.

That mostly metallic barium rather than barium oxide evaporates from well broken down coated filaments follows from experiments performed by C. J. Davisson in these laboratories several years ago. It was found that the material that evaporated produced rather large resistance leaks across glass surfaces between metallic terminals. When air was let into such tubes, the resistance increased greatly and rapidly. Commercial hydrogen, presumably slightly impure, caused no rapid changes in resistance. Metallic barium would be expected to produce these results while barium oxide would not.

These experiments, it seems to us, prove conclusively that metallic barium evaporates from a well broken down oxide coated filament. If the temperature is not too high and if no electrons are drawn from the filament, it appears that practically nothing else evaporates. At sufficiently high temperatures barium oxide must also evaporate.

(2) Evaporation of oxygen. When current is drawn from a coated filament at a sufficiently high temperature and if this current is not limited by space charge, oxygen evaporates. Some of this oxygen is deposited on the tungsten ribbon in Fig. 2 and decreases its activity. Thus, when filament F_3 in tube 12-J was at a temperature of about 800°K and the plates were at a positive potential of about 100 volts, it was found that the activity of the tungsten ribbon decreased progressively. In one particular case, the current to the center plate was about 1.0 milliampere and the activity of the tungsten ribbon was decreased by a factor of two for every 2 hours. By drawing large currents we have been able to reduce the activity of the tungsten filament by a factor of 200.* If the tungsten ribbon was subsequently raised to tempera-

filament to the next but for a given filament it was probably quite constant since the activity did not change appreciably with changes in glowing temperature.

[18] Zwikker, Physica **8**, 241, (1928).

† At about 1250°K the evaporation rate of barium from metallic barium is about 10^8 times as great as the rate of evaporation of barium from a well broken down coated filament.

* From the fact that the activity of the tungsten ribbon can be reduced by more than a factor of two, we may conclude that the oxygen which strikes one side of the ribbon must

tures higher than about 1600°K, the activity increased for a time and then became almost constant. If the temperature was raised again, the activity increased rapidly at first and then more and more slowly.** At 1800°K, the activity reached that of clean tungsten in something like ten minutes.

Practically all of this oxygen must leave the coated filament in an uncharged condition, for the rate at which it collects on the tungsten ribbon is not affected by the potential of the tungsten ribbon. If an appreciable amount of the oxygen were negatively charged and if the tungsten ribbon were made negative with respect to the coated filament, the rate of deactivation of the tungsten ribbon should be appreciably decreased. We have made several experiments in several tubes to test this point and have never found any evidence that the oxygen was negatively charged. This is rather surprising in view of Barton's result[19] which is frequently quoted in the literature. It may be that the condition of his filament was considerably different from that of ours and from that in ordinary tubes.

By determining the rate of deactivation of the tungsten ribbon as a result of various treatments imposed upon the coated filaments, it is a rather simple matter to determine the factors upon which the rate of evaporation of oxygen depends. Such experiments have shown that the rate of oxygen evaporation increases with (1) the temperature of the filament, (2) the amount of current drawn from it, (3) the plate potential and (4) the composition or state of the oxide. Thus far, the exact manner in which it depends on these factors has not been determined accurately. The first two factors were to be expected. That the oxygen evaporation increases rapidly with the positive plate potential is somewhat surprising since one might expect the potential difference across the oxide at a given temperature to depend only on the current through it. Experiment, however, shows very definitely that if the emission is limited by space charge, no oxygen or very little oxygen is liberated compared to the amount liberated when the plate voltage is increased such that the current is limited by emission. When the plate is at a negative potential, no oxygen evaporates. It should be pointed out that the temperatures at which it is possible to obtain oxygen at an appreciable rate are considerably lower than those required to obtain barium at an appreciable rate. It is therefore possible to obtain oxygen without barium by one procedure, and barium without oxygen by another.

An important observation was this: it was comparatively easy to obtain oxygen from filament F_3, the unbroken down coated filament in tube 12-J, soon after the tube was sealed off the pumps. However, after a considerable quantity of oxygen had been removed and the filament had become more active, it required large currents, 10 to 20 mils, and high plate potentials, 150 to 200 volts, to obtain appreciable quantities of oxygen. We take this

migrate and reach the other side of the ribbon at the testing temperatures of about 1400°K. Subsidiary experiments especially with the shielded tube 89-B showed that no oxygen could reach the back side of the tungsten ribbon by being reflected from the walls of the tube.

** The reason for this behavior is that the rate of evaporation at a given temperature decreases rapidly as θ decreases.

[19] Barton, Phys. Rev. **26**, 360 (1925).

to mean that originally an appreciable part of the current through the oxide was carried electrolytically by oxygen and barium ions; after the filament was broken down and barium was dispersed through the oxide, a much smaller part of the current was carried by ions.

From the experiments described in this section, we conclude that when current is drawn from a coated filament at a sufficiently high temperature and this current is not limited by space charge, oxygen evaporates. Most of this oxygen must be uncharged. The rate at which it appears increases rapidly with the plate potential, and it decreases as more barium is dispersed through the oxide.

(3 Activation due to barium on barium oxide. There are two ways by which barium can be caused to appear at the surface of the oxide: one is by sending electrons into the oxide from an outside source and thereby elec-

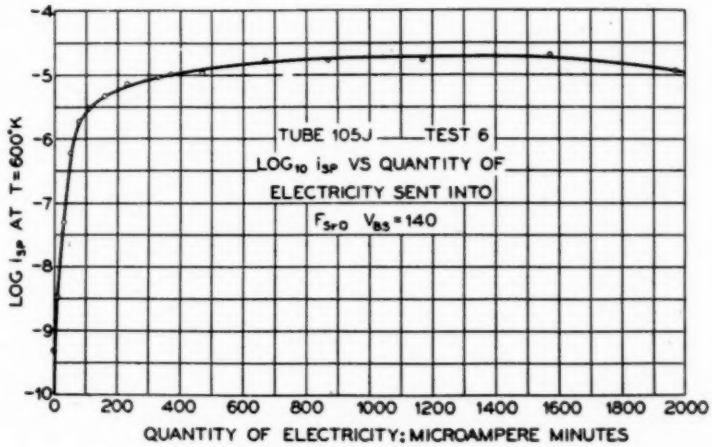

Fig. 5.

trolizing the oxide; the second is by vaporizing barium from another filament which, under proper conditions, may be another oxide coated filament. The barium which is thus brought to the surface of the oxide should change the activity of the filament. If barium on barium oxide is analogous to barium on tungsten the log of the activity should increase rapidly at first, then more and more slowly until it passes through an optimum beyond which it should decrease. When the oxide coated filament is subsequently glowed and the barium is thereby caused to diffuse or vaporize from the surface, the activity should again increase to an optimum and then decrease to its normal value. The following experiments and figures show that this is exactly what happens.

Figure 5 shows a logarithmic plot of the activity of a strontium oxide uncombined filament as a function of the amount of electricity, expressed in microampere minutes, sent into it from an outside source through a P. D. of 140 volts. The activity is here defined as the emission current from the entire 10 cm length of the filament at approximately 600°K and 70 volts

plate potential. For some points this activity was determined by extrapolation from higher or lower temperatures. Note that the activity increased to an optimum value which was about 30,000 times its initial value after about 1200 microampere minutes had been sent into the filament. Subsidiary tests showed that all parts of the filament did not reach their optimum at the same time. This causes the peak to be considerably flatter and somewhat lower than it would otherwise be. Such non-uniformities are to be expected and are extremely difficult to avoid. If they had been avoided, we estimate that the optimum would have come at 300 mic-minutes. Subsidiary tests also showed that the initial test point in Fig. 5 did not correspond to clean strontium oxide, for subsequent more severe glowing reduced the activity below this value. If the current through the oxide were entirely electrolytic and if the microscopic surface area were the same as the measured

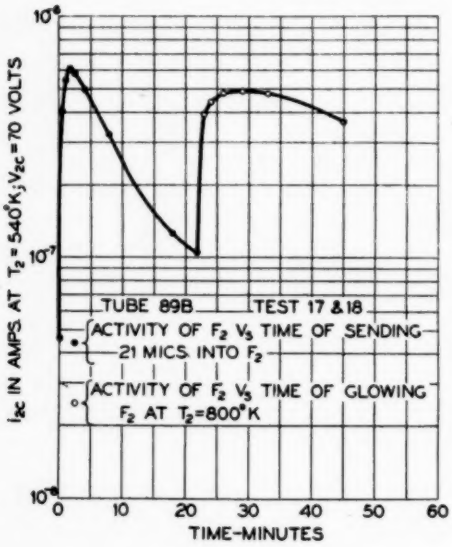
I_{2c} IN AMPS. AT T_2 = 540°K; V_{2c} = 70 VOLTS
TUBE 89B TEST 17 & 18
ACTIVITY OF F_2 V_3 TIME OF SENDING 21 MICS. INTO F_2
ACTIVITY OF F_2 V_3 TIME OF GLOWING F_2 AT T_2=800°K
TIME-MINUTES

Fig. 6.

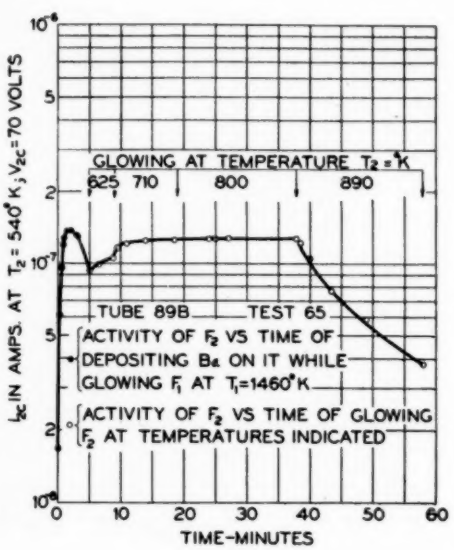
I_{2c} IN AMPS. AT T_2 = 540°K; V_{2c} = 70 VOLTS
GLOWING AT TEMPERATURE T_2 = °K
625 710 800 890
TUBE 89B TEST 65
ACTIVITY OF F_2 VS TIME OF DEPOSITING Ba ON IT WHILE GLOWING F_1 AT T_1=1460°K
ACTIVITY OF F_2 VS TIME OF GLOWING F_2 AT TEMPERATURES INDICATED
TIME-MINUTES

Fig. 7.

macroscopic area, about 2.0 microampere minutes per cm² should suffice to cover the surface with a monatomic layer of metallic strontium. From these facts we may conclude that very roughly 1/200 of the current through this particular oxide was carried by strontium ions.

The first part of Fig. 6 shows a similar curve for test 17, tube 89-B, filament F_2. In this case 21 microamperes were sent into the coated filament for a total of 22 minutes. At the end of this time F_2 was glowed at 800°K for 23 minutes. The activity was tested under standard conditions at the times for which points are plotted. The activity passed through an optimum which is about 25 percent lower than the optimum for the preceding curve. This small discrepancy in the optima is no greater than is usual in this type of curve and is possibly due to slight differences in the degree of uniformity of covering.

If we compare Figs. 5 and 6 we note that the peak is much sharper in 6 than in 5. This is undoubtedly due to the fact that in Fig. 6 the degree of non-uniformity at the peak is much less than it is in Fig. 5 since the activity in Fig. 6 refers to 1.27 cm of the center portion of the filament while that in Fig. 5 refers to the entire 10 cm length.

A still more striking difference between these two figures is that in Fig. 6 the optimum activity is only about 13 times the initial activity while in Fig. 5 it is about 30,000 times the initial activity. This is undoubtedly due to the fact that in Fig. 6 the filament surface was nearly completely covered with barium at the initial activity.

The proof of this statement is based on test 61A, tube 89-B. In this test the broken down coated filament F_1 was flashed at 1450°K in order to vaporize barium onto F_2 and also onto F_W. (See Fig. 2 for the relative positions of the oxide coated and tungsten filaments.) The activity of F_2 changed in the manner practically identical with that given in the first part of Fig. 7 for test 65 except that the curve was extended for 20 minutes instead of 5; from 5 to 20 minutes it decreased at a slower and slower rate. During the same time the activity of F_W followed a course given by Fig. 1, the peak occurring after 14 minutes of flashing F_1. Note that F_2 reached its optimum activity before two minutes of flashing while F_W reached its optimum after 14 minutes. Since F_2 was about twice as far from F_1 as was F_W from F_1, the amount of material reaching F_2 in a given time is about 1/2 as great as that reaching F_W. Consequently it required only 1/14 or about 7 percent as much material to bring F_2 to its optimum as it did to cover F_W with a monatomic layer. On the hypothesis that the optimum activity occurs at a monatomic layer, we may conclude that F_2 was 93 percent covered at the initial value in Fig. 7. This initial value could be repeatedly obtained after glowing at about 1300°K for several minutes, and was roughly the same as in Fig. 6.

Fig. 7 shows the change in activity of F_2 while F_1 was glowed at 1460°K for 5 minutes. Note that the activity passes through an optimum after barium is deposited on F_2. Subsequent glowing of F_2, at the temperatures and times indicated in Fig. 7, caused the activity to pass through practically the same optimum as before.

It is very instructive to compare Figs. 6 and 7. In one case barium was brought to the surface by electrolysis while in the second case it was deposited by vaporization. In both cases the activity of F_2 passed through an optimum. In both cases subsequent glowing caused the activity to go backward through an optimum practically equal to that of the optimum which preceded it. The slight differences between the two cases are easily accounted for by the treatment given the filament between tests 17 and 65. Unfortunately we do not yet have two such curves for the filament in identical conditions and especially in an initially rather inactive state.

That the amount of barium brought to the surface by electrolysis is directly proportional to the quantity of electricity sent into the oxide coated filament may be inferred from Fig. 8. This is a plot of the logarithm of the emission from the central inch of filament F_3 at a temperature of 475°K and

a plate voltage of 31.5 volts vs. the mic-minutes of current sent into F_3 while F_3 was at 475°K. Each set of points shown in this figure represents a complete curve by itself. For one set of points, the current sent into the filament was 6.0 microamperes; for others, 15, 60, and 380 microamperes respectively. From the fact that the different sets of points all fall on the same curve, we may conclude that the number of ions brought to the surface depends only on the product of the current and the time and not upon either variable alone. This is readily understandable if the amount of barium brought to the surface is directly proportional to the quantity of electricity sent into the filament.

In Fig. 8 the initial activity is very close to the optimum activity. While we have no proof in this particular instance that this means that the surface is practically completely covered, we have no hesitation in inferring this from analogy with the data discussed above for tube 89-B. Similar data in tube

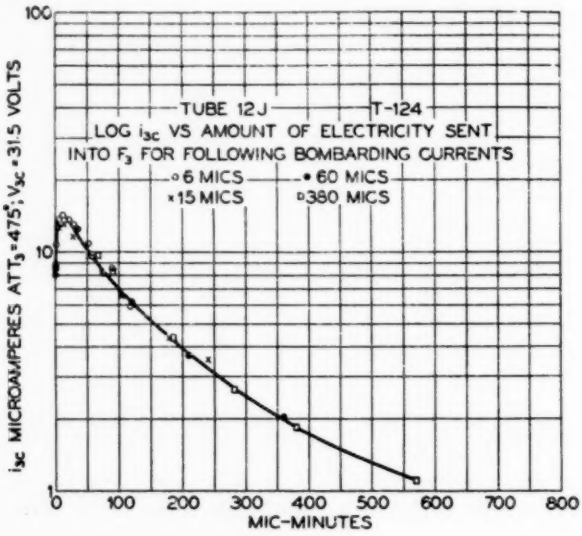

Fig. 8.

12-J could not be obtained since the filament F_1 was burned out rather early in the history of the tube. Before the curve shown in Fig. 8 was taken, filament F_3 had been well activated by breaking it down. Its activity could not be decreased appreciably by glowing it even at fairly high temperatures such as 1300°K for a time sufficient to vaporize hundreds of layers of barium from it. Possibly by glowing it at temperatures near the melting point of the core, we might have decreased the activity slightly.

While we have no curve showing the rise in activity of F_3 while barium was being vaporized onto it from F_1, we do have a curve which shows what happened to the activity of F_3 after about three layers of barium had been deposited on it. This is shown in Fig. 9 in the form of power emission curves. The line or lines on the extreme right show the initial activity in test 1 soon after the tube was pumped. After about three layers of barium had been vaporized onto F_3, the emission was that given by points 1 and 2 in the lower left-hand corner of the figure. Even at as low a temperature as 500°K the

activity increased due to barium disappearing from the surface. At any temperature such time changes were usually rapid at first and then slowed down until they were fairly steady.* The temperature was then changed to a higher value at which the activity increased again. This process continued up to points 7 and 8. For still higher temperatures the activity decreased at each temperature. After point 12 the temperature was decreased. At the lower temperature the activity was now quite steady. In this condition the activity was still appreciably higher than it was in the initial state, pre-

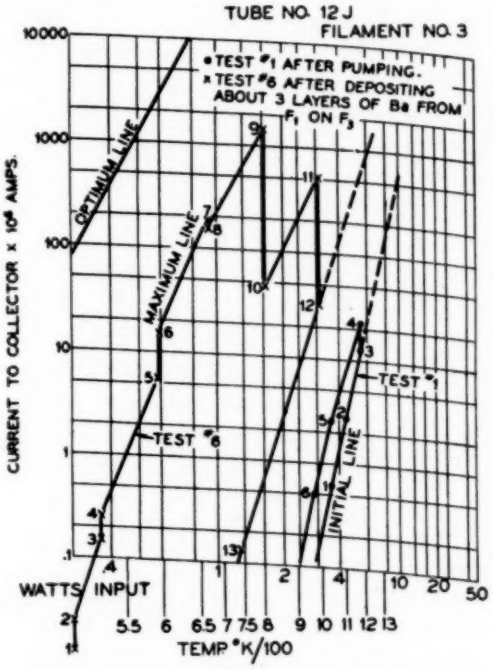

Fig. 9.

sumably because some barium was still left on the surface even after glowing at approximately 1000°K. Note that the maximum line is about 100,000 times as active as the initial line. By subsequent treatment of the filament, the activity was raised almost to that of the optimum line given in the upper left corner. This line is about 10^7 times as active as the initial line.

The evidence presented in connection with Figs. 5, 6, 7, 8, and 9, proves conclusively that the activity of an oxide coated filament can be greatly modified by depositing barium on its surface. We could give many more curves similar to the ones which have been given, but feel that this is unnecessary.

The amount of barium on the surface of the oxide is not the only factor which determines the activity, for otherwise the activity of all oxide coated filaments should be the same for an optimum amount of barium on the surface. Experiment shows that this is not so. The optimum line for filament

* The reason for this behavior is that the rate of evaporation at a given temperature decreases rapidly as θ decreases.

F_3 in tube 12-J is shown in Fig. 9. The optimum line for F_2 in tube 89-B was approximately parallel to this line but was a factor of 25 below it. The optimum line for filament F_1 tube 89-B, was again approximately parallel to the optimum line for F_3 tube 12-J, but was a factor of 500 below it. That the optimum lines for the same filament at various stages of its breakdown process may differ is suggested by the position of the "maximum line" and "optimum line" in Fig. 9. There is some question as to the part that oxygen played in the determination of the "maximum line," but for this line as well as for the "optimum line," the surface was quite likely covered with an optimum amount of barium.

(4) Diffusion of barium in the oxide. That the barium which is produced by electrolysis diffuses into and through the oxide can be deduced from a number of experimental facts. One of these is the activation resulting from the breakdown process. The barium is deposited on the oxide-core interface and must diffuse through the oxide to the surface before it can increase the activity.

Another argument for diffusion is this; hundreds of layers of barium can be vaporized from a well broken down filament without appreciably altering its appearance or its activity. This barium could not possibly have been on the surface of the oxide at one and the same time, for otherwise, (1) the surface would have had a metallic appearance, (2) the activity could not have been affected by adding more barium, and (3) the rate of vaporization would have been much higher than was found to be the case. Hence the barium must have diffused through the oxide to the surface.

A semi-quantitative proof of diffusion is based on the life of these filaments. It is a well-established fact that these filaments retain an appreciable percentage of the original oxide even after furnishing a current of 20 milliamperes from a cm^2 for at least two years or approximately 15,000 hours. We shall show below that more than one part in one thousand of the current through the oxide is carried by ions. Hence at 15,000 hours, 300 milliampere hours or 18,000 milliampere minutes of ion current must have reached the surface. If each ion carries a charge equal to that on the electron and if a single layer of barium corresponds to about 7×10^{14} atoms per cm^2, it requires about two microampere minutes of ion current per cm^2 to produce one layer. Hence the number of layers of barium that should be deposited at the current and time specified above is more than 9,000,000. Actually there are only about 20,000 layers of oxide on a filament and only a portion of these disappear during the treatment. Hence it follows that by far the largest part, about 0.998, of the barium which is produced by electrolysis must diffuse into the oxide, and must recombine with oxygen to form barium oxide.

The rate at which the barium diffuses from the surface into the oxide may be determined from curves such as that shown in the second part of Fig. 6. In this case the surface concentration of barium was greater than that corresponding to equilibrium conditions and hence the barium disappeared from the surface rapidly at first and then more slowly. This barium either evaporated or diffused into the oxide. That only a small part evaporated

appears from the following calculation. In Fig. 6 we estimate that at 800°K about 0.05 layers left the surface between times 30 and 45 minutes. This corresponds to a rate of one layer in 300 minutes or about 3×10^{-3} layers per minute for an average θ of about 0.98. From curve 3 in Fig. 4 for which θ was about 0.90 we can obtain that at 800°K, the rate of evaporation was about 3×10^{-7} layers per minute or only 1/10,000 of the rate of disappearance. It seems improbable that the evaporation rate increases as much as one thousand-fold when θ changes from 0.90 to 0.98. Hence most of the barium must have left the surface by diffusion and the diffusion rate must be approximately the same as the total rate of disappearance.

Whenever the barium surface concentration exceeds the equilibrium concentration, the rate at which the surface concentration approaches the equilibrium concentration is rapid at first and then decreases more and more. This is readily deduced from the shapes of the glowing curves like those in Figs. 6 and 7. One would hardly expect that the diffusion inward should cease when the equilibrium concentration is reached. It appears very likely that there is a constant interchange of atoms between the surface and the interior of the oxide. We should expect that the rate of diffusion to the surface should be directly proportional to the volume concentration of barium in the oxide while the rate of diffusion from the surface should increase exponentially with the absolute value of the surface concentration. The latter expectation is based on the picture that it takes a definite amount of work to take an atom from the surface into the interior and that this amount of work decreases as the surface concentration increases; in other words, that the diffusion inward process is analogous to the evaporation process.* When a steady state is reached at any glowing temperature just as many atoms come to the surface as leave the surface. From this picture we should expect that the surface concentration should not differ greatly when the volume concentration is changed by even as great a factor as 10. This may explain why the activity is not very greatly dependent on the amount of barium stored in the core and oxide coating.

(5) The effect of oxygen on the activity. It is a well-known fact that when current is drawn from a coated filament the activity of this filament changes rapidly at first and then more and more slowly. The magnitude and even the direction of the change in activity depend greatly upon the composition of the oxide, the plate potential, the degree of breakdown and the temperature of the filament.

For a well broken down filament we have invariably found that the activity decreases rapidly and then more and more slowly. This is illustrated in the first part of Fig. 10. Curve 1 shows how the emission current in milliamperes decreased at a temperature of 715°K and 60 volts plate potential. At intervals the activity was tested at a lower temperature, 475°K. This activity is plotted in microamperes as curve 2.

It was shown above that if the temperature and the plate potential are high, oxygen is formed by electrolysis and evaporates. Presumably, there-

* See reference 15. The reason for this behavior is, that the rate of evaporation at a given temperature decreases rapidly as θ decreases.

fore, the decay in activity is caused by oxygen which has come to the surface and some of which stays there because the temperature does not remove it rapidly. Because of its electron affinity some of the oxygen should be negatively charged and if the oxygen stays on top of the surface layer of barium it should produce electrical fields which hinder the escape of electrons. Consequently the activity should decrease. If more and more oxygen is brought to the surface the rate at which it disappears from the surface either by evaporation or by diffusion should increase rapidly until the rate of disappearance is equal to the rate of production. We thus have a satisfactory picture of the cause of the decay in activity when current is drawn.

This view is supported by experiments in which oxygen was vaporized onto the broken down filament from another oxide filament. The activity of the broken down filament was reduced by more than a factor of ten. The slope

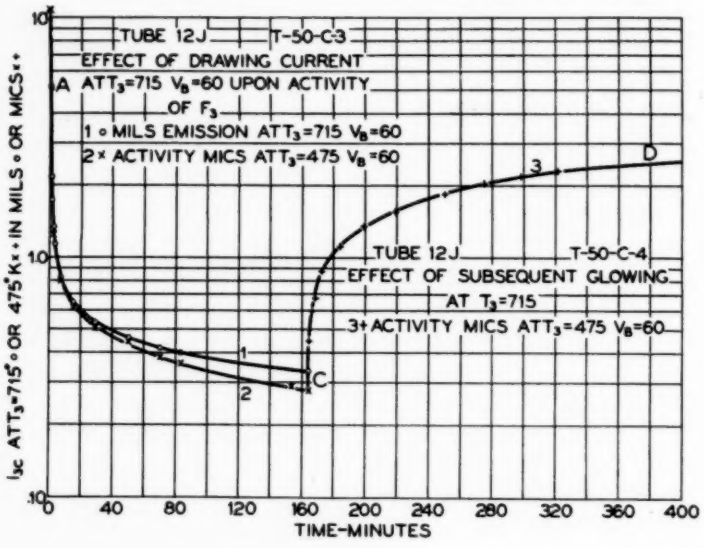

Fig. 10.

of the log i vs. θ curve was practically constant while the activity decreased by a factor of five; then the slope gradually became less.

Of course, one could postulate that the oxygen which comes to the surface combines with the barium and decreases the activity by decreasing the surface barium concentration. This, however, is unlikely since it was shown above that barium and oxygen do not permanently combine chemically when they are present on a hot tungsten surface. Even more convincing is the experimental fact (test 34, tube 89-B) that when the barium concentration was more than the optimum and oxygen was then brought to the surface, the activity decreased rather than increased. If the oxygen combines with the barium, the barium concentration should decrease and thus come nearer to the optimum concentration which should result in an increase in the activity.

If the filament is merely glowed at the same temperature at which current has been previously drawn the activity increases rapidly at first and then

more and more slowly. This is illustrated by curve 3 in Fig. 10. In general the activity either never or only extremely slowly reaches the initial activity. If, however, the filament is glowed at a high temperature such as 1200°K, the initial activity can be readily restored.

The explanation for this activation on glowing is fairly apparent. Some of the oxygen which was deposited on the surface by electrolysis is caused to leave the surface by thermal agitation. As the oxygen surface concentration gets nearer and nearer to its equilibrium value, the rate of disappearance of the oxygen decreases more and more.

Thus far we have described the effects of oxygen on the activity in a well broken down filament. We shall now proceed with the effects of oxygen in filaments which have not been broken down. The best data on this sub-

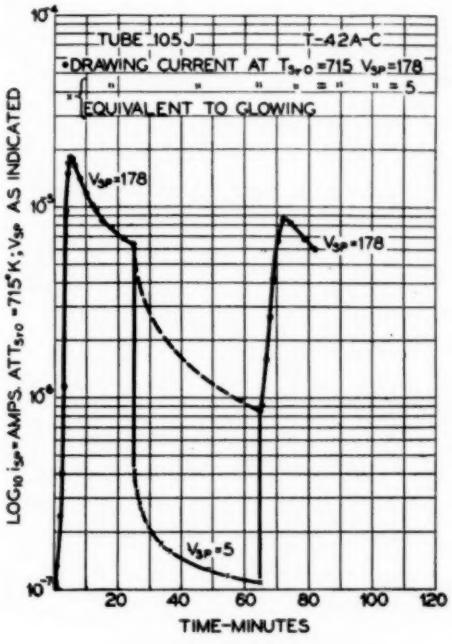

Fig. 11.

ject were obtained with an uncombined strontium oxide filament. The results were confirmed with an uncombined barium oxide filament and to some extent in a barium oxide plus strontium oxide combined filament. They are thus quite general and well established even though similar results have never been reported in the literature.

When current was drawn from the unbroken down strontium oxide filament in tube 105-J at a temperature less than 950°K and a plate potential of 178 volts, the log of the emission increased slowly, then more rapidly, then more slowly again until it reached a peak or maximum value beyond which it decreased and asymptotically approached a steady value. A typical curve is shown in the first part of Fig. 11. The rate of activation and the height of the peak increased considerably with the plate potential. For sufficiently

small plate potentials such as 30 volts the activity never passed through a peak value but merely increased to its steady value.

When the filament was glowed at the same temperature at which current had been drawn, the activity decreased rapidly at first, then more and more slowly. This activity was determined under testing conditions which did not alter the activity: either both the temperature and the plate potential were decreased, or else the plate potential alone was decreased to a low value. The solid line in the second part of Fig. 11 shows the decrease in the activity when the plate potential was reduced to 5.0 volts. The dashed line above this solid line shows the instantaneous emission that would have occurred if the plate potential had been changed back to 178 volts at any particular instant. This was actually done at time 65 minutes with the result shown in the third part of the figure. A peak was again obtained, but this peak was lower and occurred later than the first peak. In order to duplicate the first curve it was found necessary to glow the filament at a much higher temperature such as 1200°K for 5 or 10 minutes.

If the data of the first curve in Fig. 11 are used to plot a curve of the log of the activity vs. mic-minutes of current drawn from the filament, a straight line is obtained for the initial portion of the curve. The slope of this line is a measure of the rate at which some activating material is coming to the surface. A series of experiments has shown that the slope of this line (1) increased rapidly with the plate potential, (2), decreased as the temperature increased, (3) increased when the surface was slightly covered with an active material vaporized from the plates, (4) decreased if the filament was not thoroughly glowed after the preceding test, (5) decreased markedly as the degree of breakdown increased. The height of the peak emission divided by the initial emission varied in this same manner with these five factors. The mic-minutes required to reach the peak (1) decreased with the plate potential (2) decreased as T increased, (3) and (4) changed slightly with the third and fourth factor given above, (5) decreased from about 20 to about 2 mic-minutes per cm² when the filament was broken down. In the case of a barium oxide uncombined filament in tube 123-J the peak came at about 60 mic-minutes per cm².

At first sight it might appear that this peak was due to barium as in the case of Figs. 5, 6 and 7. The following reasons show that this cannot be so: (1) the barium is deposited on the core and the temperature is so low that it seems highly improbable for the barium to diffuse rapidly enough to the surface of the oxide to account for the rapid increase in activity; (2) the glowing curve in Fig. 11 decreases rather than increases as it did in Figs. 6 and 7; (3) the activity at the peak is very variable and depends on the conditions prevailing during the treatment while in the barium case the optimum activity does not depend on these same conditions; (4) the optimum activity due to barium is about 50,000 times the initial activity while for this peak phenomenon the peak activity is less than 1000 times the initial activity.

The hypothesis which we tentatively propose for this peak on drawing current is an extension of what is already known. Due to electrolysis, oxygen is brought to the surface. As will be shown below the factors that determine

the amount of electrolysis are of the same sort as those that determine this peak phenomenon namely, plate potential, temperature and composition of the oxide. Hence it is natural to ascribe this peak phenomenon to oxygen. From analogy with caesium on tungsten it is to be expected that a little oxygen increases the activity while more oxygen decreases it. Whether the activity is increased or decreased depends upon just where the oxygen is located with reference to the surface barium atoms. If the oxygen is beneath the barium layer, the activity is raised because the negative oxygen induces more positive barium ions and the moment of the additional barium ions and their images more than counterbalances the moment of the oxygen ions and images. If on the other hand, the oxygen is on top of the surface layer of barium, the activity is decreased because now the moment due to the oxygen is greater than the moment due to the barium.

By combining the hypothesis with the experimental facts we may draw the following conclusions: oxygen is deposited by electrolysis just beneath the partial surface layer of metallic barium or strontium. If the temperature is high enough some or all of this oxygen rather rapidly arrives at the top of the barium layer where it forms an outer oxygen layer which is a more stable layer than the inner oxygen layer. If the temperature is low enough the first oxygen that is deposited stays in the inner layer. As the oxygen concentration increases, the field tending to pull electrons and negative oxygen ions toward the plane of the barium ions increases and some of the oxygen reaches the top of the barium layer. At the peak the factors tending to increase the activity are balanced by those tending to decrease it. Beyond the peak the net result of electrolysis is the increase in concentration of the outer layer of oxygen. We believe that some of the oxygen also diffuses inward into the oxide. If the filament is glowed either before or after the peak, oxygen leaves the inner layer; it reaches the outer layer or diffuses into the oxide.

To be consistent we need to apply this hypothesis to the case of well broken down filaments in which emission is accompanied by a decrease in activity. For well broken down filaments the field which tends to pull electrons and also negative ions into and beyond the plane of the positive Ba ions is very great so that even at very low temperatures the oxygen is rapidly pulled into the outer layer. It may also be that in well broken down filaments the inner oxygen layer is already near its maximum concentration, and any additional oxygen is forced to go to the outer layer. This latter view would fit in well with the observed fact that the maximum activity which can be obtained depends on one or more factors besides the optimum amount of barium. The study of the effect of oxygen on the activity is still far from complete.

(6) Diffusion of oxygen. That oxygen diffuses from the surface into the oxide follows from the same sort of evidence as that presented above for the diffusion of barium. The argument which was presented there and which was based on the life of the filament can be applied word for word for oxygen.

Another line of evidence for the diffusion of oxygen is this: if current is drawn from a broken down coated filament even at as low a temperature as 550°K the activity decreases. After the decrease amounts to a factor of

about three, the filament can be glowed at this same temperature. It is then found that the activity increases due to the glowing. This increase in activity is presumably due to the disappearance of oxygen from the surface. We should hardly expect oxygen to evaporate under these conditions: at any rate, we have never been able to detect it. Consequently we must conclude that the oxygen diffuses into the interior of the oxide.

As more and more oxygen diffuses into the interior the concentration of oxygen in the oxide increases. Some of this oxygen presumably recombines with metallic barium; some of the oxygen must diffuse back to the surface at a rate which is presumably proportional to the concentration of oxygen in the oxide. If current is drawn from the filament for a long time at a constant temperature and plate potential, the net diffusion inward decreases and may eventually approach zero especially if the temperature is high enough so that oxygen evaporates.

(7) Factors which determine the amount of electrolysis. Only a relatively small part of the current through the oxide can be carried by positive barium ions and negative oxygen ions. The ratio of ion current to total current for barium is not necessarily the same as for oxygen. For barium this ratio depends upon the temperature and the composition of the oxide; it is independent of the speed with which electrons from the outside strike the filament. For oxygen this ratio depends upon the composition of the oxide and the field strength at the surface of the filament when current is drawn from it; presumably it also varies with the temperature.

The ratio barium ion current to total current can be determined from the data for curves like those in Figs. 5, 6 and 8. The calculations based on Fig. 5 are given above: it was found that roughly one part in 200 of the current was carried by strontium ions. A similar computation for Fig. 6 leads to the conclusion that in this case 1/240 of the current is carried by barium ions. For this calculation we have used the following data: at the initial activity the fraction of the surface covered with barium was 0.90 while at the optimum it was 1.00; this 0.1 layer was deposited in 36 mic-minutes or 48 mic-minutes per cm^2; 2 mic-minutes per cm^2 of ion current were taken to correspond to one layer. A similar computation for Fig. 8 gave the result that about 1/300 of the current was carried by barium ions.

A series of tests showed that when the temperature of the coated filament was purposely raised above that prevailing in the tube while electrons were sent into it, a curve was obtained which was similar to that in Fig. 8 except that the mic-minute axis was increased by a constant factor. From this we conclude that the ratio of barium ion current to total current decreases by about a factor of 2.0 when the temperature is increased from about 300°K to about 600°K.

In another series of tests it was shown that the curve similar to that in Fig. 8 did not depend upon the potential of the oxide coated filament with respect to the source of the electrons. To obtain this result, it was however, necessary that the distribution of the current from one filament to the other was not altered when the potential between the filaments was changed.

Hence, the amount of electrolysis is not dependent upon the speed with which the electrons strike the oxide.

Our knowledge of the factors that determine the ratio of oxygen ion current to total current is based partly on the factors that determine the rate of evaporation of oxygen which were discussed in a previous section. It was there shown that the evaporation rate depended greatly on the composition or state of the oxide and also on the plate potential. Presumably the rate of oxygen production varies in the same manner as the rate of evaporation.

The rate of oxygen production was also studied by determining the decrease in log i as a function of the mic-minutes drawn from the filament. The initial slope of a plot of these variables is a measure of the oxygen ion current to the total current. From a large number of tests it follows that this ratio decreases with the degree of breakdown of the filament. Presumably this means that as more and more metallic barium is dispersed through the oxide a larger and larger proportion of the current is carried by electrons.

Another series of tests on about 10 different filaments has shown that the amount of oxygen produced per milliampere minute increases rapidly with the positive plate potential and that if the current is limited by space charge comparatively little oxygen is produced. This conclusion is again based on the initial slopes of log i vs. milliampere minute curves.

It has been tacitly assumed that the rate of oxygen production varies directly with the electron current. This tacit assumption is difficult to prove since every factor which changes the emission current seems at the same time to change the rate of oxygen production. Since, however, it is shown above that the rate of barium production is directly proportional to the electron current, we can quite safely assume that the rate of oxygen production is also directly proportional to the current.

The fact that the oxygen yield depends so markedly on the plate potential presumably means that part of the potential difference between the filament and plate is used up in the oxide but that the P.D. across the oxide is not directly proportional to the electron current through the oxide. In other words, the conductivity of the oxide does not obey Ohm's law. From the fact that little or no electrolysis takes place when the current is limited by space charge, we are inclined to believe that there is little or no potential difference across the oxide in this case. The electrons get through the oxide not because of a field in the oxide but because of a diffusion pressure similar to that which has been shown to exist in an arc.

We have no evidence at present that the oxygen yield varies with the temperature but from analogy with the barium yield, it seems probable that the oxygen yield per milliampere minute decreases somewhat as the temperature increases.

(8) Time changes in coated filaments. A rather complete study has been made of the changes in emission that occur in time as a function of the temperature, the plate potential, the immediate previous treatment and the remote but violent previous treatment. This has been done for various types of filament. We shall first describe the time changes that occur in a barium

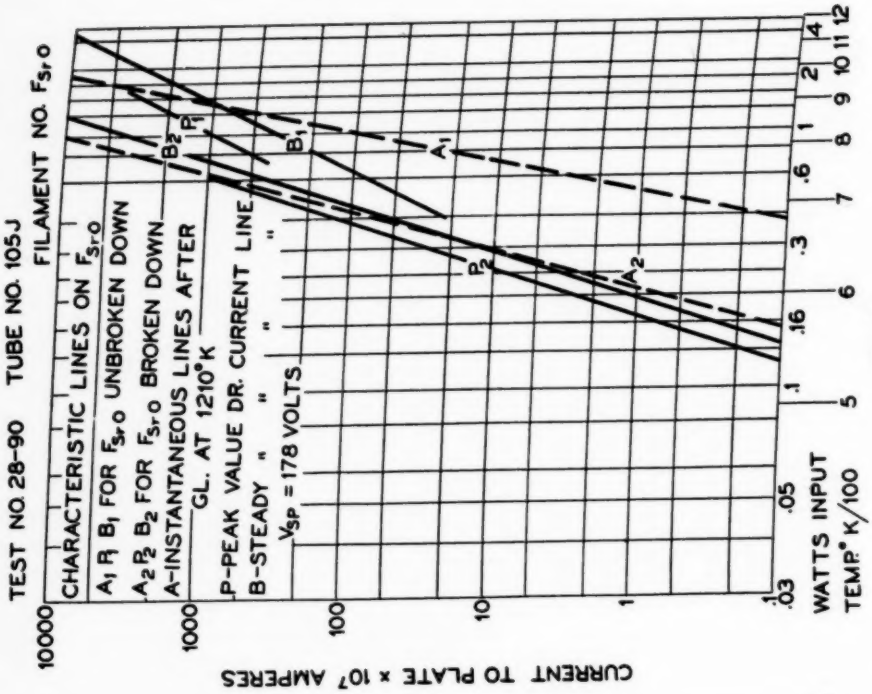
TEST NO. 28-90 TUBE NO. 105J FILAMENT NO. $F_{Sr\,O}$
CHARACTERISTIC LINES ON $F_{Sr\,O}$
A_1 P_1 B_1 FOR $F_{Sr\,O}$ UNBROKEN DOWN
A_2 P_2 B_2 FOR $F_{Sr\,O}$ BROKEN DOWN
A-INSTANTANEOUS LINES AFTER GL. AT 1210°K
P-PEAK VALUE DR. CURRENT LINE
B-STEADY " " "
V_{SP} = 178 VOLTS
CURRENT TO PLATE x 10^7 AMPERES
WATTS INPUT
TEMP° K/100

Fig. 13.

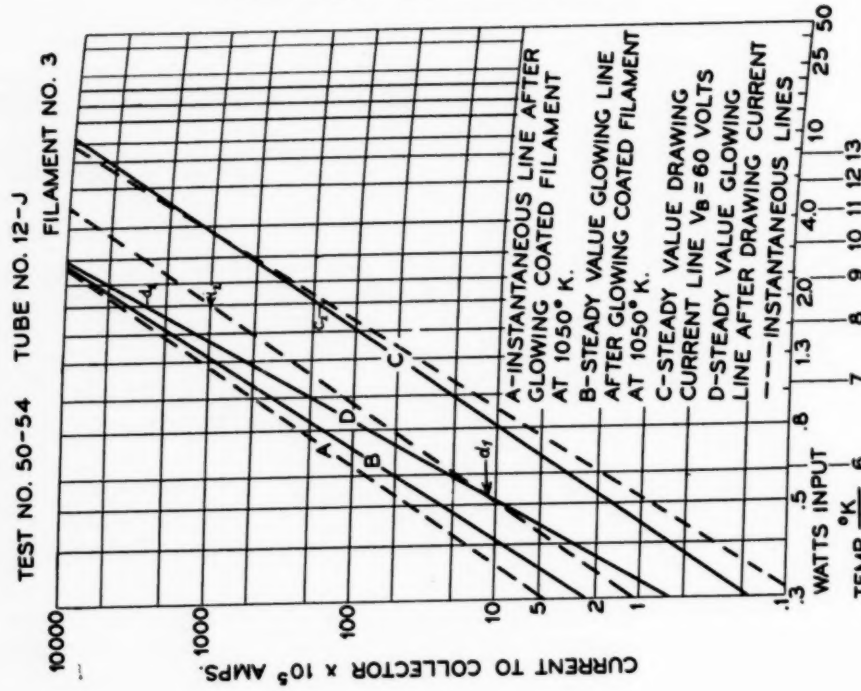
TEST NO. 50-54 TUBE NO. 12-J FILAMENT NO. 3
A-INSTANTANEOUS LINE AFTER GLOWING COATED FILAMENT AT 1050° K.
B-STEADY VALUE GLOWING LINE AFTER GLOWING COATED FILAMENT AT 1050° K.
C-STEADY VALUE DRAWING CURRENT LINE V_B = 60 VOLTS
D-STEADY VALUE GLOWING LINE AFTER DRAWING CURRENT
---INSTANTANEOUS LINES
CURRENT TO COLLECTOR x 10^5 AMPS.
WATTS INPUT
TEMP $\frac{°K}{100}$

Fig. 12.

oxide+strontium oxide combined broken down filament. Then we shall discuss the changes in an uncombined filament, first, before breakdown and later after some breakdown has occurred.

These time changes can best be described in terms of power emission curves. It was first found that the effect of any immediate previous history of the filament could be wiped out by a one to ten minute glowing at about 1050°K. The activity at a low testing temperature could repeatedly be restored to a definite value by this treatment. In the case of filament F_3 tube 12-J, this activity is represented by the uppermost dashed line *A* in Fig. 12. Since the emission decreased when current was drawn, it was in some cases necessary to extrapolate the current to zero time. At low temperatures the time changes are so slow that this need not be done. A typical decay curve has been shown in curve 1 of Fig. 10 for a temperature of 715°K. If current is drawn for a sufficiently long time, these decay curves become practically flat. The emission for this steady value on drawing current is represented by a point on line *C* Fig. 12 at the treating temperature. By glowing at 1050°K and drawing current at other deactivating temperatures until the emission became practically steady, other points on the *C* or steady value drawing current line were obtained.

If the filament is glowed at the treating temperature after a point on the *C* line has been obtained, the emission increases rapidly at first then more and more slowly until it becomes practically flat. This is illustrated by curve 3 in Fig.10. The emission for this flat porton of the curve is then plotted against the treating temperature, and a series of such points at various temperatures constitute the *D* line in Fig. 12.

The rate at which these time changes take place increases rapidly as the temperature is increased. Thus at a temperature of 600°K it might take something like 10 hours to go from a point on the *A* line to a corresponding point on the *C* line, while at 900°K it would take only several minutes for the same transition.

If at any stage in a deactivation curve (*A*-*C*) or a subsequent activation curve (*C*-*D*) the temperature is suddenly changed to a higher or to a lower value and if the instantaneous emission is obtained for this new temperature, it will be found to lie on a line such as one of the dashed lines in Fig. 12. These lines are called instantaneous lines. They are roughly parallel to one another. These instantaneous lines are the only ones which truly represent the activity.

The *B* line is obtained by glowing at 1050°K, reducing the temperature to a lower value for a considerable time, applying the plate voltage and observing the emission at the instant the plate voltage is applied. If the plate voltage is kept on, the current will again end on the *C* line.

With such a diagram of steady value and instantaneous lines it is possible to predict the time changes that will occur in a coated filament under any set of circumstances provided it is known where the state of the filament can be represented by a point on this diagram. For example, suppose we know that the state of a filament is such as to be represented by a point d_1 on the

D line at a low temperature T_1. Suppose we now wish to know what happens if the temperature is increased to T_2 and (a) no current is drawn or (b) current is drawn. In the first case the activity will be given by i_2 in Fig. 12 and will increase to d_2. In the second case the current will decrease from i_2 to c_2.

All the lines represented in Fig. 12 are for a single plate potential of 60 volts. For a different plate potential an entirely new set of curves would hold. If the filament is given a severe treatment a complete new set of lines results.

We shall next consider uncombined filaments. Fig. 13 shows two sets of power emission lines which show the type of time changes that occurred in an uncombined strontium oxide filament before it was broken down (lines with subscript 1) and after it was partially broken down (lines with subscript 2). The dashed line A_1 represents the instantaneous emission current obtained at various temperatures after the filament had been thoroughly glowed at 1200°K. At any temperature below about 950°K the emission current increased with time, came to a peak value which is represented by a point on the P_1 line at that temperature, and then decreased to a steady value represented by a point on the B_1 line. Above about 950°K the current no longer passed through a peak but attained a steady value which again fell on the B_1 line.

After large currents had been drawn from the filament for considerable periods of time so that the filament was partially broken down, the analogous instantaneous line A_2, the peak line P_2, and the steady value line B_2 were obtained. At a given temperature the instantaneous activity had increased one hundred to five hundred-fold. The angles between A_2 and P_2, and A_2 and B_2 were now considerably smaller than the analogous angles in the preceding case. The point at which the peak phenomena disappeared was shifted to lower currents and to lower temperatures. These and other sets of such lines for different degrees of breakdown show that the peak phenomena become less pronounced and are shifted to lower temperatures as the breakdown process continues. The angle between the instantaneous line and the steady value drawing current line decreases as the breakdown process increases. These deductions fit in well with Fig. 12 for which no peak phenomena were observed and for which the angle between the instantaneous line A and the steady value glowing line C is very small.

From the discussions which have been given in preceding sections it follows that the only lines whose slopes may properly be used to obtain work functions are the instantaneous lines. If the data represented by the A_1 and A_2 lines in Fig. 13 and the A line in Fig 12 are replotted in the customary way, i.e., $\log i - 2 \log T$ vs. $1/T$, straight lines are obtained whose slopes yield work functions of 1.8, 1.3, and 0.53 volts respectively. Since it is questionable that the work function of a composite surface is independent of the temperature, no great significance is to be put on any work functions determined in this manner. As far as they go, however, the values for the work functions are quite satisfactory, since the value 0.53 volts is for a filament

which was in an unusually active condition. It might be well to point out that if work functions had been based on the steady value drawing current lines there might have been an error by more than a factor of two.

From the discussion of time changes given in preceding sections, the reader can appreciate the significance of these various lines. Their complete interpretation must be left until an even more exhaustive study has been made.

Summary

The activity of a coated filament depends upon the surface concentration of metallic barium, the surface concentration of oxygen, on the relative positions of the barium and oxygen, and on the composition of the underlying oxide. Barium can be deposited on the surface either by evaporation from an outside source, which may be another coated filament, or else by electrolysis due to sending electrons into the filament from an outside source. In either case the barium on the barium oxide acts similar to barium on tungsten: as the amount of barium increases, the log of the emission at a given temperature increases rapidly at first and then more and more slowly until it passes through an optimum value beyond which it decreases. Oxygen may also be deposited on the surface either by evaporation or by electrolysis due to drawing current from the filament itself. The effect of this oxygen on the activity is quite complex: in general it is similar to the effect of oxygen in the case of barium on oxygen on tungsten; if the oxygen is between the surface layer of barium and the oxide, it increases the activity while if the oxygen is above the surface layer of barium it decreases the activity. Both barium and oxygen diffuse quite readily from the surface into the oxide and vice versa. The rate of diffusion increases rapidly with the temperature and with the concentration gradient near the surface. When current is sent into the oxide or drawn from the oxide most of it is carried by electrons, but a small portion is carried by oxygen and barium ions. The ratio of ion current to total current depends upon the temperature, the composition of the oxide, and in the case of drawing current on the plate potential. The complex changes in activity that occur in time when the filament is treated in various ways can best be described in terms of various "power-emission" or equivalent Richardson lines, namely, instantaneous lines, steady value glowing lines, steady value drawing current lines, and peak lines. These complex time changes can in a general way be interpreted in terms of the proposed theory. Some of the features require further study.

Acknowledgment

The author welcomes this opportunity to express his gratitude to those who have preceded him in the development and study of oxide coated filaments in this laboratory, particularly H. D. Arnold, W. Wilson, J. E. Harris, M. J. Kelly and C. J. Davisson. He also gratefully acknowledges the benefit derived from numerous discussions with C. J. Davisson. E. K. Jaycox deserves great credit for diligently and carefully performing the large number of experiments.

A NEW METHOD FOR THE STUDY OF VOLTAGE-INTENSITY RELATIONS AND ITS APPLICATION TO THE MERCURY 2537A LINE

By Floyd C. Ostensen
Physics Laboratory, University of Minnesota

(Received August 15, 1929)

Abstract

Method for eliminating secondary electrons in the study of the voltage-intensity relations in spectra—All previous measurements of the relation between the intensity of spectrum lines and the velocity of the exciting electrons have been subject to uncertainties due to the presence of secondary electrons. To eliminate these effects a beam of electrons is so concentrated by a magnetic field as to prevent their striking any metal surfaces until they reach a collector which traps all secondaries. This arrangement insures that the light emitted from the path of such a beam is produced solely by electrons which have a specified velocity (to within the Maxwellian distribution).

Voltage-intensity characteristics for Hg 2537 up to 7.4 volts—The above method was applied to a study of the variation with electron velocity of the intensity of λ2537 in the Hg spectrum. The results obtained agree in a general way with those of others. A maximum intensity is found at about 6.0 volts which agrees within 0.2 volts of the values given by White and by Hanle. The rate at which the intensity drops off beyond the maximum is, however, considerably greater than that given by previous workers. This may be attributed to the elimination, in the present work, of secondary electrons.

Introduction

FOR a more complete understanding of the dynamics of the collision process between electrons and atoms, a knowledge of the probability of excitation of the atom to a given energy state as a function of electron energy is necessary. There are two experimental methods of attacking this problem: (1) from a study of the number of electrons which, at any given speed, lose the energy corresponding to the given energy state of the atom; and (2) from a study of the intensity of the spectrum lines which are emitted as a result of the excitation process. The latter method is practically limited to the study of the efficiency of excitation to the lowest excited state of the atom and must be carried out under conditions which do not permit of anything happening to the atom between the excitation and the radiation processes.

Unfortunately an examination of the existing literature shows a rather wide discrepancy, not only in the results as obtained by the two methods, but also in the results of different observers who have used the same method.

One source of error in practically all spectroscopic studies of excitation efficiencies has been the presence, in the primary beam of electrons, of large numbers of secondary electrons of undetermined speed. In principle, the apparatus almost invariably used[1] in such studies is illustrated in Fig. 1.

[1] D. R. White, Phys. Rev. **28,** 1125 (1926); P. Bricout, J. de Physique et le Radium **9,** 88 (1928); W. Hanle, Zeits. f. Physik **54,** 848 (1929); W. Hanle, Naturwissenschaften **15,** 832 (1927); W. D. Crozier, Phys. Rev. **31,** 800 (1928); J. Valasek, Phys. Rev. **29,** 817 (1927); J. H. Lees, H. W. B. Skinner, Nature **123,** 836 (1929); M. G Peteri, W. Elenbaas, Zeits. f. Physik **54,** 92 (1929).

It consists of a source of electrons F, a grid G to which is applied the variable accelerating potential, and a plate P which serves to collect the electrons which pass through the grid. The region of spectroscopic observation is the field-free space between G and P, and it is usually assumed that the electrons in this region have a velocity corresponding to the potential applied to G (with proper corrections for contact e.m.f., etc.). No one who has studied the velocity distribution of the electrons in such an arrangement can fail to have been impressed by the large number of electrons which have speeds less than that corresponding to the applied potential. These slower electrons

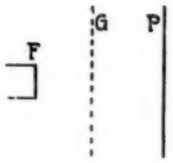

Fig. 1. Arrangement of electrodes customarily used in a study of the excitation function of spectrum lines.

are presumably secondary electrons which come from P and G by reflection or otherwise. Their number varies greatly with the nature and geometry of the electrodes. The importance of correcting for their presence has been realized by others but, in view of the uncertainties involved, it is desirable to devise a method which eliminates them entirely from the region of observation.

In what follows such a method will be described and its use will be illustrated by some preliminary measurements on the voltage-intensity relations for the 2537A line of the mercury spectrum.

Apparatus and Method

The apparatus is sketched in Fig. 2. The boxes A, B, C, are made of molybdenum. To support them in rigid alignment, short tungsten rods fastened to the boxes are sealed into a glass frame. The entire assembly is next inserted in a Pyrex tube which is then closed and attached to the vacuum

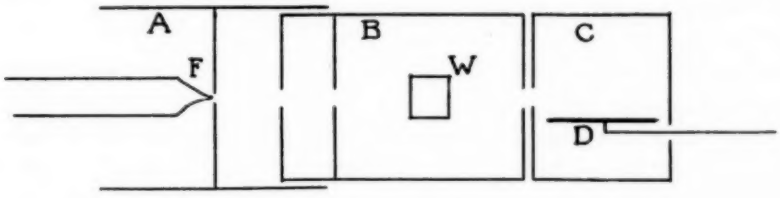

Fig. 2 Diagram of apparatus used in the present study.

system. Box A is maintained at the potential of the mid-point of the filament. A magnetic field of 200 gauss from two Helmholtz coils mounted with their axes parallel to the axis of the boxes prevents any lateral spread of the electron beam. The diaphragms in boxes B and C are of such size that no electrons from the filament will strike them. The box C contains a plate

parallel to the electron beam but removed from it by 5 mm. This plate is maintained at a positive potential of 1200 volts with respect to box *C* and serves to remove electrons from the beam and prevent the return of secondaries to *B*. The electrons are accelerated from the filament *F* to the box *B*. The space within *B* is field-free. The mean free path of the electrons should be about ten times the distance from the filament to the collector. The window *W* in box *B* is one of two openings opposite each other. One of the openings faces a horn in the glass tube which is painted on the outside with black enamel and serves as a light well. The light to be studied passes out through the opening *W* and through a quartz window to whatever photometric device may be chosen for the particular purpose in view.

Voltage-Intensity Relation for 2537A in Mercury Vapor

To illustrate the applicability of the method, it was applied to the study of λ2537 of Hg. For this purpose the pressure of Hg was limited by the presence of ice on the trap. The voltage was varied by steps of 0.2 volts from 4.6 to 7.0 volts, except near the maximum, where a closer study was made. In some of the work the filament was placed farther in front of box *A* than indicated in the diagram. This necessitated a field between box *A* and the mid-point of the filament. The results obtained with both filament arrangements gave essentially the same curve.

A quartz lens focused the light on a photographic plate. Eastman 40 plates were used. A special plate holder made possible an entire run on one plate. On the same plate graded exposures to the light were made by interposing in the light path metal screens which had been calibrated with a thermopile to determine the percentage radiant energy transmitted. These exposures were taken with the applied voltage which gave the maximum intensity, and this enabled us to determine the relation between the blackening on the photographic plate as read on the microphotometer and the energy delivered to the plate. Since all pictures were taken with 90 seconds exposure, there was no need to assume the validity of the reciprocity law for time and intensity of radiation. The plates yielded very nearly a straight-line relation between the logarithm of energy and the deflection on the microphotometer. Photographs taken at 4.1 applied volts showed no stray light. The current to the plate was measured and was about 27 microamperes. Unfortunately because of imperfect alignment there was a slight current to the front face of box *B*.

The results of the measurements are plotted in Fig. 3. Their reproducibility can be estimated from a comparison of the positions of the circles and dots which represent two independent sets of observations. In the figure the voltage scale is arbitrarily shifted so that the curve, extrapolated to zero intensity, will cut the axis at 4.86 volts.

The chief points of interest in the curve are the steep initial rise and the abrupt decline beyond the maximum, together with the indication that the curve is a composite of two curves, one with a maximum at about 5.5 volts and the other with a maximum at about 5.95 volts. Since the whole radiation

from the beam was focused on the photographic plate it is not possible to decide whether these two maxima are characteristic of λ2537 alone or whether at about 5.7 volts a new radiation, possibly a molecular band, is added to

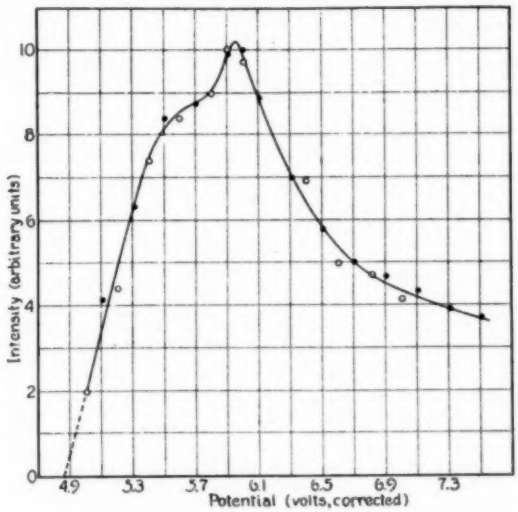

Fig. 3. Variation with electron energy of the intensity of Hg 2537.

λ2537. In this connection it may be significant that in critical potential measurements under similar conditions a critical potential at 5.7 volts is always found.

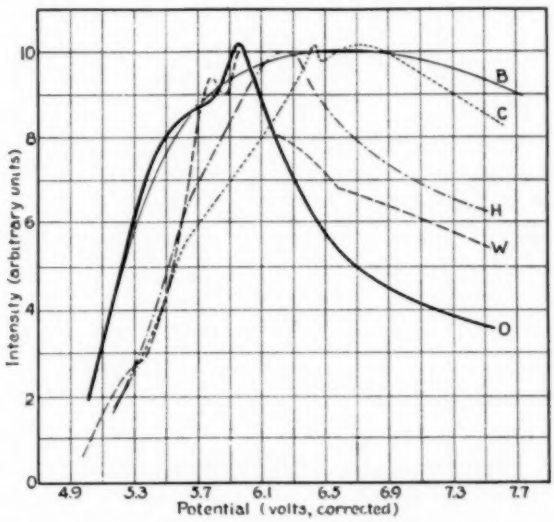

Fig. 4. Comparison of present curve (O) with the results of others. B, Bricout; C, Crozier; H, Hanle; W, White (see reference 1).

In Fig. 4 the present curve is plotted together with all curves previously published on λ2537. The most prominent distinction of the present curve is the much more rapid decline from the maximum. The reason for this is

undoubtedly the elimination of secondary electrons which in this region would be particularly effective in increasing the amount of radiation.

A detailed comparison of the present curve with the others is impossible because, in addition to the elimination of secondary electrons, the vapor pressure was here very much lower than in the other cases. The experimental conditions in Hanle's curve are probably most nearly like those of the present work and the differences in the curves are probably to be ascribed largely to the elimination of secondary electrons. In White's curve which most nearly agrees with the present one in position of maximum, the vapor pressure was so high (saturated vapor pressure at about 100°C) that most of the fine structure is attributed by White to secondary effects. It is difficult to reconcile the present curve with those of Bricout or of Crozier.

Sources of Error in the Present Work

Space charge made it impossible to take a velocity distribution. The voltage scale is uncertain, but is arbitrarily extrapolated to give zero intensity at 4.86 volts. Space charge might tend to compress or extend the applied voltage scale. A rough calculation has shown this to be 0.1 volt or less for the range of voltages studied. Space charge is known not to make the velocity distribution any broader than usual. This is also born out by the sharpness of the curve. Space charge probably causes a velocity gradient in the beam. However, in this work it was possible to study a portion of the beam 0.15 cm in length. Velocity gradient could not cause much loss of homogeneity in this length of beam.

Electrons spiral about the magnetic lines of force and make the path in mercury vapor uncertain. This is due only to the component of velocity perpendicular to the path of the beam. This should not be more than a few tenths of a volt. The only effect on the shape of the curve would be the difference in the perpendicular component for different velocity electrons. This is a second order correction. In addition to this, the radius of the spiral is proportional to the square root of the voltage. This divides by two any percent of error due to this source. Furthermore the ratio of the perpendicular component of velocity to the total should be practically the same over this range of velocities.

It might be supposed that the radiation given out by atoms excited by electrons of 6.0 or 7.0 volts would have a slightly different fine-structure from that of the light given out by atoms excited by electrons of 5.0 volts. This might cause the absorption coefficient of the mercury vapor to change considerably, and would mean that the observed curve would not represent the true intensity. Hanle tested this by putting additional mercury vapor in the path of the light and taking another test. He concludes that the shape of the curve is, within experimental error, independent of the length of path in mercury vapor.

In conclusion, I wish to thank Professor John T. Tate who suggested the problem and its method of attack and under whose guidance the work was done. Thanks are also due to the entire staff, especially Mr. Wm. Haliday, Mr. Charles Johnson, and Mr. E. Greinke for help with the apparatus and the glass work.

THE MAGNETIC MOMENT OF THE OXYGEN ATOM

By O. E. Kurt[1] with T. E. Phipps
Laboratory of Physical Chemistry, University of Illinois

(Received October 2, 1929).

Abstract

The magnetic moment of the oxygen atom has been investigated by the atomic ray method of Stern and Gerlach. The atomic oxygen was formed by means of an electrodeless ring discharge and the ray was detected by its oxidizing action on freshly sublimed litharge. When the ray was passed through an inhomogeneous magnetic field the resulting image consisted of an undeviated central line and two broad lines displaced symmetrically, one on each side. Hydrogen was substituted for oxygen and the procedure was repeated. The separations obtained in the two cases provided the data necessary for the calculation of the effective magnetic moment of the oxygen atom. The experimental magneton values were zero and ± 1.67. The magneton numbers expected from the spectroscopic ground term of oxygen are 0, $\pm 3/2$, and ± 3. The effective magneton numbers which (due to overlapping of the images) would result from these values are zero and ± 1.71. The agreement is within the limits of experimental error.

Introduction

THE experimental method employed in this investigation is that developed by Stern and Gerlach.[2] Rays of atoms possessing a magnetic moment are deflected into separate rays when passed through an inhomogeneous magnetic field at right angles to the direction of the field. The deflection s_a experienced by those atoms in the ray having the most probable velocity is

$$s_a = 1/4 \cdot M/RT \cdot \partial H/\partial s \cdot (L_1^2 + 2L_1L_2) \qquad (1)$$

where M is the magnetic moment in gauss-cm per mol; L_1 is the length of the pole pieces of the magnet, or the distance the atoms must travel through the magnetic field; L_2 is the distance from the end of the field to the target; $\partial H/\partial s$ is the value of the inhomogeneity of the field in the path traversed by the atomic ray. In this equation $\partial H/\partial s$ is assumed constant throughout the path of the ray in the field. If the magnetic moment for one element is known, then the magnetic moment for another element can be calculated from the relative deflections obtained under identical conditions in the two cases. This method obviates the tedious mapping of the field necessary in the evaluation of $\partial H/\partial s$. The equation employed is

$$M_2 = M_1 \cdot s_{a_2} T_2 / s_{a_1} T_1 \qquad (2)$$

where M_1 and M_2 may be expressed either in gauss-cm or in Bohr magnetons. In this investigation the hydrogen atom, assumed to have a magnetic mo-

[1] This communication is an abstract of a thesis submitted in partial fulfilment of the requirements for the degree of Doctor of Philosophy in Chemistry at the University of Illinois.

[2] Stern, Zeits. f. Physik **7**, 249 (1921); Gerlach and Stern, Zeits. f. Physik **8**, 110 (1922); **9**, 349, 353 (1922), Ann. d. Physik **74**, 673 (1924); **76**, 163 (1925).

ment of one Bohr magneton, is used as the reference substance in Eq. (2). Magneton values for the oxygen atom have been determined and compared with theoretical predictions.

Experimental

The electrodeless ring discharge. A long discharge tube of the R. W. Wood type with aluminum electrodes was used in the early attempts to prepare atomic oxygen. This method was found unsatisfactory since under optimum conditions for the discharge the aluminum electrodes were oxidized with a considerable evolution of heat, and a consequent decrease in the pressure due to the "clean-up" of the active species.

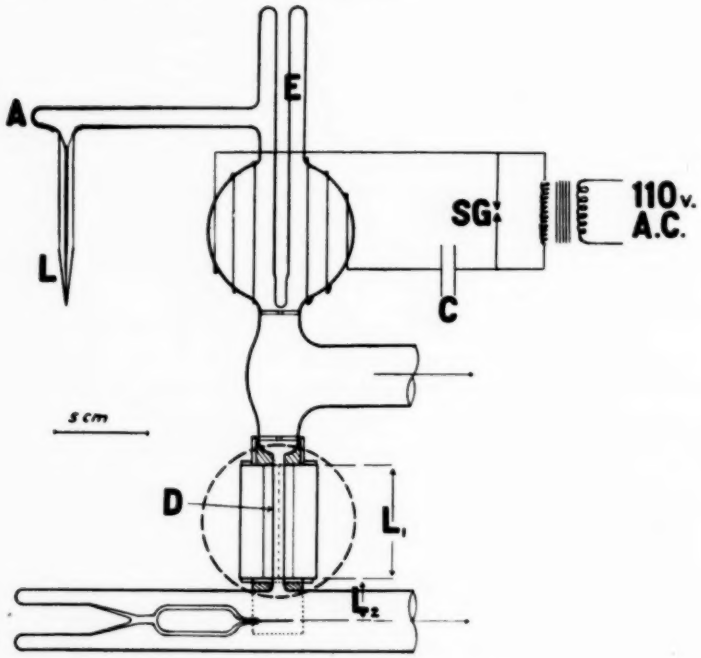

Fig. 1. Diagrammatic sketch of apparatus.

The electrodeless ring discharge was found to be a more satisfactory method. The electrical circuit is shown in Fig. 1. The secondary of a 1 k.w. 25000 volt transformer was connected with stranded leads of No. 8 B. & S. insulated copper wire through a condenser C of about 0.015 μf capacity, to six turns of copper tubing, about 0.3 cm in outer diameter, spaced equally around a Pyrex bulb of 200 cc capacity. The condenser consisted of 15 plates, each having an area of 500 cm^2. Two thicknesses of double-strength window glass between plates served as a dielectric, and the entire condenser was immersed in transformer oil. The spark gap SG consisted of two zinc electrodes, each having an area of 2 cm^2, placed about 1.5 cm apart.

In the preliminary experiments precautions were taken to insure the purity and dryness of the oxygen admitted to the discharge bulb. However,

ordinary commercial tank oxygen was found satisfactory and was used in all later experiments. The oxygen was admitted through a glass capillary, adjusted to give a suitable pressure in the discharge bulb.

The discharge was found to pass at any pressure between 0.007 and 0.45 mm. After experience had shown that the greatest chemical activity was found at a pressure of about 0.13 mm, this pressure was adopted in all later experiments. An intense line spectrum against a black background was observed under these conditions by means of a Zeiss pocket spectroscope. As seen by the eye in daylight, the discharge consisted of a general glow filling the bulb, with streamers of a different color following the directions of the coil. At low pressures the glow was a blue-gray while at high pressures a distinct pink color appeared in the blue. The streamers in both cases had a greenish blue appearance. Impurities such as mercury vapor and nitrogen were detected by their characteristic lines in the spectrum and by the changed appearance of the glow. Heating the walls of the bulb or running the discharge continuously for several hours had the effect of removing the impurities and intensifying the oxygen spectrum. The effect of water vapor as an impurity was unique and will be discussed at length in a later paragraph.

The detection of atomic oxygen. Freshly sublimed litharge was found to be an excellent detector at room temperature of atomic oxygen. The presence of water vapor, even in small traces, intensified the oxidizing conditions in the discharge. An extended investigation into the effect of varying amounts of water vapor upon the discharge led to the results summarized below.

Mixtures of oxygen and water vapor containing as much as 40 mol percent water vapor oxidized litharge in a few seconds to brown lead dioxide, when in direct contact with the discharge. Lead dioxide could be distinguished by chemical test from litharge and metallic lead, since it is very slightly soluble in 25 percent nitric acid, and gives a green color with an acetic acid solution of diphenylamine. If water vapor were in excess of about 40 mol percent the action was distinctly reducing, as in a hydrogen discharge; lead dioxide was reduced to litharge and litharge to metallic lead under these conditions. It was found that lead thus formed would be reoxidized directly to lead dioxide without the intermediate formation of litharge, when the conditions in the bulb became oxidizing.

The effect with dry hydrogen, with hydrogen saturated with water vapor at room temperature, or with water vapor alone in the discharge bulb was the stepwise reduction of lead dioxide to litharge, and of litharge to metallic lead, when these were in direct contact with the discharge. However, at a distance from the discharge, as under molecular ray conditions, lead dioxide was reduced to litharge but litharge was not reduced to metallic lead. This peculiar result has been noticed by another investigator.[3] Not only did the chemical effects indicate the presence of atomic hydrogen in all of these cases, but the Balmer series was observed to be very intense, and small particles on the walls of the discharge bulb glowed brightly. Both of these phenomena are characteristic of hydrogen atoms, and were never observed when dry

[3] DeHemptinne, Ann. Soc. Sci. Bruxelles **47B**, 143 (1927).

oxygen was admitted to a discharge bulb whose walls had been well outgassed. A very dry condition however, was not as conducive to intense oxidizing effects as was the presence of even a trace of water vapor. Hence in subsequent experiments the oxygen was saturated with water vapor at room temperatures before being introduced into the discharge bulb.

The detection of atomic oxygen with blue molybdenum oxide was also investigated. Since it was necessary to heat the oxide to a temperature of 200°C before oxidation by oxygen atoms occurred, it was considered less satisfactory than litharge.

The slit system. To produce a ray of atoms, an all Pyrex slit system was sealed to the discharge bulb as shown in Fig. 1. This consisted of two slits, 0.12 cm long and 0.005 cm wide, aligned with each other at a distance of 6.6 cm.[4] The space between the slits was connected with tubing 3.0 cm in diameter through a liquid air trap to a high speed mercury vapor pump. The second slit was connected to the target chamber by means of the small tube *D*. The target chamber was connected through a liquid air trap to a second high speed mercury vapor pump.

The target. The target consisted of a microscope cover glass held in an all Pyrex clamp so designed that the cover glass could be easily removed and mounted, for convenience in handling and photographing, on a microscope slide. No sealing wax or cement was used in holding the target. Repeated failures to obtain images when sealing wax or de Khotinsky cement were present in the vacuum led finally to the conclusion that these substances had a desensitizing effect upon the litharge surface. (This effect was not noticed with molybdenum oxide surfaces exposed to rays of hydrogen atoms.) The litharge was active only when freshly prepared and kept in a vacuum. Even in a vacuum it became less sensitive if the walls of the target chamber were heated, for the purpose of outgassing.

The litharge was deposited upon the microscope cover glass by sublimation. An oxyhydrogen flame was directed against a surface of molten litharge, thus producing a dense cloud of very fine particles. In order to obtain a fine-grained surface the cover glass was held close to the molten litharge. Under the best conditions surfaces were produced which showed no grain under high magnification. A transparent pale yellow layer about 4×10^{-5} cm in thickness was produced in this manner.

The magnetic field. A large DuBois magnet, an exact replica of the magnet used in a previous investigation,[5] was used in this research. The pole pieces were similar to those employed by Leu[6] and in accordance with his observations the inhomogeneity of the field may be assumed to be uniform throughout the region traversed by the ray. A cross-sectional view of the pole pieces is shown in Fig. 2. These were 6 cm long and were placed 0.3 cm apart. The slot was 0.6 cm wide. The edge of the 60° wedge-shaped piece

[4] The method of constructing these slit systems was devised by one of the authors, and will be published later.

[5] Phipps and Taylor, Phys. Rev. **29**, 308 (1927).

[6] Leu, Zeits. f. Physik **41**, 551 (1927).

was 0.1 cm wide. The position of the small Pyrex tube D and the path of the ray between the pole pieces are shown in Fig. 2.

Procedure. The apparatus assembled for a run is shown in Fig. 1. The discharge bulb was placed above the magnet, since in this position the discharge suffered less disturbance from the magnetic field than in any other position. Even in this position the current in the magnet coils could not exceed 5 amperes without causing serious interference with the discharge. The leak L (Fig. 1) was adjusted to give a pressure of 0.13 mm with oxygen in the discharge bulb. The pressure was measured by means of a McLeod gauge attached through a liquid air trap to the system at the point A. Before passing the discharge it was necessary to seal off the McLeod gauge to avoid "clean-up" of the atomic oxygen by the mercury of the gauge.

A run was then made with oxygen. The current in the primary of the transformer was about 13 amperes and that in the magnet coils was about 3.5 amperes. The re-entrant tube E in the discharge chamber permitted the insertion of a thermometer or thermocouple into the discharge for measuring the temperature near the first slit. The temperature remained fairly steady

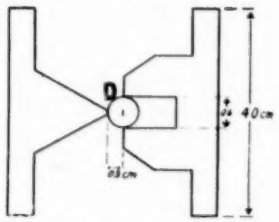

Fig. 2. Diagrammatic shetch of pole pieces (cross-section).

at about 340°C during the run. A thermometer was employed since a thermocouple was found unsatisfactory due to a disturbing effect of the discharge upon it.

An undeviated central line appeared after about two hours as a brown streak of lead dioxide on a pale yellow litharge background. After about nine hours faint lines on each side of the central line appeared. The run was continued for twenty hours,[7] after which the target was removed and attached to a microscope slide. In order to facilitate measurements of the image, photomicrographs of the image (7X) were taken (Fig. 3). It was found that blue transmitted light gave the best photograph of the oxygen image. Cramer's Super-contrast plates were employed. A density study of the re-

[7] In a preliminary run without the magnet, with 20 amperes in the primary circuit, images were visible in the vacuum within fifteen minutes. In the run with the magnet described above it was necessary to use a smaller current for a longer time due to the low capacity of the transformer. It was at first a source of surprise that twenty hours of running should be necessary to bring out the side lines to an intensity which made photographing possible. This is probably due (1) to the fact that the magnet current reduces the intensity of the discharge considerably, (2) to the fact that the magnetic field broadens the deflected ray and thus reduces its intensity, and (3) to the inadequacy of the transformer for continuous duty with large primary currents. Beyond this, however, it is probable that some unknown condition was unfavorable in this particular run.

sulting photographic negative was then made with a Moll Recording Microphotometer (Fig. 5a). A microphotometer study of the original image was unsuccessful, probably due to the slight difference in transmission coefficients of litharge and lead dioxide for the longer wave-lengths.

Fig. 3. Photomicrograph of oxygen image (7X).

Fig. 4. Photomicrograph of hydrogen image (7X).

The method employed in this investigation involves a comparison under identical conditions of the relative deflections of rays of oxygen and hydrogen atoms. The next step then was the substitution of hydrogen for oxygen

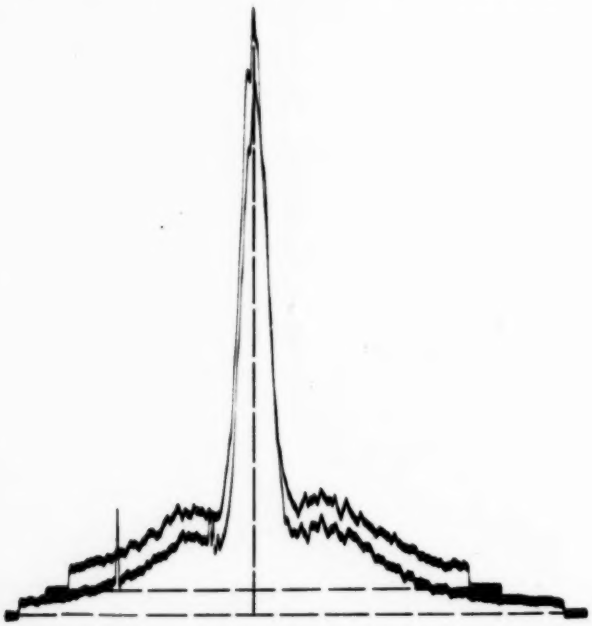

Fig. 5a. Microphotometer record of negative of oxygen photomicrograph.

in the discharge bulb. Molybdenum trioxide was used as a detector. The current in the primary of the transformer was 16 and that in the magnet coils was 3.5 amperes. The temperature of the discharge as recorded by the

thermometer near the first slit was 328°C. After fifty minutes the double-line splitting characteristic of the hydrogen atom appeared. The run was continued for three hours, after which the target was removed from the vacuum and photographed (Fig. 4).

Appearance of the images. Fig. 3 shows the photomicrograph of the oxygen image taken by transmitted blue light. From the image it can be seen that the inner edge of the deflected ray is relatively sharp compared with the

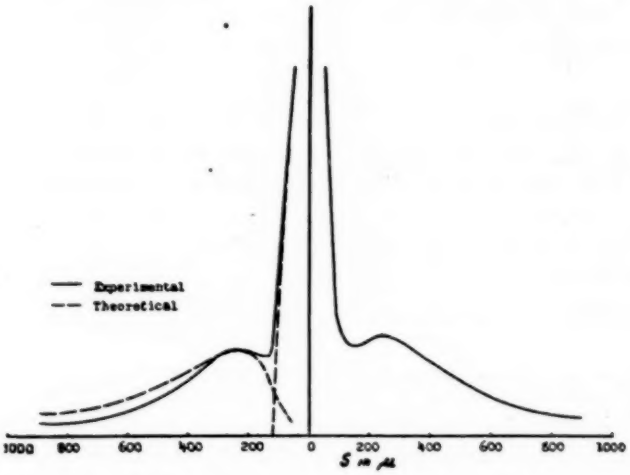

Fig. 5b. Smooth curve constructed from Fig. 5a.

outer edge, where the density falls off very gradually. This condition is unfavorable to the direct determination of points of equal density in the deflected ray, a procedure necessary to the calculation of the results. For this reason the microphotometer record (Fig. 5a) was made from the negative. Measurements were then made from Fig. 5b, which is a smooth curve constructed from Fig. 5a. The unsymmetrical appearance of the microphotometer curve for the two side lines in Fig. 5 is due to the fact that the

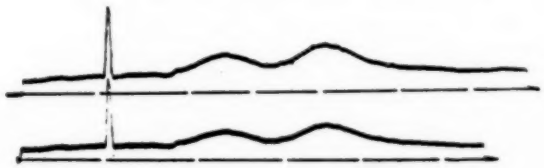

Fig. 6a. Microphotometer record of negative of hydrogen photomicrograph.

value of $\partial H/\partial s$ is not constant over the entire region traversed by the ray. served by means of light scattered along the X axis.

In the case of the hydrogen image also it was found advantageous to make the measurements from a microphotometer record of the negative. The density curve and the smooth curve constructed from it are given in Figs. 6a and 6b.

Since the value of $\partial H/\partial s$ is more constant on the side of the ray toward the slotted pole piece, all measurements were made from the corresponding side (left side) of the microphotometer curves.

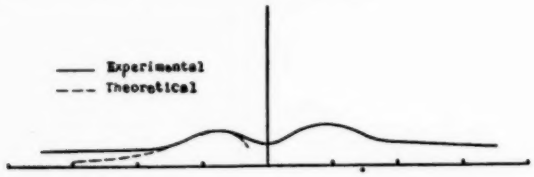

Fig. 6b. Smooth curve constructed from Fig. 6a.

Results and Calculation of Magneton Values

In order to calculate the relative magnetic moment of the oxygen atom from Eq. (1) it is necessary to know the value of s_a for both hydrogen and oxygen. This value however cannot be measured directly from the microphotographs of the images but must be calculated by means of an equation derived by Stern[8] from a consideration of the width of the undeflected ray and the Maxwellian distribution of velocities of the atoms in the ray. This equation is

$$s_a = 3s_1s_2/(s_2-s_1)\left[\ln(s_2/s_1)+a^2/s_1^2\left\{2-4s_a/3s_1+s_a^2/6s_1^2\right\}\right] \qquad (3)$$

where s_1 and s_2 are points on the inner and outer edge, respectively, of the deflected streak, which have the same intensity; a is one-half of the width of the undeflected ray. Values of s_1 and s_2 for oxygen were obtained from

Table I
Dimensions of Apparatus

Distance between the slits	6.6 cm
Distance from the second slit to the target	9.6 cm
Length of the pole pieces, L_1	6.0 cm
Distance from the end of the field to the target, L_2	2.3 cm
Width of the first slit	0.0045 cm
Width of the second slit	0.005 cm
Length of the slits	0.12 cm
One-half the width of the undeflected line, a	0.0060 cm

Measurements from Microphotometer Records

Substance	T °K		s_1 μ	s_2 μ	s_a μ	M Bohr magnetons
Hydrogen	601		100	214	383	
			129	179	405	
				Avg.	394	1
Oxygen	613	Experimental	171	300	636	
			186	286	649	
				Avg.	642	1.67
		Theoretical	175	310	658	
			190	290	666	
				Avg.	662	1.71

[8] Stern, Zeits. f. Physik **41**, 563 (1927).

measurements upon Fig. 5b, and for hydrogen were obtained from Fig. 6b. These values are given in Table I.

From these values of s_1 and s_2 corresponding values of s_α for oxygen and hydrogen were calculated by means of Eq. (3). These values were then substituted in Eq. (2) to obtain the average value of ± 1.67 Bohr magnetons for the relative effective magnetic moment of the oxygen atom,—besides the value of zero.

Discussion of errors. The maximum probable error of s_α for oxygen is about three percent, and for hydrogen about four percent, and for each of the values of T about one percent. The value of $\partial H/\partial s$ is sufficiently uniform throughout the region traversed by the ray so that any error introduced by the use of Eq. (1) instead of a more exact equation is negligible.

Theoretical prediction of the magnetic moment. The ground term of the oxygen atom has been calculated by Hund[9] from a consideration of atomic structure to be a ^3P triplet state. This prediction has been confirmed by spectroscopic data.[10] The atom has one stable state, the $^3P_2$ state, and two metastable states, the $^3P_1$ and $^3P_0$ states. Since the term values for the triplet level are known, the relative probability of each state can be calculated from the equation

$$W=(2j+1)e^{-E/kT}=(2j+1)e^{-h\Delta\nu c/kT}. \tag{4}$$

The values of the probability W calculated for each state appear in column 4, Table II. The magneton values in column 5 have been calculated according to the usual method[9] for each of the P terms.

TABLE II. *Probabilities of the normal states.*

state	term values[10]	$\Delta\nu$	W	magneton values
$^3P_2$	109833 cm^{-1}	0	5	± 3, $\pm 3/2$, 0
$^3P_1$	109674	159	2.07	$\pm 3/2$, 0
$^3P_0$	109607	226	0.59	0

By summing up the probabilities for the magneton values in the separate states the total probability for each of the values is obtained. These are given in Table III. They are used later in calculating the resultant effective magnetic moment of the oxygen atom.

TABLE III. *Probabilities of the magneton values.*

magneton values	W
$+3$ or -3	0.438
$+3/2$ or $-3/2$	0.741
0	1

The theoretical intensity distribution curve for hydrogen is presented in Fig. 7, based upon the value of s given in Table I. The equation of Stern[8]

$$J/J_0=\tfrac{1}{2}\left[e^{-y}(y+1)\right]_{s\alpha/s-\alpha}^{s\alpha/s+\alpha} \tag{5}$$

[9] Hund, "Linienspektren" (1928).

[10] Hopfield, Nature **112**, 437 (1923); Phys. Rev. **21**, 710 (1923); Astrophys. J. **59**, 114 (1924).

was employed, in which J is the intensity of the deflected ray at a distance s from the center of the undeflected ray; s_a and a are the same quantities which appear in Eq. (3); and J_0 is the average intensity of the undeflected ray.

From the value of s_a for the hydrogen atom ($M=1$, $T=601°K$) were calculated values of s_a for the oxygen atom ($M=\pm 3/2$ and ± 3, $T=613°K$). Similar intensity distribution curves were plotted for these values (curves B and C in Fig. 7). Curves B and C are intensity distribution curves respectively for $M=3/2$, and $M=3$ with the proper statistical weights given to the values of J/J_0, shown in Table III. Curve D which is a summation curve from curves B and C represents the intensity distribution which should

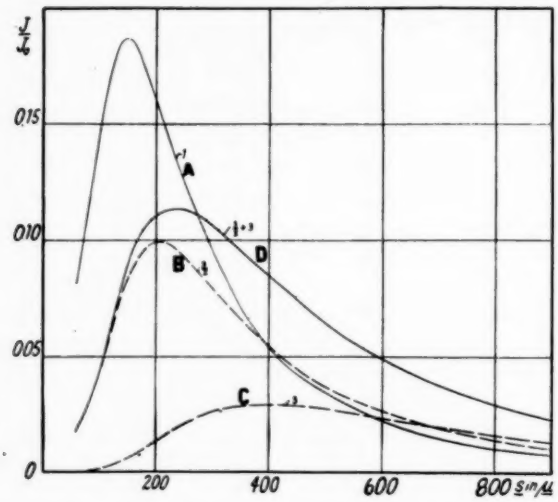

Fig. 7. Intensity distribution curves calculated as follows
A for $M=1$, $s=394\mu$. B for $M=3/2$, $s=580\mu$.
C for $M=3$, $s=1160\mu$. D is a summation of B and C.

obtain for the oxygen image. This curve appears also in Fig. 5b, for convenience in comparing it with the experimental intensity distribution curve. The theoretical curve is not expected to coincide with the experimental density distribution curve since the latter may be distorted in the direction of the intensity axis. However values of s_a and hence of M calculated from corresponding values of s_1 and s_2 taken from the two curves should agree. The extent of the agreement can be seen from a comparison of s_a (exp.) with s_a (theoret.) for comparable values of s_1 or s_2, as given in Table I, or from a comparison of the two curves in Fig. 5b. The experimental values of the effective magnetic moment of the oxygen atom, zero and ± 1.67 agree within the limits of experimental error with the theoretical values zero and ± 1.71 Bohr magnetons.

In conclusion the writers wish to thank Professors A. P. Carman and E. H. Williams of the Department of Physics for their kindness in allowing the use of the large Dubois magnet, and Mr. H. N. Swenson of the Department of Physics for his aid in making the microphotometer records.

ON THE THEORY OF THE SMEKAL-RAMAN EFFECT IN HYDROGEN-LIKE ATOMS

By Boris Podolsky* and Vladimir Rojansky
University of California, Berkeley, and Washington University, St. Louis

(Received October 11, 1929)

Abstract

It has been shown by Schrödinger and O. Klein that the Kramers-Heisenberg formulas for dispersion and incoherent scattering can both be obtained by an extension of Schrödinger's method for treating dispersion, the terms in the Hamiltonian involving squares of the potentials being neglected. The resulting formulas agree with those of Dirac. They are, however, inconvenient for calculations, as they contain summations with respect to all energy levels combining with the pair of levels under consideration, and thus imply complicated integrations when a continuous spectrum is present. This paper treats the problem of a hydrogen-like atom, acted on by light the wave-length of which is large compared to the size of the atom and the frequency of which is not too near a resonance frequency, and develops a method which obviates the necessity of integrating over the continuous range. It is an extension of the method used by one of us in treating the dispersion by atomic hydrogen. It is applied in detail to the first two levels of H. Formulas are derived for the intensities of the Smekal-Raman lines with a shift corresponding to the first absorption line.

IT HAS been pointed out by several investigators that the Smekal-Raman effect is to be expected from the formula of Kramers and Heisenberg,[1] which has also been derived entirely on the new mechanics by Dirac,[2] Schrödinger[3] and O. Klein.[4] This formula, when applied to a system possessing both a discrete and a continuous spectrum, involves a summation over the discrete range and an integration over the continuous range, and, due to the complexity of the integration, is inconvenient for the actual calculation of the intensities of the expected lines. In the present paper a theory is developed for handling the case of a hydrogen-like atom which yields intensity formulas involving only summations, and thus permits the numerical evaluation of intensities with relative ease. The width of the spectral lines is neglected in the discussion, and the final formulas involve the resonance denominators characteristic of the formula of Kramers and Heisenberg.

We start with the usual Hamiltonian function for a hydrogen-like atom in an electromagnetic field[5] in which the effects of relativity and electron spin are neglected:

$$H=1/2\mu\cdot\Sigma(p_i+eA_i/c)^2-e\phi, \quad i=1,2,3 \tag{1}$$

* National Research Fellow.

[1] H. A. Kramers and W. Heisenberg, Zeits. f. Physik **31**, 681 (1925).

[2] P. A. M. Dirac, Proc. Roy. Soc. **114A**, 710 (1927).

[3] E. Schrödinger, Ann. d. Physik **81**, 109 (1926).

[4] O. Klein, Zeits. f. Physik, **41**, 407 (1927).

[5] See for example H. Weyl, *Gruppentheorie und Quantenmechanik*, p. 88 (1928).

where μ is the mass of the electron, ϕ the scalar and $\boldsymbol{A}=(A_1, A_2, A_3)$ the vector potential, all quantities throughout this paper being expressed in Gaussian units. If $\boldsymbol{A}$ is so chosen that ϕ is merely the electrostatic potential due to the nucleus, $e\phi$ can be included in H_0, the Hamiltonian function for the unperturbed atom. Also, if $\mathrm{div}\boldsymbol{A}=0$, p_i and A_i commute, and (1) reduces to

$$H=H_0+e/\mu c\cdot\Sigma A_i p_i+e^2/2\mu c^2\cdot\Sigma A_i^2,\quad i=1,2,3. \tag{2}$$

If we assume the incident radiation to be a plane polarized light wave of frequency ν propagated along the Y axis, with the electric vector along the Z axis, the components of the vector potential may be taken to be $A_x=A_y=0$, $A_z=-cF\sin 2\pi\nu(t-y/c)/2\pi\nu$, where c is the velocity of light, and F the amplitude of the electric vector. We now neglect the size of the atom in comparison with the wave-length of the incident light,[6] neglect the last summation[7] in (2), and obtain the wave equation

$$[H_0+(h/2\pi i)\partial/\partial t]\Psi=(eF/2\pi\nu\mu)\sin 2\pi\nu t\cdot p_z\Psi, \tag{3}$$

the right hand side of which we regard as the perturbation term. Let a solution of the unperturbed problem be $\Psi_0(n)\exp[2\pi E(n)t/hi]$, so that

$$[H_0-E(n)]\Psi_0(n)=0, \tag{4}$$

where n stands for the three quantum numbers. We assume that the solution of (3) is of the form

$$\Psi(n)=\{\Psi_0(n)+\Psi_1(n)\}\exp[-2\pi iE(n)t/h]. \tag{5}$$

Substituting (5) into (3), using (4), and neglecting the term in $F\Psi_1(n)$, we obtain the equation to be satisfied by $\Psi_1(n)$:

$$[H_0-E(n)+(h/2\pi i)\partial/\partial t]\Psi_1(n)=(eF/2\pi\nu\mu)\sin 2\pi\nu t\cdot p_z\Psi_0(n). \tag{6}$$

It is seen from (6) that to be periodic, with the period $1/\nu$, $\Psi_1(n)$ must be of the form

$$\Psi_1(n)=u_1e^{2\pi i\nu t}-u_2e^{-2\pi i\nu t}, \tag{7}$$

where the u's are functions of coordinates only, satisfying the equation

$$[H_0-E(n)\pm h\nu]u=-\frac{heF}{8\pi^2\mu\nu}\frac{\partial\Psi_0(n)}{\partial z}, \tag{8}$$

[6] Definite limitations on the wave-length of the incident light will be imposed later in connection with Eq. (15).

[7] Neglecting this summation is contrary to Dirac's treatment of this problem, for he considers that this term is necessary to obtain the correct dispersion formula. The fact that the present method also leads to the correct dispersion formula can be traced to the difference in the assumed physical conditions in the two methods. Here we look for that solution of the wave equation in which the terms due to the perturbation contain factors periodic in time with the period of the incident radiation. The solution so obtained is interpreted by a generalization of the method of Heisenberg, Zeits. f. Physik **33**, 879 (1925), and E. Schrödinger, Ann. d. Physik **79**, 734 (1926).

where $p_z\Psi_0$ has been eliminated through its equivalent $(h/2\pi i)\partial\Psi_0/\partial z$, and where, as in what follows, the upper sign refers to the subscript 1 and the lower to the subscript 2. Thus to an eigenfunction $\Psi_0(n)\exp[2\pi E(n)t/hi]$ of the unperturbed atom there corresponds an eigenfunction $\Psi(n)$ of the perturbed atom of the form:

$$\Psi(n)=\left\{\Psi_0(n)+u_1e^{2\pi i\nu t}-u_2e^{-2\pi i\nu t}\right\}e^{-2\pi iE(n)t/h}. \tag{9}$$

The form of the matrix elements corresponding to the dipole moment $e\mathbf{r}=\mathbf{P}$, on neglecting terms involving two of the u's as factors, is now

$$\begin{aligned}\mathbf{P}(nn')&\equiv e\int\bar{\Psi}(n)\mathbf{r}\Psi(n')d\tau\\&=\mathbf{I}_0e^{2\pi i\nu(nn')t}+\mathbf{I}_1e^{2\pi i[\nu+\nu(nn')]t}+\mathbf{I}_2e^{-2\pi i[\nu-\nu(nn')]t},\end{aligned} \tag{10}$$

where $\nu(nn')=[E(n)-E(n')]/h$, and where the $\mathbf{I}$'s are functions of the quantum numbers only.

We now interpret $2|\mathbf{I}_0|$, $2|\mathbf{I}_1|$, and $2|\mathbf{I}_2|$ just as we would the coefficients of the Fourier expansion of the dipole moment in the classical theory, except that this dipole moment is here associated with a transition from the state n to the state n'. Thus

$$|\mathbf{I}_1|^2\cdot 8\pi^3[\nu+\nu(nn')]^4/c^3 \tag{11}$$

is the energy radiated with the frequency $\nu+\nu(nn')$ per unit time, per unit solid angle, in the direction perpendicular to $\mathbf{r}$. For the case $n=n'$, $\mathbf{I}_1=\mathbf{I}_2$, $\mathbf{P}(nn')=2\mathbf{I}_1\cos 2\pi\nu t$, and $2\mathbf{I}_1$ is the amplitude of the equivalent oscillating dipole in the state n. In the same way $\mathbf{I}_0$ and $\mathbf{I}_2$ give the energy radiated with frequency $\nu(nn')$ and $\nu-\nu(nn')$ respectively.

In order to obtain Dirac's result, it is necessary to expand the perturbation terms (5), as well as the right hand side of (6), into a series of the form $\sum_s c(s)\Psi_0(s)$. As a consequence of the use of Ψ_0's for this expansion the intensity coefficients I_0, I_1, and I_2 will contain a series, each term of which connects the initial and the final state with some other state. This tempts one to interpret the process of transition from a state n to another state n' as consisting not only of the direct jump $n\rightarrow n'$, but also of the double jumps $n\rightarrow s\rightarrow n'$, where s stands for any state which combines with both n and n'.

2. In using Eq. (9) it is inconvenient to expand the u's in terms of the Ψ_0's because these form a *complete* orthogonal set *only* if the continuous range of the functions, corresponding to the hyperbolic orbits, or to the imaginary values of the total quantum numbers, is included. Instead, we use a set of functions given by

$$T(\sigma,\lambda,\kappa;\alpha)=\left\{\left[\frac{1}{2\pi}\right]^{1/2}e^{i\kappa\phi}\right\}\left\{\left[\frac{(2\lambda+1)(\lambda-|\kappa|)!}{2(\lambda+|\kappa|)!}\right]^{1/2}P_\lambda^{|\kappa|}(\cos\theta)\right\}M_\sigma^\lambda(2\alpha r), \tag{12}$$

where

$$M_\sigma^\lambda(2\alpha r)=\left\{\frac{(2\alpha)^{\lambda+1}}{(\sigma+\lambda)!}\left[\frac{(\sigma-\lambda-1)!}{(\sigma+\lambda)!}\right]^{1/2}e^{-\alpha r}r^\lambda L_{\sigma+\lambda}^{2\lambda+1}(2\alpha r)\right\}, \tag{13}$$

in which α is any constant, σ, λ, and κ are integers satisfying the conditions $\sigma > \lambda \geq |\kappa|$, and $L_{\sigma+\lambda}^{2\lambda+1}(2\alpha r)$ is the Laguerre associated function.[8] The functions T satisfy the differential equation

$$\nabla^2 T - (\alpha^2 - 2\alpha\sigma/r)T = 0, \tag{14}$$

and it can be shown[9] that for any constant real value of α the functions given by all allowed values of σ, λ, and κ form an orthogonal and normalized set which is complete with respect to a function decreasing rapidly with increasing r, such as $r\partial\Psi_0/\partial z$. We set

$$\alpha = \alpha(n) = +\left\{-8\pi^2\mu[E(n) \mp h\nu]/h^2\right\}^{1/2}, \tag{15}$$

and restrict ourselves to the values of ν which yield a real α. This restriction is physically equivalent to our earlier assumption that the size of the atom is negligible in comparison with the wave-length of the incident light, though the equivalence should be regarded as accidental. We also set

$$\eta = 4\pi^2\mu e^2 Z/h^2, \tag{16}$$

and (8), upon the substitution of H_0 and a slight simplification, becomes

$$\nabla^2 u(n, l, m) - (\alpha^2 - 2\eta/r)u(n, l, m) = (eF/h\nu)\partial\Psi_0(n, l, m)/\partial z, \tag{17}$$

where all the quantum numbers have been written out. If we now put

$$r\partial\Psi_0(n, l, m)/\partial z = \Sigma_{\sigma,\lambda,\kappa}\, a(n, l, m;\ \sigma, \lambda, \kappa)T(\sigma, \lambda, \kappa;\ \alpha), \tag{18}$$

$$u(n, l, m) = \Sigma_{\sigma,\lambda,\kappa}\, b(n, l, m;\ \sigma, \lambda, \kappa)T(\sigma, \lambda, \kappa;\ \alpha), \tag{19}$$

we find, with the help of (14), that (17) is satisfied if we set

$$b(n, l, m;\ \sigma, \lambda, \kappa) = eFa(n, l, m;\ \sigma, \lambda, \kappa)/2h\nu(\eta - \alpha\sigma). \tag{20}$$

Thus the use of the Ψ_0's for the expansion of the u's is not necessary. The essential thing is to obtain a solution of (3) in the form (9). Since the T's are not the eigenfunctions, the states s in the process $n \to s \to n'$ will not be the eigenstates, and the interpretation of the process as a double jump loses its significance, being a spurious relation dependent on the use of the Ψ_0's.

The method here presented, with a slightly different notation, was applied to the treatment of dispersion in a previous paper.[10] As an illustration of its application to the Smekal-Raman effect we shall consider here only transitions between the states of principal quantum numbers 1 and 2, when observed by means of light scattered along the X axis.

3. We shall be concerned only with the following particular cases of (10):

$$\begin{aligned} P_z(n, l, m;\ n', l', m') = {} & I_0(n, l, m;\ n', l', m';\ z)e^{2\pi i\nu(nn')t} \\ & + I_1(n, l, m;\ n', l', m';\ z)e^{2\pi i[\nu+\nu(nn')]t} \\ & + I_2(n, l, m;\ n', l', m';\ z)e^{-2\pi i[\nu-\nu(nn')]t}, \end{aligned} \tag{21}$$

[8] E. Schrödinger, Ann. d. Physik **80**, 486 (1926).

[9] Courant and Hilbert, *Meth. d. Math. Physik I*, Ch. 5, §5, p. 239 (1924).

[10] B. Podolsky, Proc. Nat. Acad. Sci., **14**, 253, (1928) and F. Reiche, Zeits. f. Physik **53**, 168 (1929).

and similar expressions with z replaced by y. We let $n=1$, $m=l=0$, and $n'=2$; on performing the calculations it then turns out that all the I's corresponding to the permissible values of m' and l' vanish except the following:

$$I_0(1,0,0;\ 2,1,0;\ z)=e\int \bar{\Psi}_0(1,0,0)z\Psi_0(2,1,0)d\tau,$$

$$I_0(1,0,0;\ 2,1,\pm 1;\ y)=e\int \bar{\Psi}_0(1,0,0)\,y\Psi_0(2,1,\pm 1)d\tau, \tag{22}$$

$$I_1(1,0,0;\ 2,0,0;\ z)=e\int \bar{\Psi}_0(1,0,0)zu_1(2,0,0)\,d\tau$$

$$-e\int \bar{u}_2(1,0,0)z\Psi_0(2,0,0)d\tau, \tag{23}$$

$$I_2(1,0,0;\ 2,0,0;\ z)=e\int \bar{u}_1(1,0,0)z\Psi_0(2,0,0)d\tau$$

$$-e\int \bar{\Psi}_0(1,0,0)zu_2(2,0,0)d\tau. \tag{24}$$

We may write $\Psi_0(n, l, m)$, properly normalized, in the form

$$\Psi_0(n,l,m)=(\eta^{1/2}/n)T(n,l,m;\ \eta/n). \tag{25}$$

Since we need $u(1, 0, 0)$, and $u(2, 0, 0)$, we first obtain, by the use of (25):

$$r\frac{\partial\Psi_0(1,0,0)}{\partial z}=\left\{\left(\frac{1}{2\pi}\right)^{1/2}\right\}\left\{\left(\frac{3}{2}\right)^{1/2}P_1{}^0(\cos\theta)\right\}\left\{2\left(\frac{\eta^5}{3}\right)^{1/2}re^{-\eta r}\right\}, \tag{26}$$

and

$$r\frac{\partial\Psi_0(2,0,0)}{\partial z}=\left\{\left(\frac{1}{2\pi}\right)^{1/2}\right\}\left\{\left(\frac{3}{2}\right)^{1/2}P_1{}^0(\cos\theta)\right\}\left\{\left(\frac{\eta^5e^{-\eta r}}{6}\right)^{1/2}\frac{(4r-\eta r^2)}{4}\right\}. \tag{27}$$

Comparing Eqs. (26), (27), (18), and (12), we obtain:

$$2re^{-\eta r}(\eta^5/3)^{1/2}=\sum_{\sigma=2}^{\infty}a(1,0,0;\ \sigma,1,0)M_\sigma{}^1(2\alpha(1)r), \tag{28}$$

and

$$(4r-\eta r^2)(\eta^5e^{-\eta r}/96)^{1/2}=\sum_{\sigma=2}^{\infty}a(2,0,0;\ \sigma,1,0)M_\sigma{}^1(2\alpha(2)r). \tag{29}$$

Since the M's satisfy the orthogonality relation

$$\int_0^\infty M_\sigma{}^\lambda(2\alpha r)M_{\sigma'}{}^\lambda(2\alpha r)rdr=\delta_{\sigma\sigma'}, \tag{30}$$

we find that

$$a(1,0,0;\,\sigma,1,0)=2(\eta^5/3)^{1/2}\int_0^\infty r^2e^{-\eta r}M_\sigma{}^1(2\alpha(1)r)dr, \tag{31}$$

$$a(2,0,0;\,\sigma,1,0)=(\eta^5/96)^{1/2}\int_0^\infty (4r^2-\eta r^3)e^{-\eta r/2}M_\sigma{}^1(2\alpha(2)r)dr. \tag{32}$$

The integrals in these equations are calculated with the help of the relation

$$J(s,\beta;\,\sigma,\lambda;\,\alpha)\equiv\int_0^\infty r^se^{-\beta r}M_\sigma{}^\lambda(2\alpha r)dr$$

$$=\left[\frac{(\sigma+\lambda)!}{(\sigma-\lambda-1)!}\right]^{1/2}\frac{(\beta+\alpha)^{\lambda-s}}{(2\alpha)^\lambda}\left(\frac{d}{dx}\right)^{s-\lambda-1}\{x^{s+\lambda}(1+x)^{\sigma-\lambda-1}\}, \tag{33}$$

where $x=-2\alpha/(\alpha+\beta)$.

We introduce the notation $\beta(n)=-h\nu/E(n)$, $q_1(n)=[1+\beta(n)]^{1/2}$, and $q_2(n)=[1-\beta(n)]^{1/2}$; then, since $E(n)=-2\pi^2\mu e^4Z^2/h^2n^2$, Eq. (15) becomes $\alpha_1(n)=\eta q_1(n)/n$ and $\alpha_2(n)=\eta q_2(n)/n$. Substituting the relations (31), (32), and (33) into Eqs. (19) and (20), and then into Eqs. (23) and (24), and eliminating the α's by means of the q's, we finally obtain

$$I_1=\frac{2^{11}e^2F}{3\sqrt{2}h\nu\eta^2}\sum_{\sigma=2}^{\infty}\frac{(\sigma+1)!}{(\sigma-2)!}\Bigg\{\frac{q_1{}^4(2)}{2-\sigma q_1(2)}\,\frac{\{[1-q_1(2)][2-q_1(2)]\}^{\sigma-3}}{\{[1+q_1(2)][2+q_1(2)]\}^{\sigma+3}}[4-\sigma q_1(2)]$$

$$[1-\sigma q_1(2)+q_1{}^2(2)]-\frac{q_2{}^4(1)}{1-\sigma q_2(1)}\,\frac{[1-2q_2(1)]^{\sigma-4}[1-q_2(1)]^{\sigma-2}}{[1+2q_2(1)]^{\sigma+4}[1+q_2(1)]^{\sigma+2}}[4-9\sigma q_2(1) \tag{34}$$

$$+4(2+\sigma^2)q_2{}^2(1)-4\sigma q_2{}^3(1)]\Bigg\}.$$

The expression for I_2 is similar, and can be obtained directly from the expression for I_1 by substituting $q_1(1)$ for $q_2(1)$, substituting $q_2(2)$ for $q_1(2)$, and changing the sign in front of the whole expression from plus to minus.

These formulas involve only summations and, in conjunction with (11), enable one to calculate the intensity of the Smekal-Raman lines with a shift corresponding to the first absorption line, provided that the frequency of the incident light is not too near a resonance frequency of the atom (note the resonance denominators), and that the size of the atom is negligible in comparison with the wave-length of the incident light.

We wish to acknowledge our indebtedness to Mr. Harvey Hall and to Mr. G. G. Harvey for much assistance in checking this work.

ON LIFE AND CONCENTRATION OF METASTABLE ATOMS AND THE QUENCHING OF MERCURY RESONANCE RADIATION

By E. Gaviola
Department of Terrestrial Magnetism, Carnegie Institution of Washington

(Received October 2, 1929).

Abstract

A complete and general study of the dependence of life and concentration of metastable mercury atoms, optically excited, on experimental conditions, on foreign gas-pressures, and on intensity of illumination is given. This study explains why the life can not be larger than 10^{-2} second under laboratory conditions and why foreign gases act so differently in regard to the accumulation of excited atoms. The theoretical results are in good agreement with all experimental data available. An improved and more general formula for the quenching of mercury resonance radiation is obtained. The efficiencies of collisions of the second kind of metastable mercury atoms with N_2, A, and He molecules are calculated numerically. It is shown that the concentration of metastable atoms increases only with the square root of the intensity of the exciting light and not with the exciting light itself as generally assumed.

I. Life of Metastable Atoms

In A previous publication[1] I have mentioned that a provisional measurement of the transition probability of the "forbidden" line 2656 ($2^3P_0 \rightarrow 1^1S_0$) indicates that the life of a metastable mercury atoms is, when undisturbed, of the order of magnitude of 10 seconds. On the other hand all the measurements of that life made under laboratory conditions give values for it that range from 10^{-3} to 10^{-2} second. The gap between the two values is considerable. It is therefore of interest to analyze the factors that in the laboratory shorten the life so many times and to see how these factors work depending on experimental conditions. The metastable atoms that we shall consider are the ones on the level 2^3P_0. They are the only ones of importance for photosensitized fluorescence and chemical reactions. Metastable atoms are produced mainly and practically exclusively in all the cases we are considering by collisions of the second kind of resonance atoms (2^3P_1) with other molecules (Fig. 1). They are destroyed in many different ways which we shall consider one by one. Let us begin by considering a vessel with a quartz window containing saturated mercury vapor at room temperature and illuminated with the

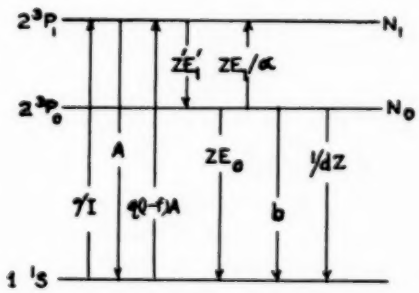

Fig. 1. Diagram of transitions regarding metastable atoms.

[1] E. Gaviola, Phil. Mag. 6, 1181 (1928).

light of a water-cooled, magnetically-deflected, mercury arc. The intensity of illumination should not be too strong. The case of strong illumination will be considered further on. Under these conditions the few metastable atoms that will be produced will almost with certainty reach the wall owing to the long mean free path at 10^{-3} mm pressure and they will be destroyed as a result of it. All experimental evidence favors the assumption that collisions with solid walls destroy all excited atoms including metastable ones. Now owing to the fact that the resonance line is reduced to one-half 5 mm vapor, the mean distance of a metastable atom from the entrance wall when it is produced is 5 mm and since the mean thermal velocity is 1.7×10^4 cm/sec, the mean time that atoms will take for hitting the entrance wall will be of the order of a small multiple of 10^{-5} second. The presence of the other walls of the vessel will decrease that time. The mean life of a metastable atom "in vacuum" can therefore not be longer than say $1/2\times10^{-4}$ second. This time could be increased only by lowering the temperature and at the same time increasing the dimensions of the vessel. The latter alone would not help owing to the fact that at room temperature most metastable atoms will, be produced only a few millimeters away from the entrance wall and they will have a good chance of hitting this wall independent of the distance of the others. Now let us assume that we introduce slowly into the vessel a foreign gas which does not or nearly does not destroy metastable atoms by collisions of the second kind. As such we may use H_2O, N_2, A, or He, which have been freed from hydrogen. The life, τ_0, of the metastable atoms will now increase in proportion to the foreign gas pressure owing to the diminishing of the diffusion rate towards the walls. At the same time the number of collisions of a metastable atom with foreign gas molecules will increase in proportion to the pressure. Now Foote[2] has called attention to the fact that at room temperature out of 6000 molecules one has a speed sufficient to perform a collision of the first kind bringing the metastable atom to the resonance level. A metastable atom will survive then on the average only $6000/E_1$ collisions, if E_1 is the efficiency factor for collisions of the first kind. The life, τ_0, will then reach a maximum value when on the average a metastable atom suffers $6000/E_1$ collisions before hitting the walls. The maximum will be reached at a pressure of a few millimeters depending on the factor E_1. If we increase the foreign gas pressure, τ_0 will be still mainly determined by the time of $6000/E_1$ collisions, but since this time decreases with the pressure, τ_0 will decrease in proportion to the inverse pressure. Let us put all this in better form: The probability of hitting the wall is $1/(c+Zd)$, if c is the probability at pressure zero, d a constant inversely proportional to the diffusion coefficient and Z the number of gas kinetic collisions, which is proportional to the pressure. If collisions with the wall were the only death reason, the life, which we will call τ_1, would be the inverse of the probability given above

$$\tau_1=c+dZ. \tag{1}$$

This is a straight line which cuts the ordinate axis at the point c and has a slope d that depends on the diffusion constant of the particular gas and especi-

[2] P. D. Foote, Phys. Rev. **30**, 288 (1927).

ally on the position of the volume element that we are considering in regard to the walls; for a volume element near a wall, d will have a smaller value than for an element farther away from it.

On the other hand the probability of suffering a collision of the first kind is ZE_1/α. Here α is the average number of collisions required for one of them to have sufficient energy to perform a collision of the first kind. This number is given by Boltzmann's formula $\alpha = e^{-w/kT}$ where w is the difference of energy between the 2^3P_1 and 2^3P_0 states. The life, considering only collisions of the first kind, is then

$$\tau_2 = \alpha/ZE_1. \tag{2}$$

The resultant life τ_0 is, if we take both processes into consideration, the inverse of the sum of both probabilities

$$1/\tau_0 = 1/\tau_1 + 1/\tau_2.$$

To simplify the formulas we will neglect c in (1) because it is small in comparison with dZ for all pressures above a tenth of a millimeter. We write then

$$\tau_1 = dZ \tag{3}$$

and obtain with it

$$\tau_0 = 1/(ZE_1/\alpha + 1/dZ). \tag{4}$$

Figure 2 illustrates τ_1, τ_2 and τ_0 as functions of the pressure Z assuming arbitrary values for d and E_1. We see that τ_0 is mainly limited by wall collisions

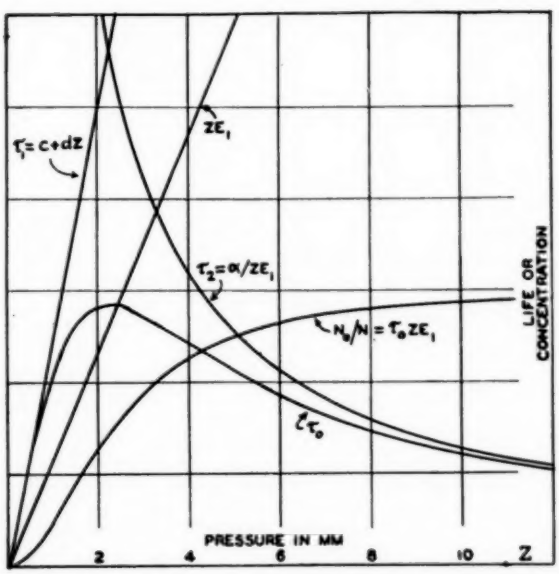

Fig. 2. Dependence of life and concentration on foreign gas pressure.

at pressures below one millimeter, while it is determined mostly by collisions of the first kind beyond 4 millimeters pressure. τ_0 can be increased only by lowering the temperature (increase of α) or by choosing a gas with small

efficiency E_1. Differentiating τ_0 in regard to Z we find that τ_0 has a maximum for $ZE_1/\alpha = 1/dZ$, that is, when the probabilities of hitting the wall and suffering a collision of the first kind are equal. Now, what are the numerical values of E_1 and d for the gases that come into consideration? Under the assumptions made so far, metastable atoms are destroyed at higher gas pressures only by collisions of the first kind. Under stationary conditions the number of transitions producing metastable atoms $N_1Z'E_1'$ (Fig. 1) must be equal to the number of transitions destroying those which are N_0ZE_1/α. We have then

$$N_0ZE_1/\alpha = N_1Z'E_1'$$

and since for higher pressures $N_0 = \alpha N_1$ as we shall see presently,

$$ZE_1 = Z'E_1'. \tag{5}$$

If we set arbitrarily $Z = Z'$, which amounts to saying that the collision section of the metastable atoms shall be set equal to that of resonance atoms in every case then we see that the efficiency of collisions of the first kind, of metastable atoms, is equal to the efficiency of collisions of the second kind, of resonance atoms. These last efficiencies have been calculated in a pre-

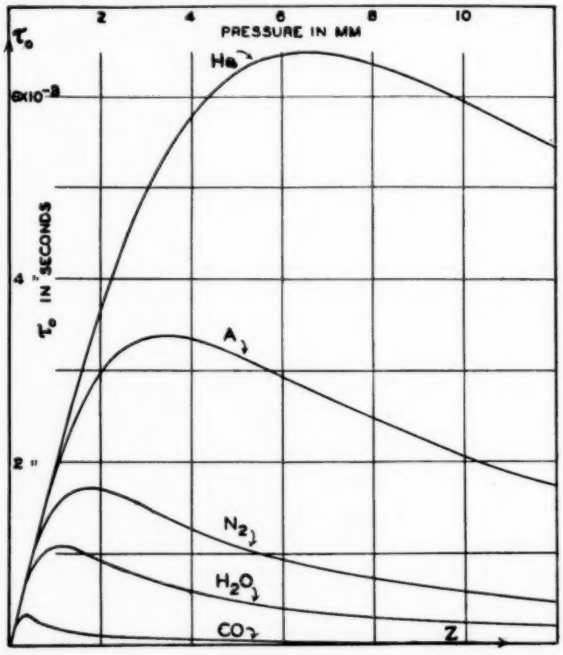

Fig. 3. Life, τ_0, as a function of the foreign gas pressure under ideal conditions.

ceding paper[3] to which we shall refer in the following, and we shall use the values given in Table II there.

The value of d depends primarily, as we said before, on the position of the volume element considered in regard to the walls and on the diffusion con-

[3] E. Gaviola, Phys. Rev. **33**, 309 (1929).

stant for metastable atoms in each particular gas. This last is not known. The dependence of d on position can be calculated exactly, but we shall not do it here to avoid lengthening the paper unnecessarily. We shall assume arbitrarily $d=2\times10^{-3}P/Z$ sec/mm (P is the pressure in millimeters) in the following for all gases. This value is in accordance with previous calculations of similar cases[4] and represents more or less an average for the experimental conditions primarily considered here. Using these numerical values we obtain the curves of Fig. 3 for τ_0. The ordinates give the life in seconds and the abscissae the pressure in millimeters.

The influence of collisions of the second kind and of impurities. So far we have assumed that collisions of the second kind of metastable atoms with foreign gas molecules have an efficiency zero. Now if an impurity in the form of H_2 or O_2 is present in the foreign gas, which will generally be the case if no special precautions are taken, this efficiency can not be zero. Moreover experimental evidence seems to show that some gases like CO have an efficiency of their own in destroying metastable atoms independent of impurities. Let us consider now how τ_0 is affected by collisions of the second kind of metastable atoms. τ_0 will be limited not only by the probabilities of hitting the wall and collisions of the first kind but also by the probability of a collision of the second kind ZE_0 if E_0 is the efficiency factor for this last type of collisions. Thus

$$\frac{1}{\tau_0}=\frac{1}{dZ}+\frac{ZE_1}{\alpha}+ZE_0=\frac{1}{dZ}+Z\left(\frac{E_1}{\alpha}+E_0\right)$$

and if we make

$$E_1/\alpha+E_0=E \tag{6}$$

then E is the total efficiency of a collision in destroying a metastable atom. τ_0 now takes the form

$$\tau_0=1/(ZE+1/dZ). \tag{7}$$

This expression is the same formula (4) of the previous case with the only difference that instead of E_1/α we have now E, which is in general slightly larger. The curves of Figure 2 then will still represent the form in which τ_0 varies with pressure, the ordinate will have to be reduced in general, and for higher pressures the reduction factor will be $E_1/\alpha E$. To give a numerical example, if we use N_2 with so much impurity in it that $E=2E_1/\alpha$ then the curve that will represent N_2 in this case is the one that corresponded to water in Figure 3. (This is because E_1 water $=2E_1$ nitrogen.)

The influence of formation of molecules, absorption of light and impurities of the vessel. It is known that in the case of a collision of a metastable mercury atom with a normal one there is a certain probability for the formation of a Hg_2 molecule. This probability will not depend on the pressure of the foreign gas. The same is true for the probabilities of absorbing lines of the arc like 4046 and of colliding with some impurity (H_2) which develops in the ves-

[4] Meissner and Graffunder, Ann. d. Physik **84**, 1041 (1927).

sel as a result of the illumination. To these we can add the probability of emission of 2656. We will denote by b the sum of the probabilities of all these processes which do not depend on the pressure. Then

$$\tau_0 = 1/(ZE + 1/dZ + b) \tag{8}$$

is the most general expression for the life of metastable atoms.

The term b will be small in comparison with $1/dZ$ for small pressures and it will be negligible in comparison with ZE for large Z; only for intermediate pressures will it affect the curve τ_0 in which case the effect will be to flatten down the maxima of the curves of Figure 2. Altogether then we see that the form of the τ_0 curves is mainly determined by diffusion on one side and by collisions of the first and second kind on the other, and that the value of τ_0 can not under laboratory conditions be increased practically beyond say 10^{-2} second at room temperature.

II. Relative Number of Metastable Atoms

The number of metastable atoms will be under all conditions given simply by the number of such atoms produced per second multiplied by their life τ_0. Metastable atoms are produced in all cases considered here mainly and

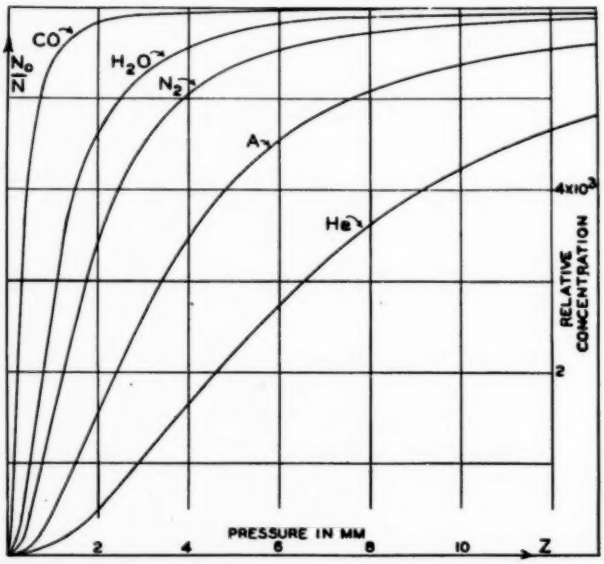

Fig. 4. Relative concentration of metastable atoms as a function of the foreign gas pressure under ideal conditions.

practically exclusively by collisions of the second kind of resonance atoms with foreign gas molecules. The number of atoms brought to the 2^3P_0 level per second is therefore N_1ZE_1 [Figure 1 and Eq. (5)] and the number of metastable atoms

$$N_0 = N_1ZE_1\tau_0. \tag{9}$$

The ratio N_0/N_1 has been plotted in Figure 2 as a function of the pressure. We see that this ratio will increase at first with the square of the pressure

owing to the fact that both ZE_1 and τ_0 increase with pressure and that it will rapidly approach the asymptotic value α. As we see, the form of the N_0/N_1 curve is very different from the one of the τ_0 curve and the maximum in the life will in general not correspond to a maximum in the concentration.

Let us now calculate N_0 under the ideal assumptions $E_0=0$ and $b=0$. τ_0 is then given by formula (4) and

$$\frac{N_0}{N_1}=\left(\frac{1}{\alpha}+\frac{1}{dE_1Z^2}\right)^{-1} \tag{10}$$

In Figure 4 I have plotted this ratio for the gases we are considering as a function of the pressure using for α, d, and E_1 the same values as before. We see that all the curves tend more or less rapidly towards the asymptotic value α given by Boltzmann's formula. A comparison of Figures 3 and 4 shows the curious result that for a given pressure the gas that allows the metastable atoms to live longest is the one which produces the smallest concentration of them. This shows again that life and amount by no means behave similarly.*

Case $E_0 \neq 0$

If we assume that $E_0 \neq 0$ the life τ_0 is given by formula (7) and the amount N_0 will be

$$\frac{N_0}{N_1}=ZE_1\tau_0=\left(\frac{E}{E_1}+\frac{1}{dE_1Z^2}\right)^{-1}$$

and if we put

$$E_1/E=\alpha' \tag{11}$$

we have

$$\frac{N_0}{N_1}=\left(\frac{1}{\alpha'}+\frac{1}{dE_1Z^2}\right)^{-1}. \tag{12}$$

This formula is identical with formula (10) with the only difference that instead of α we have now α' which is somewhat smaller than α. Formula (12) will be represented then by curves similar to the ones in Figure 4 that will converge asymptotically towards a constant value α'. This yields the interesting result that the Boltzmann distribution between 2^3P_0 and 2^3P_1 will not hold now any more even at high pressures in spite of the rapid interchange between the two levels.

The fact that N_0/N_1 becomes constant for high pressure does not mean that N_0 itself will be constant. It was so in the ideal case considered before

* Formula (10) and the curves of Figure 4 are not exact for any particular volume element v. They are exact for the average taken over the whole volume. This is due to the fact that the metastable atoms generated in a volume element v, and which have an average life τ_0, do not stay in v owing to diffusion; they distribute more or less all over the vessel, depending on the pressure. At higher pressures when the influence of diffusion disappears, formula (10) and curves of Figure 3 will be exact also for a particular volume element. An exact calculation of the dependence of N_0 on pressure and position can be made as will be shown later.

when it was assumed that $E=0$. This however, leads to $N_1=$ constant and N_1 will no longer be constant in the case $E_0=0$.

CASE $b \neq 0$

Let us consider the influence of formation of molecules, absorption of light, and of impurities of the vessel on the amount N_0. The life τ_0 is given now by formula (8). Therefore

$$\frac{N_0}{N_1}=ZE_1\tau_0=\left(\frac{1}{\alpha'}+\frac{1}{dE_1Z^2}+\frac{b}{ZE_1}\right)^{-1} \tag{13}$$

The term b/ZE_1 will be small compared with $1/dE_1Z^2$ for small pressures and it will be negligible in comparison with $1/\alpha'$ for high pressures. The curves of Figure 4 will then represent (13) adequately for small and for large pressures (replacing α by α') but for the intermediate range the presence of b/ZE_1 will flatten down the curves.

To obtain N_0 itself as a function of the pressure we have to multiply (13) by N_1. The values of $N_1=f(Z)$ can be obtained from the quenching curves of Stuart[5] or they can be calculated directly. We shall do the latter because with the help of Stuart's curves we shall be able to obtain the numerical values of E_0 and of b for some of the gases.

III. THE QUENCHING OF RESONANCE RADIATION

The quenching of mercury resonance radiation originally calculated by Foote in a very interesting paper[2] has been recently treated by Klumb and Pringsheim[6] in a more complete and very elegant way. The latter authors restricted themselves to the calculation of N_0 and did not take into consideration the reabsorption factor $q(1-f)$. To avoid repetition, I have used here Klumb and Pringsheim's results in the calculation of N_1 paying attention to the factor $q(1-f)$, and without neglecting the term τ/T_c^0 (in Klumb and Pringsheim's symbols). I give here therefore the expression for N_1 and refer to the publication[6] for its deduction. It is

$$\left(1-\frac{q}{2}\right)\frac{N_1}{N_1^0}=\left\{1+\frac{(ZE_0+b)\tau/(1-q/2)}{1/\alpha'+1/dE_1Z^2+b/ZE_1}\right\}^{-1}=J \tag{14}$$

where $N_1^0/(1-q/2)$ is the number of resonance atoms for $Z=0$, τ their mean life at $Z=0$, and q the reabsorption factor. $(1-q/2)N_1/N_1^0=J$ is proportional to the amount of resonance radiation observed and it represents the value directly measured by Stuart. For pressures above a few millimeters diffusion can in general be neglected and therefore we can put $1/dE_1Z^2=0$. Then (14) goes over into

$$J=\left\{1+\frac{(ZE_0+b)\tau/(1-q/2)}{1/\alpha'+b/ZE_1}\right\}^{-1} \tag{15}$$

[5] H. Stuart, Zeits. f. Physik **32**, 262 (1925).
[6] H. Klumb and Peter Pringsheim, Zeits. f. Physik **52**, 610 (1928).

Formula (15) is identical with formula (10) of Foote[2] if we translate his constants in the following way: $p \rightarrow Z$, $c \rightarrow b$, $b \rightarrow E_1$, $d \rightarrow E_1/\alpha$, $e \rightarrow E_0$ and $f\tau \rightarrow (1-q/2)/\tau$. We can therefore rectify (15) in the same way in which Foote did with his formula. We can thus write it as follows:

$$\frac{\alpha\tau/(1-q/2)}{1/J-1} - \frac{\alpha}{ZE_1} = \frac{1}{ZE_0+b} \tag{16}$$

If we plot therefore the inverse of the quantity at the left using Stuart's values for J, we will obtain for pressures above a few millimeters a straight line, the slope of which will give us E_0, and its value for $Z=0$ will be equal to b. Table I gives the values used and the results obtained in that way. We have set $q=1/4$ as in the paper referred to in footnote 3.

TABLE I

Gas	Z	ZE_1	E_1	b	ZE_0	E_0
CO	28. $\times 10^6 p$	28. $\times 10^6 p$	1	—	—	—
H_2O	6.4 "	2.5 "	0.4	—	—	—
N_2	6 "	1 "	0.2	1300	87	15. $\times 10^{-6}$
A	5 "	0.26 "	0.05	570	10	2 "
He	14 "	0.071 "	0.005	330	3	0.2 "

The values of b and E_0 for CO and H_2O cannot be obtained in this way due to the neglect of diffusion. We have seen that our calculation is correct only for pressures above a few millimeters; the quenching curves of CO and H_2O are only known for a few millimeters pressure and therefore an estimation of b and of E_0 cannot be made in this way for these gases. The values of b and E_0 obtained for N_2, A, and He are probably correct and give an idea of the experimental conditions of Stuart. We cannot ascribe to these values any specific meaning because b is the sum of the probabilities of four independent processes: emission of 2656, formation of molecules, absorption of light, and collisions with vessel impurities; and E_0 embodies collisions of the second kind with foreign gas molecules and with impurities that may be present. If we arbitrarily interpret E_0 as solely due to impurities (H_2) we would have to assume that Stuart had one molecule of hydrogen in 10,600 of N_2, in 66,500 of A, and in 1,860,000 of He. These values differ greatly from the ones obtained by Foote assuming $E_1=1$ for all processes (see his Table II), and are more likely to correspond to experimental conditions.

IV. Absolute Number of Metastable Atoms

Now that we have obtained the expression for N_1 and the numerical values of E_0 and b we can return to our metastable atoms. Multiplying (14) and (13) we obtain

$$N_0 = N_1^0/(1-q/2)/[1/\alpha' + (ZE_0+b)\tau/(1-q/2) + 1/dE_1Z^2 + b/ZE_1] \tag{17}$$

as the final expression for the amount of metastable atoms as a function of the pressure. We know now all the constants entering in (17) and we can therefore plot N_0 as a function of the pressure Z. This has been done in Figures

5 and 6 for the gases we are considering. We would obtain the same curves for N_2, A, He, using formula (13) and for N_1 the values taken from Stuart's curves. The ordinates of Figures 5 and 6 indicate the number of metastable atoms in a volume unit assuming that $N_1^0=1$; that is the unit of volume absorbs 10^7 light quanta of 2537 per second. As long as the illumination is not too strong the values of N_0 for each pressure will be directly proportional to the absorbed light intensity. We shall consider presently the case of strong illumination. As said before we could not obtain the values of b and

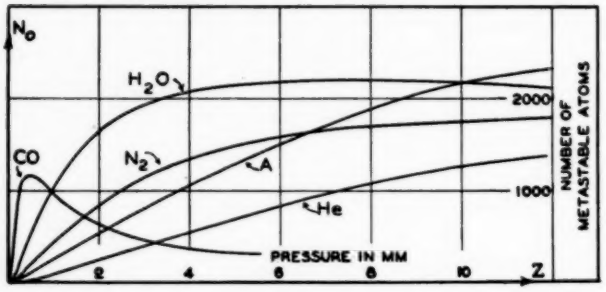

Fig. 5. Number of metastable atoms as a function of the foreign gas pressure if 10^7 quanta are absorbed per second.

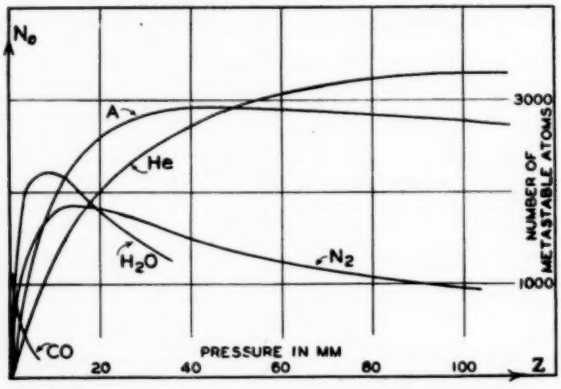

Fig. 6. Number of metastable atoms as a function of the foreign gas pressure for $N_1^0=1$ (10^7 quanta absorbed per second).

E_0 for CO and for H_2O owing to the neglect of diffusion. The curves for these two gases in Figures 5 and 6 have been obtained using formula (17) and assuming arbitrarily $b=1300$, $E_0=14\times10^{-6}$ for H_2O and $b=1300$, $E_0=177\times10^{-6}$ for CO. These values have been chosen so that for N_0 they give curves that are in agreement with the previous experimental results of the author.[1] They probably do not correspond to the experimental conditions of Stuart.

Let us see how the values of E_0 and b influence the shape of our curves N_0. A large E_0 (impurities proportional to the pressure) will displace the maximum of N_0 towards smaller pressure without flattening it much and at the same time it will make N_0 decrease rapidly for higher pressures; a large b (impurities independent of pressure) will displace the maximum towards higher pressures and it will flatten it considerably. This last has been experi-

mentally shown by Klumb and Pringsheim admitting a constant small amount of H_2 together with the nitrogen[6] (Figure 4, p. 618 in Klumb and Pringsheim's paper). The curves of Figures 5 and 6 are in general qualitative and sometimes even quantitative agreement with the experimental results of Donat,[7] Loria,[8] Klumb and Pringsheim,[6] Pool,[9] and Gaviola.[1] So for instance, the curves for the intensity of the photo-sensitized fluorescence of thallium as a function of the pressure of argon obtained by Donat are in very good agreement with the A curve of Figure 6; he found maxima for all the lines at 40-mm pressure and we see that this corresponds exactly to the maximum in the amount of metastable atoms. Since according to Loria at low pressure, N_2 is more efficient than A and according to Donat the reverse is true at high pressures, we see that the apparent contradiction between their results is removed and conciliated by Figure 5. The fact that Klumb and Pringsheim obtain a maximum in the nitrogen curve already at 1 mm pressure, would indicate that they measured the absorption of 4047 Å at some distance from any wall so that their diffusion curve (τ_1 in Figure 1) was very steep, which corresponds to a large d. The result obtained by Klumb and Pringsheim with water is almost certainly due to the pressure of free hydrogen mixed with the water vapor. According to my experience water vapor contains always some free hydrogen even before it is illuminated with the arc. Finally the curve obtained by Pool for $N_0(a)$ as a function of the nitrogen pressure is in very good agreement with our N_2 curve (Figure 6). The curve of Pool for $\tau_0(b)$ as a function of the nitrogen pressure is also in good general agreement with our curve of Figure 3. It ought to be mentioned though that according to our theory the τ_0 curve ought to increase linearly starting from zero, which the $\tau_0(b)$ curve of Pool does not do. I am not able to explain this divergence.

For a given illumination the maximal concentration of metastable atoms that can be obtained is then primarily limited by the ratio $\alpha = e^{-w/kT}$ and by the amount of impurities contained in the admixed gas. α can be increased by lowering the temperature T, but this would diminish rapidly the density of the mercury vapor in the vessel, so that no real gain would result. We can increase N_0 only by increasing the intensity of the primary light, but this has also a limit as we shall see in the following paragraph.

V. Dependence on Illumination

So far we have disregarded collisions between two excited atoms. As long as the illumination is not strong the number of excited atoms will be small in comparison with the number of normal atoms and collisions between two metastable atoms will occur rarely. But if we increase constantly the intensity of the exciting light, the number of metastable atoms will increase at first linearly with it and the probability of a collision of two metastable atoms will grow with the square of the illumination. Now Beutler and

[7] K. Donat, Zeits. f. Physik **29**, 345 (1924).
[8] S. Loria, Phys. Rev. **26**, 573 (1925).
[9] M. L. Pool, Phys. Rev. **33**, 22 (1929).

Josephy[10] have shown that by a collision of two metastable atoms there is a great probability for one of them to take over the whole energy, the other becoming normal. Both metastable atoms cease then to be such as a result of the collision. This process will put an additional limit to the life and concentration of metastable atoms.

The life was given in the general case by formula (8). It will be diminished now by the additional probability of hitting another metastable atom, which will be proportional to their number N_0. We will call it cN_0. Then

$$\tau_0=(ZE+1/dZ+b+cN_0)^{-1}=(a+cN_0)^{-1} \tag{18}$$

if we put the part independent of the illumination

$$(ZE+1/dZ+b)^{-1}=1/a. \tag{19}$$

On the other hand, the number N_0 is given always by formula (9)

$$N_0=ZE_1N_1\tau_0$$

in which N_1 is proportional to the intensity of illumination I. We can write then

$$N_0=hI\tau_0 \tag{20}$$

where h is a factor of proportionality. Combining (18) and (20) we obtain the quadratic expression

$$cN_0^2+aN_0-hI=0 \tag{21}$$

and its solution is

$$2cN_0=(a^2+4chI)^{1/2}-a. \tag{22}$$

As we see N_0 will increase only with the square root of the light intensity. We obtain in the same way for the life

$$\tau_0=\left[(a^2+4chI)^{1/2}-a\right]/2chI. \tag{23}$$

τ_0 will then decrease at the same time as N_0 increases. Now Klumb and Pringsheim[6] have observed that the absorption of the line 4047 does not increase in proportion to the illumination I if N_2 at pressures above 0.05 mm is present. The absorption reaches a certain saturation at a value of 0.55. They explain this by pointing out that since the cold vapor absorbs only the core of the line of the arc, once the whole core is absorbed no further absorption can take place. Their explanation is surely correct. It may be but one factor in the phenomenon since formula (22) shows that we can expect N_0 to grow only with the square root of the illumination. The curves of Figure 6 in Klumb and Pringsheim's paper could very well be reproduced using formula (22) assuming a suitable value for c. A repetition of Klumb and Pringsheim's experiment using two absorption vessels of equal section and different length would show how much of the saturation in the absorption is due to the different widths of the arc and absorption lines and how much to collisions between two metastable atoms.

The considerations and formula developed here for the metastable atoms of mercury apply, *mutatis mutandis*, to any metastable molecules excited optically.

[10] H. Beutler and B. Josephy, Phil. Mag. **5**, 222 (1928), Naturwiss. **15**, 540 (1927).

ENERGY CHANGES BY A VARIATION FROM THE CRYSTALLOGRAPHIC GROUP

By H. M. Evjen
California Institute of Technology, Pasadena

(Received October 11, 1929).

Abstract

The purpose of the paper may be briefly stated as follows: To investigate the possibility of energy minima by a systematic departure from the perfectly symmetrical crystalline lattice. A geometrically simple variation is considered. The surface (100-plane) of a heteropolar crystal of the face-centered type is contracted uniformly in patches, and the interior planes are likewise contracted in patches by amounts decreasing linearly with the distance from the surface. In this way a "mosaic" structure of a type previously suggested in the literature[1] is obtained. A numerical calculation of the change in potential energy is carried out for rock-salt with certain simplifying assumptions. The change in energy is obtained as a power series in terms of the maximum displacement of the ions. Due to the slow convergence of this alternating series an approximate remainder term is introduced to take care of powers higher than the third. The series contains two parameters, namely the linear extension of the patches and the depth of the cracks. The function, in general, is found to have two minima with respect to the displacement of the ions, one at zero displacement, and a second at a finite displacement. The second minimum, depending on the parameters, may be negative with respect to the former. The function also has minima with respect to the two parameters, thus proving the static stability of a mosaic structure of definite dimensions. These considerations with only minor changes, are also applicable to a mosaic structure in the interior of the crystal.

THE potential energy of two ions may be written in the form:

$$E=-(e^2/r)+A/r^{\alpha} \tag{1}$$

where the first term represents the energy due to the inverse square Coulomb forces, and the second term phenomenologically stands for the energy due to the repulsive forces between ions, which are necessary for static equilibrium. A and α in general depend on the kind of ions considered.[2] In the following, however, we shall confine our attention to crystals of the rock-salt type and shall assume that these constants are the same for each of the three combinations of ions which occur. This greatly simplifies the calculations, and is permissible in first approximation, in as much as we are not primarily interested in quantitative results. In the case of rock-salt then, the best value of α will be that corresponding to a Na-ion against a Cl-ion, namely 9.[2] With this constant fixed and the value of the lattice constant known, the value of A may be computed in the usual manner from the minimum energy condition. With Bragg's[3] value for the lattice constant of rock-salt, namely 2.81×10^{-8} cm, we obtain $A=25.8\times10^{-82}$.

[1] F. Zwicky, Proc. Nat. Acad. Sci. **15**, No. 3, March, 1929.
[2] Lennard-Jones and Dent, Proc. Roy. Soc. **A121**, 247 (1928).
[3] Bragg, X-Rays and Crystal Structure, 306, (1924).

This calculation is based on the assumption of an infinite space lattice, perfectly symmetrical, with a lattice constant everywhere the same. Needless to say, this assumption has been amply justified in the case of a great number of physical properties. In the case of certain other properties,[4] there has been a great discrepancy between theory and facts, a discrepancy which has recently led to a questioning of the above mentioned assumption.[5] It is then a matter of considerable interest to investigate the energetic aspects of a systematic departure from the space lattice of perfect symmetry. As to the type of variation to be considered there are several possibilities. These might perhaps be classified as follows: (1) Variations utilizing the loss in potential energy by contraction of planes, lines, and dipoles, from the lattice constant of the solid to that of the plane, line, or dipole respectively. (2) Variations utilizing the loss in energy by expansion of planes of homogenous polarity. (3) Variations utilizing the former two principles in combination with a rearrangement of the ions leading to losses in energy comparable with the heat of sublimation. The most favorable variation probably would be of the third type, and probably would be geometrically somewhat complicated. If, however, we can establish the existence of energy minima outside of the crystallographic group by a geometrically simple variation of the first type, our main purpose will be fulfilled. Very reliable quantitative results can hardly be expected anyway, except perhaps as to order of magnitude, since the existence of energy minima outside of the crystallographic group would in some measure invalidate our previous computation of the ionic constants α and A, constants which we shall have to use in the establishment of the minima.

The following variation, then, will be considered: Starting with an ideal rock-salt crystal, a boundary 100-plane will be contracted in square patches, the contraction of two neighboring ions being everywhere the same, namely $d/(p-1)=\delta$, except at the edges where the displacement will be d. p is the number of ions in a line element of the patch. During this first step of the variation the interior lattice planes are kept rigid. The resulting change in energy will be due to two sources: (1) Change due to the ions in the contracting plane, and (2) change due to the ions of the interior planes. As a second step in the variation the interior planes are similarly contracted by amounts decreasing linearly with the distance from the surface.

The energy of an isolated plane, contracted as outlined above, may be written:

$$E=\frac{1}{2}\sum_{l=-\infty}^{\infty}\sum_{m=-\infty}^{\infty}\sum_{r=1}^{p}\sum_{s=1}^{p}\left[\frac{(-1)^{l+m}e^2}{[(la-k_1\delta)^2+(ma-k_2\delta)^2]^{1/2}}+\frac{A}{[(la-k_1\delta)^2+(ma-k_2\delta)^2]^{\alpha_2}}\right] \tag{2}$$

where a is the lattice constant, and k_1 and k_2 are integers depending on l and r, m and s respectively in a manner such that

[4] See f. ex. F. Zwicky, Phys. Zeits. **24**, 131 (1923).

[5] See reference 1.

$$\frac{1}{p}\sum_{r=1}^{p}k_1^2=R\left(\frac{l}{p}\right)\left[p-R\left(\frac{l}{p}\right)\right]$$
$$\frac{1}{p}\sum_{s=1}^{p}k_2^2=R\left(\frac{m}{p}\right)\left[p-R\left(\frac{m}{p}\right)\right] \qquad (3)$$
$$\frac{1}{p}\sum_{s=1}^{p}k_2^3=-R\left(\frac{m}{p}\right)\left[p-R\left(\frac{m}{p}\right)\right]\cdot\left[p-2R\left(\frac{m}{p}\right)\right]$$

where the symbol $R(m/p)$ stands for remainder in m/p.

The change in energy now may be obtained by expanding the expression 2 in powers of $d/a=\delta_e$, and summing the pure number series occurring as coefficients in this expansion. The expansion converges for $d/a<1$. The coefficients of the three first terms in this expansion have been evaluated.[6] The higher orders in the expansion may, to good approximation, be said to arise entirely from the ions forming the boundaries of the patch. This enables us to replace the higher orders by an approximate remainder,[6] so that for reasonably great values of $p(p>10)$ the following functional relation is obtained between the average change in energy per ion, ΔE and δ_e:

$$pa\Delta E/e^2=1.9417-1.4753\delta_e+\{1.14p/(p-1)-0.6235\}\delta_e^2$$
$$-\{0.04-7.66/(p-1)^2\}\delta_e^3-2/(1+\delta_e)+0.0583/(1+\delta_e)^9 \qquad (4)$$

In addition to this there will be a decrease in energy due to polarization caused by the asymmetries of the mosaic configuration. This change in energy will be given by:

$$p^2\Delta E=-\frac{\alpha}{2}\sum_{t=1}^{p}\sum_{q=1}^{p}\{\overline{\Delta X^{qt}}^2+\overline{\Delta Y^{qt}}^2\}$$

where the first term in a Taylor expansion gives:[6]

$$\Delta X^{qt}=-\sum_{-\infty}^{\infty}(-1)^l\cdot\frac{2ek_1}{a^3l^3}\delta+\sum_{-\infty}^{\infty}\frac{e\delta}{a^3}\frac{k_1(m^2-2l^2)-3k_2lm}{[l^2+m^2]^{5/2}}\cdot(-1)^{l+m}$$

so that the second order change in energy will be:

$$pa\Delta E/e^2=-0.366(p/p-1)^2\cdot\delta_e^2 \qquad (5)$$

α being the average polarizability of the ions.[7]

The higher orders here may be neglected, so that the change in energy due to the ions of the contracting plane may be written:

$$pa\Delta E/e^2=1.9417-1.4753\delta_e+\{1.14p/(p-1)-0.366(p/p-1)^2-0.6235\}\delta_e^2$$
$$-\{0.04-7.66/(p-1)^2\}\delta_e^3-2/(1+\delta_e)+0.0583/(1+\delta_e)^9 \qquad (6)$$

The energy of a displaced ion in the surface due to the interior of the crystal may be written:

[6] H. M. Evjen, Thesis, California Institute of Technology, 1929.
[7] Born and Heisenberg, Zeits. f. Physik. **23**, 388, (1924).

$$E=\sum_{l=1}^{\infty}\sum_{m=-\infty}^{\infty}\sum_{n=-\infty}^{\infty}\left[\frac{(-1)^{l+m+n}e^2}{[(la)^2+(ma-h_1\delta)^2+(na-h_2\delta)^2]^{1/2}}+\frac{A}{[(la)^2+(ma-h_1\delta)^2+(na-h_2\delta)^2]^{a_2}}\right] \tag{7}$$

where h_1 and h_2 depend on p in such a way that

$$\frac{1}{p}\sum_{r=1}^{p}h_1^2=\frac{1}{p}\sum_{s=1}^{p}h_2^2=\frac{(p^2-1)}{12}. \tag{8}$$

Again an expansion by the binominal theorem gives the change in energy. Only even powers of d occur in this expansion. The second order change has been evaluated.[6] If account is taken of the Lennard-Jones contraction perpendicular to the surface,[2] it is:

$$pa\Delta E/e^2=0.0228p(p+1)/(p-1)\delta_e^2 \tag{9}$$

The total change in energy by the first step in the variation now may be written:

$$\begin{aligned}pa\Delta E/e^2=1.9417-1.4753\delta_e&+\{1.14p/(p-1)-0.366(p/p-1)^2\\&-0.6235+0.0228p(p+1)/(p-1)\}\delta_e^2\\&-\{0.04-7.66/(p-1)^2\}\delta_e^3-2/(1+\delta_e)\\&+0.0583/(1+\delta_e)^9.\end{aligned} \tag{10}$$

From which it is seen that this first step in the variation, which in itself forms a highly artificial variation out of the crystallographic group, already gives rise to energy minima. For certain values of p the change in energy may be represented as depicted in Fig. 1. The function also will be seen to

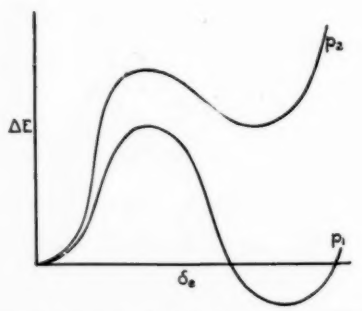

Fig. 1. Change in energy by a variation from the crystallographic group.

possess a minimum with respect to p, showing that the patches, if formed in this way, would tend to assume a definite size.

The simultaneous minimum in δ_e and p, however, falls outside of the region of convergence of the expansion, so that the value of p for which this occurs can only be roughly estimated. It is of the order of 10.

The smallness of the patches formed in this way is due to the restraining influence of the fixed space lattice represented by Eq. (9), which is distinguished by the fact that it contains p to a higher power than the contribution of the plane, (Eq. 6). When we carry out the second step of our variation this restraining influence will be seen to be practically annihilated. That is, when the boundary plane is already contracted, the forces of interaction between the planes will tend to contract the neighboring interior planes. It is not deemed necessary, therefore, actually to compute the energy of interaction between the planes by the second step of the variation, as an upper limit to the total change in energy of interaction is given by the expression (9) divided by the number of planes contracted; and this will be seen to be a rather small contribution, since the term now has lost its distinction of containing p to a higher power than the contribution of the planes. In the place of the actual value of this positive contribution we shall therefore use the upper limit.

Aside from this small change in energy due to the interaction between the planes, the change will be made up of a sum of expressions of the type 6. If this expression be denoted by $f(\delta_e)$, the sum in question will be:

$$S=\sum_{q=1}^{n} f(\delta_e \cdot q/n). \tag{11}$$

In summing the last two terms of $f(\delta_e \cdot q/n)$, the summation may be replaced by an integration, so that, writing $p=xn$, the total change in energy by the complete variation may be written:

$$pa\Delta E/e^2=1.9417-0.7376\delta_e+0.502\delta_e^2-0.0116\delta_e^3 -(2ln(1+\delta_e))/\delta_e+(0.0073/\delta_e)[1-1/[1+\delta_e]^8]+\phi(n,x) \tag{12}$$

where

$$\begin{aligned}\phi(n,x)=0.0228x\delta_e^2+\frac{\delta_e}{n}\Bigg[&-.0.736+\left(0.121+\frac{0.136}{x}\right)\delta_e+(0.02+0.26/x \\ &+0.014/x^2)\frac{\delta_e}{n}\Bigg]-\left[0.022-\frac{(1.915/x^2-0.022)}{n}\right]\frac{\delta_e^3}{n} \\ &-\frac{2}{\delta_e}ln\left(1+\frac{\delta_e}{n}\right)-\frac{2}{n\delta_e}ln\frac{1+\delta_e}{1+\delta_{e/n}} \\ &-\frac{n}{n-1}\frac{0.0073}{\delta_e}\left[1-\frac{1}{(1+\delta_e/n)^8}\right]+\frac{0.0073}{n\delta_e}\left[1-\frac{1}{[1+\delta_e]^8}\right]\end{aligned} \tag{13}$$

This functional relation again may be represented graphically by the type of curves shown in Fig. 1. The function possesses minima with respect to x and n as well as δ_e, showing that the mosaic structure, if formed in this way, would have definite dimensions. Again the absolute minimum occurs outside of the region of convergence, and the values of x and n for which maximum stability obtains can be only roughly estimated. x seems to be of

the order 1, and n of the order 25, which agrees roughly with previous phenomenological estimates.[8]

If the previous calculation had been carried out for planes very far removed from the boundaries of the crystal the final result would have been essentially the same. The only difference in the calculation would have been the introduction of factor 2 in the constant of expression 9, which again would mainly have the effect of decreasing somewhat the value of the ratio x at the absolute minimum, an effect which we should expect.

Beyond establishing the possibility of energy minima outside of the crystallographic group, the previous calculation is of interest in that it suggests the possibility of a coexistence of different modifications of the same crystallographic group below certain temperatures.

[8] A. Smekal, Zeits. f. techn, Physik **7**, 535 (1926); **8**, 561(1927) and reference 1.

LETTERS TO THE EDITOR

Prompt publication of brief reports of important discoveries in physics may be secured by addressing them to this department. Closing dates for this department are, for the first issue of the month, the twenty-eighth of the preceding month; for the second issue, the thirteenth of the month. The Board of Editors does not hold itself responsible for the opinions expressed by the correspondents.

The Nature of Cosmic Radiation

In a communication in Naturwissenschaften [16, 1044, (1928)] Bothe and Kohlhörster have described absorption experiments with the new Geiger tube counter which indicate that cosmic radiation is of a corpuscular nature. In a more detailed description of the experiments given in the same periodical [17, 271, (1929)] they estimate that if this radiation is of high speed electrons, it must have an original energy of at least 10^9 electron volts.

Although the absorption experiments seem definitely to indicate that the view of these authors is correct, more direct information on this point could be secured from experiments of the same kind with a magnetic field instead of absorption screens. With a magnetic field of 7000 gauss and 24 centimeters in diameter, it should be possible to bend electrons of 10^8 volts velocity so that most of those passing through a tube counter above the field would fail to pass through a similar counter directly below it and the magnetic field. Hence, the softer portion of the radiation would be cut off from the lower counter and the number of coincidences reduced, since the radiation comes mainly in a vertical direction.

Experiments have been started with such an arrangement using an air gap of 5 cm between the pole pieces of the electromagnet. Preliminary experiments indicate a definite decrease in the number of coincidences observed when the magnetic field is used, in confirmation of the views of Bothe and Kohlhörster. More data, however, are needed to make this point certain and a full account will appear later in the Bureau of Standards Journal of Research.

L. F. CURTISS

Bureau of Standards,
October 30, 1929.

The Kinetic Correction in Fluid Flow

When the viscosity of a liquid is determined from the rate of efflux, (E), through a capillary, a correction is made for the kinetic energy of the liquid. There is no existing method of doing this if the fluid deviates from the law of Poiseuille. Since a portion of the pressure, (P), is used in imparting energy of motion, this suggests that the correction be applied to the pressure. The work done per second on the liquid is

$$W = EPg$$

The kinetic energy of the same liquid is

$$T = \int_0^{2\pi}\int_0^R (r\,dr\,d\theta\,\rho v)v^2/2$$

v is the velocity component parallel to the axis of the capillary. The energy used in overcoming internal friction is $T-W$. The pressure used in overcoming internal friction is therefore

$$(1) \qquad P' = P - (\pi\rho/Eg)\int_0^R v^2 r\,dr$$

If the efflux is known as a function of the pressure, say $E=f(P)$, where the rate of flow is small; then this equation can be corrected for kinetic energy by writing $E=f(P')$.

The method requires that v be known as a function of r. For many fluids there exists relationships such as, $E=F(R)$. The equation

$$E = -\pi\int_0^R r^2(\partial v/\partial r)\,dr$$

defines a value of $\partial v/\partial r$. This together with the condition that $v=0$, at $r=R$, gives a velocity function which can be substituted in Eq. (1). The value of $\partial v/\partial r$, (or v), is however not unique; for to any function thus found,

as v, there can be added any number of other functions such as y, provided that $\int_0^R yrdr=0$. The added functions will not affect the efflux, since $E=2\pi\int_0^R vrdr$, but they will alter the kinetic energy term. Hypothetical y functions can be invented which satisfy all the known physical limitations to which v is subject. Because of this, even the agreement between theory and experiment shown by liquids obeying the law of Poisseuille, does not prove that the velocity function is uniquely determined.

The kinetic energy correction can therefore assume values other than those calculated by the usual methods. It is possible that the anomalous turbidity shown by ammonium oleate solutions, where turbulent flow starts at low values of the Reynold's number, may be associated with a large kinetic energy correction which originates in the above manner.

If the above limitation is ignored, the calculation for a viscous liquid yields the accepted kinetic energy term. For plastic flow, as defined by Bingham, the kinetic energy correction is identical with an empirical term which is often employed.

This paper will be published in one of the early numbers of "Rheology" (rhe-flow) a new quarterly dealing with phenomena connected with the flow of matter.

S. Bradford Stone

College of the City of New York
October 30, 1929.

The Nature of the Electrodeless Ring Discharge

There seems to be a misunderstanding as to the nature of the electric forces which produce an electrodeless ring discharge. It is commonly thought that the only force involved is the electromagnetic force due to the variation of the magnetic field and hence it is supposed that the electrons in the discharge move in circles around the axis of the solenoid. J. S. Townsend and R. H. Donaldson (Phil. Mag. **5**, 178, 1928) have shown that the electric force due to electric charges on the solenoid is generally very large compared to the electromagnetic force. During the course of some work on an electrodeless ring discharge, the writer has run across two lines of evidence which point to the same conclusion.

To produce the electrodeless discharge, the writer used an ordinary Colpitts circuit whose inductance, a solenoid of 15 turns, surrounded a cylindrical discharge tube containing hydrogen at 0.03 mm pressure. With the circuit oscillating at 50 meters and a tank current of about 7 amperes, a relatively intense discharge was produced. In order to increase the wave-length, additional inductance consisting of a coil of 7 turns was inserted in series with the exciting coil. However, these additional 7 turns did not surround the discharge tube. Under these conditions, the circuit oscillated at 100 meters with over 10 amperes in the tank circuit but *no discharge was produced.* As soon as the 7 additional turns were wrapped around the discharge tube as an extension of the original coil, a very nice discharge was obtained, and all other conditions were apparently the same as before. This then, seems to indicate that the *functioning of the electrodeless ring discharge depends primarily not on the current through the exciting coil but upon the potential difference between the ends of the coil.*

Another simple experiment, which would show whether the electric forces producing an electrodeless ring discharge were electromagnetic or electrostatic in nature, was suggested to the writer by Dr. G. Breit. The exciting coil was increased in diameter until there was about 2 cm clearance between coil and tube. Under these conditions, a discharge could still be obtained in the tube. Now a grounded cylinder of copper gauze closely fitting the discharge tube was inserted between the exciting coil and tube. This shield should have no effect on electromagetic forces in the discharge tube, but would completely screen it from any electrostatic forces. It was found that as soon as the tube was surrounded by the shield, the discharge ceased. Thus we must conclude that *the electrodeless ring discharge is an electrostatic and not an electromagnetic phenomenon.*

Charles J. Brasefield

University of Michigan,
October 30, 1929.

Raman Lines in the Spectrum of the Electric Discharge

A suggestion has been made by H. S. Allen[1] and extended by Deodhar,[2] that many of the faint lines in the secondary spectrum of hydrogen arise from Raman scattering in the electric discharge. It is the purpose of this note to call attention to a possible relationship between the results of Allen and of Deodhar and other observations on the secondary spectrum and also to discuss several difficulties that might prevent the acceptance of the above suggestion.

It may be recalled that Glitscher[3] plotted the intensity distribution in the secondary spectrum of hydrogen and pointed out that the frequency separations between the most intense maxima in the intensity curves and the Balmer lines, were approximately constant. This relationship was found to hold also for a group of secondary maxima and possibly for even lesser maxima. It has been pointed out since the observation of this fact that some theoretical significance may at some time be ascribed to it. It is interesting now to note that the work of Allen points out a similar relationship between the Balmer lines and some of the weak secondary lines. Both Allen and Deodhar have pointed out some very remarkable agreement between the frequency separations of some of the lines in the secondary spectrum of hydrogen and the Balmer lines. Furthermore they have found several groups of lines whose frequency separations from the Balmer lines are integral multiples of the lowest frequency separation. Although it is very tempting to call these lines Raman lines the frequency separations do not seem to be connected with anything that is known about the hydrogen molecule. There are other objections to the suggestion that the lines originate in Raman scattering and those objections will now be discussed.

The first of these objections arises when one compares the conditions in a discharge tube with those present in Rasetti's[4] Raman scattering experiments in hydrogen. The pressure of hydrogen in Rasetti's experiments was about 12 atmospheres and the exposure times varied from 10 to 40 hours. The pressure used was thus about 20,000 times as great as that in a discharge tube and the exposure times were about 1000 times as long as those usually employed in photographing discharge-tube spectra. These factors alone should make it very difficult to see how Raman scattering that takes place in a discharge at low pressures could ever be observed.

Granting however that there is some special and powerful scattering process in discharge tubes, one can mention another difficulty that arises when the intensity of these weak lines is considered. Since the frequency separations of these lines from the parent Balmer lines are integral multiples of a lowest frequency separation, it is reasonable to say that the energy levels that enter into the Raman effect combine with a common electronic level. One would then expect that if one of the Raman lines scattered by H_α, for example, is stronger than the corresponding one scattered by H_β, then all of the lines originating from H_α should be more intense than those originating from H_β. This, however, is not true as a glance at Allen's and Deodhar's notes will show. Furthermore, a group of lines should be scattered by the Lyman series and those scattered lines should be more intense than the ones scattered by the Balmer series. This follows from the fact that the frequencies of the Lyman series are nearer to the electronic frequencies of the molecule than are those of the Balmer lines. From the theory of the intensity of Raman scattering the above conclusion follows immediately.

Although the above arguments make it difficult to accept the notion that the weak secondary lines of Allen and of Deodhar are Raman lines, it seems that the relationship between them and the Balmer lines may prove of considerable interest. This is especially true because on a fine scale, it is exactly the same as the one discussed by Glitscher a long time ago.

JOSEPH KAPLAN

University of California
at Los Angeles,
November 4, 1929.

[1] Allen, Nature, January 26, 1929.
[2] Deodhar, Zeits. f. Physik **57**, 570 (1929).
[3] Glitscher, Sitzungsber. d. bayer. Akad., 1916, p. 125.
[4] F. Rasetti, Phys. Rev. **34**, 367 (1929).

To the Editor of the Physical Review

Dear Sir:

It is not until now that I have learned that by an oversight the letter j was used instead of J for the inner-quantum number in my recent paper on "The Arc Spectrum of Nickel" (Phys. Rev. **34,** 821 (1929)). I write to place it on record that this was a slip, resulting from haste in preparation of the final manuscript, just before my departure for a year's leave, and by no means a deliberate departure from the recommendation of the informal committee on nomenclature, of which I was a member.

Very truly yours,

HENRY NORRIS RUSSELL

November 1, 1929.

BOOK REVIEWS

Infra-Red Analysis of Molecular Structure. F. I. G. RAWLINS AND A. M. TAYLOR. Pp. 176, figs. 35. Cambridge University Press, London. 1929.

In recent years a great many papers both theoretical and experimental have appeared on the subject of infra-red spectra and in this book Rawlins and Taylor have performed the welcome service of reviewing and examining critically the more important of them. They have divided their book into the four chapters of Gases, Liquids, Solids, and Experimental. Of these the chapters on Liquids and Solids are especially interesting and the authors have attempted to dispose of many of the fantastic theories which have sprung up from time to time, and have suggested new experiments which should yield fruitful results.

Despite its excellence as a critical review of infra-red spectroscopy, the book lacks a certain organic unity and does not seem to emphasize sufficiently the essential points in the theory of molecular spectra. The Mathematical Appendix in particular does not seem to be adequate but perhaps a fuller treatment would have been outside the scope of the book.

Principally, however, the reviewer believes that it will prove valuable to specialists in the field of the infra-red, both because of its excellent bibliography and because of the intercorrelation which is given between widely scattered pieces of experimental work.

D. M. DENNISON

Speech and Hearing. HARVEY FLETCHER. Pp. 331, 151 figures. D. Van Nostrand Company, Inc. New York, 1929. Price $5.50.

This book is another of the series which has resulted from the "out-of hours courses" presented at the Bell Laboratories. It summarizes in part the results obtained during the past fifteen years in the comprehensive and fundamental survey and research program of the Bell Laboratories. In this work Dr. Fletcher has been the director.

The book is divided into four parts. In the first part, entitled "Speech," after brief descriptions of the organs of speech, of the formation of the English speech sounds, and of the methods of recording speech waves, a number of analyses of speech sounds are given. These give the power distribution as well as frequencies, or acoustic spectra.

Part two, "Music and Voice" contains chapters on the "Physical Properties of Musical Sounds" and "Noise." In these are given the wave forms and frequency spectra of some muscial instruments; also methods of measuring noise.

Part three, "Hearing" opens with a description of the organs of hearing. A theory of hearing is given based on that originally given by Helmholtz and modified and extended by recent investigation. It may be called a resonance theory but one in which the effects of friction are fully recognized. Quoting, "The pitch or position of a tone on the muscial scale is then dependent upon the position of the maximum stimulation along the basilar membrane. The character of the sound depends upon the position and relative intensities of agitation of the various parts of the basilar membrane."

In the chapters on "Limits of Audition," "Minimum Perceptible Differences in Sound" and "Masking Effects" the experimental results obtained are well summarized in graphs. The closing chapters of the third part treat "Binanal Effects" and "Methods of Testing the Acuity of Hearing." In this chapter are described tests of value to the physician and in the public schools.

In part four, "The Preception of Speech and Music" the loudness of sensation level of pure tones and complex sounds is first considered. In the chapter on "The Recognition of Pitch of Musical Tones" the pitch of a musical sound is defined as being that of a pure tone which has been adjusted to give the same sensation of pitch to the ear. By the use of a high

quality telephone system into which various filters could be introduced some interesting results on pitch recognition have been obtained. It was found that the pitch is determined by the common difference in the frequency of the harmonics, but only when these harmonics are multiples of the common difference. If this condition is not satisfied, no definite pitch can be recognized. These results have a bearing on the theory of hearing.

The last chapters describe methods of measuring the recognition of speech sounds and the effects of changes in intensity with and without frequency distortion; and the effects of other distortions and of noise on the recognition of speech sounds. In a very interesting group of curves are shown the relations between articulation and energy and frequency.

This book is a valuable contribution to our knowledge of "Speech and Hearing," as it compiles and records the recent work in that field. It should be of value to the physician and the psychologist as well as to the teacher of speech, the telephone engineer and the physicist.

J. W. BUCHTA

Television. H. HORTON SHELDON AND E. N. GRISEWOOD. 129 figures. Pp. 194. D. Van Nostrand Company, Inc. New York, 1929. Price $2.75.

The basic phenomena of television are described in a simple non-mathematical language. Then follow descriptions of the apparatus that is common to most systems such as the photoelectric cell, glow lamps and scanning and synchronizing devices. The particular arrangements used by the David, Bell, Jenkins and Alexanderson systems are described in separate chapters. One chapter is devoted to telephotography. The book contains a large number of photographs.

J. W. BUCHTA